ENVIRONMENTAL ANALYSIS OF BIOLOGICALLY INSPIRED SELF-CLEANING SURFACES

A Thesis
Presented to
The Academic Faculty

by

Laura Raibeck

In Partial Fulfillment
of the Requirements for the Degree
Master of Science in the
School of Mechanical Engineering

Georgia Institute of Technology
August 2008

ENVIRONMENTAL ANALYSIS OF BIOLOGICALLY INSPIRED SELF-CLEANING SURFACES

Approved by:

Dr. Bert Bras, Advisor
School of Mechanical Engineering
Georgia Institute of Technology

Dr. Dave Rosen
School of Mechanical Engineering
Georgia Institute of Technology

Dr. Jeanette Yen
School of Biology
Georgia Institute of Technology

Date Approved: June 30, 2008

ACKNOWLEDGEMENTS

I wish to thank Dr. Bert Bras, my advisor, for his help and guidance throughout my research. I also wish to thank my reading committee members, Drs. Jeannette Yen and Dave Rosen, for their comments and criticisms on my work. Dr. Michael Overcash has given me invaluable help with the chemical life cycle parts of this research. Dayna Baumeister gave me good ideas and lots of information about the biological aspects of my research.

The SRL family, especially the members of the SDM group, deserves thanks, as they have given me much support throughout my graduate career. In particular: John, who got me started on the path to becoming a researcher; Felipe and Scott, whose experiences and advice helped me avoid problems; and Caroline and Sophie, with whom I braved year one and numerous class projects

For financial support, I gratefully acknowledgement NSF DMI 0600243 for supporting the research project and the College of Engineering for my fellowship.

I would especially like to thank my partner, Jon. He has provided countless words of support and encouragement, as well as criticisms when needed. He picked up and left to Atlanta with me, perhaps the biggest sacrifice anyone has made for this work. Without him, I doubt graduate school and the completion of this thesis would have gone nearly as smoothly.

TABLE OF CONTENTS

LIST OF TABLES

LIST OF FIGURES

LIST OF SYMBOLS

α	Thermal Diffusivity
β	Volumetric Thermal Expansion
η	Efficiency
θ_a	Advancing Contact Angle
θ_c	Contact Angle
θ_r	Receding Contact Angle
θ_y	Young's Angle
ν	Kinematic Viscosity
ρ	Density
σ	Interfacial Tension
ϕ	Contact Area Fraction
c_p	Specific Heat
g	Gravity
h	Convection Coefficient
k	Thermal Conductivity
Nu	Nusselt Number
Pr	Prandtl Number
q	Heat Transfer
r	Roughness Factor
R	Thermal Resistance
Ra	Rayleigh Number
S	Shape Conduction Factor

T_f	Film Temperature
T_s	Surface Temperature
T_∞	Ambient Temperature
U	Thermal Resistance

LIST OF ABBREVIATIONS

AACA	Aluminum Acetylacetonate
BID	Biologically Inspired Design
CA	Contact Angle
COP	Coefficient of Performance
EBDM	Environmentally Benign Design & Manufacture
GPM	Gallons per Minute
GWP	Global Warming Potential
LCA	Life Cycle Assessment
LCI	Life Cycle Inventory
LCIA	Life Cycle Impact Assessment
SEM	Scanning Electron Microscope
SM	Surface to Body Mass Ratio
TACA	Titanium Acetylacetonate
TCE	Trichloroethylene

SUMMARY

Biologically inspired design is used as an approach for sustainable engineering. Taking a biologically inspired approach, one abstracts ideas and principles from nature, an inherently sustainable system, and uses them in engineering applications with the goal of producing environmentally superior designs. One such biological idea with potential environmental benefits for engineering is microscale and nanoscale surface roughness found on the Lotus plant and many other surfaces in nature. These surfaces repel water and aid in contaminant removal; this self-cleaning phenomenon is called the "Lotus Effect®," in honor of the plant first observed to exhibit it. The structures responsible for the Lotus Effect® inspired research and development of many technologies capable of creating hydrophobic, self-cleaning surfaces, and many potential self-cleaning surface applications exist beyond nature's intended application of cleaning.

While statements have been made about the environmental benefits of using a self-cleaning surface, only limited scientific data exist. Artificial self-cleaning surfaces are successfully cleaned using fog or mist. This shows that such surfaces can be cleaned with less energy and water intensive methods than the more conventional methods used to clean regular surfaces, such as spray or solvent cleaning. This research investigates the potential environmental burden reductions associated with using these surfaces on products.

A life cycle assessment is performed to determine the environmental burdens associated with manufacturing a self-cleaning surface, for three production methods: a chemical coating, a laser ablated steel template, and an anodized aluminum template.

The environmental benefits and burdens are quantified and compared to those of more conventional cleaning methods. The results indicate that self-cleaning surfaces are not necessarily the environmentally superior choice.

CHAPTER 1

INTRODUCTION

Concern for the environment and a recent trend of a focus on sustainability is causing many engineers and designers to rethink how their products and processes impact our world. The entire life cycle of products and systems should now be considered – from materials acquisition to manufacture to use and finally end of life. Engineers concerned about sustainability are not just focused on what goes into making their products, but also what the product will produce and what will be left behind.

In a world with limited resources but unlimited ingenuity, engineers and designers research new methods of producing not only technically superior, but environmentally superior products and processes. New design methods and guidelines are developed and implemented with the ultimate goal of sustainable designs, methods such as life cycle design (US EPA 1993), Design for Environment (Fiskel 1996), Ecodesign (Brezet and Hemel 1997), and Environmentally Benign Manufacturing (Allen et al. 2002).

With Nature often thought of as the ultimate model of sustainability (Benyus 1997; Beattie and Erhlich 2001), it seems obvious that designers are beginning to take more inspiration from natural systems for designing not just novel products and systems, but products and systems with lower environmental impacts. Nature, however, is useful for more than just novel concepts or functions to copy; nature can perhaps offer principles or of sustainability, which engineers can use and follow in their own systems.

Surfaces in nature have caught designers' attention. Surfaces, in particular, that occur on both plants and animals can remain clean and are able to function despite very dirty environments are of interest. The structures of these surfaces have been successfully copied with many methods for engineering applications. These surfaces,

called “self-cleaning surfaces” have found uses outside nature’s intended purpose of cleaning, and even more uses are being investigated.

Biologically inspired design is used as an approach to sustainable design. In this thesis, one biologically inspired design concept is investigated to determine if this concept is more sustainable than a traditionally designed concept. More specifically, biologically inspired self-cleaning surfaces are environmentally analyzed with a Life Cycle Assessment (LCA) and compared to traditional methods of cleaning. The results of the LCA can be used to select the environmentally superior or more sustainable design, to give more confidence to the idea that taking concepts from nature will result in environmentally superior designs, or indicating that designers must still be careful when using such ideas.

1.1 Biologically Inspired Design

Biologically inspired design is simply the using of ideas and principles of nature in an engineering context. It is also often called “biomimicry”: literally, the mimicking of life. Biologically inspired design, or biomimicry, has been used for many years to produce novel products or systems. Natural systems have faced and solved many problems that humans also encounter and seek solutions to; it is logical to use nature’s solutions to these common problems.

The most well known biomimetic design may be Velcro; it is just one of many numerous biomimetic designs. In a more abstract sense, nature has provided much inspiration for humans’ design of robotics and automation; engineers have studied how organisms move in nature and have attempted to mimic these movements. These products or systems may have been developed in a very ad hoc fashion, although now more structured methods exist to transfer ideas from nature into designs.

Biologically inspired design has two approaches: solution driven design and problem driven design. Solution driven biologically inspired design begins with biology,

while problem driven biologically inspired design starts in the engineering design world. The two approaches are described in the following two sections.

1.1.1 Solution Driven Biologically Inspired Design

Solution driven biologically inspired design begins with the discovery of an interesting biological system, which a designer hopes to replicate. The process of solution driven design is shown in Figure 1.1.

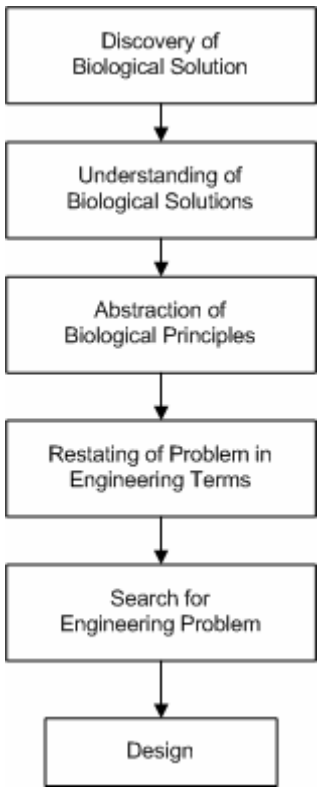

Figure 1.1: Solution driven biologically inspired design process.

A designer begins this solution driven process with a specific biological system in mind. The system of interest may have a unique movement, structure or other function. The designer then must understand how the biological system fulfilled the interesting function. Once the designer has understood how the system performs the given function, the "Understanding of Biological Solutions" step is complete.

Next, in the "Abstraction of Biological Principles" step, the designer simplifies the mechanisms the biological systems uses to fulfill the function of interest. The designer will use "solution neutral" terms to describe the biological principles. In the next step, "Restating of Problem in Engineering Terms," the designer takes the solution neutral principles and translates them to a solution to an engineering problem.

With the abstracted biological solution now translated to engineering solution, the designer can begin to find engineering problems which could be satisfied by the biologically inspired solution. This is the "Search for Engineering Problem" step. Having identified an appropriate engineering problem, the designer now can apply the principles of the biological solution and develop a new design.

An example of this process is the invention of Velcro™. An engineer in 1940s came across the burdock plant, the seeds of which became stuck to his clothes. From there, the solution driven biologically inspired design process could follow this path:

- Discovery of Biological Solution – The engineer discovers a plant that is able to attach its seeds to his clothing.
- Understanding of Biological Solution – How does the plant attach to other organisms? It is covered with long, thin hooks, which can get caught in the fur or fabric of a passerby.
- Abstraction of Biological Solution – The engineer uses solution neutral terms to describe the biological principle as "hooks attaching to loops."
- Restating of Problem in Engineering Terms – The engineer may have asked himself, "How can engineers uses hooks and loop to attach things?"
- Search for Engineering Problem – With his idea, the engineer would be able to find many areas which could use a simple, quick fastener.
- Design – The resulting product eventually became Velcro™.

1.1.2 Problem Driven Biologically Inspired Design

Problem driven biologically inspired design begins with an established engineering problem, which can possibly be solved with a biologically inspired idea. The problem driven biologically inspired design process is shown in Figure 1.2.

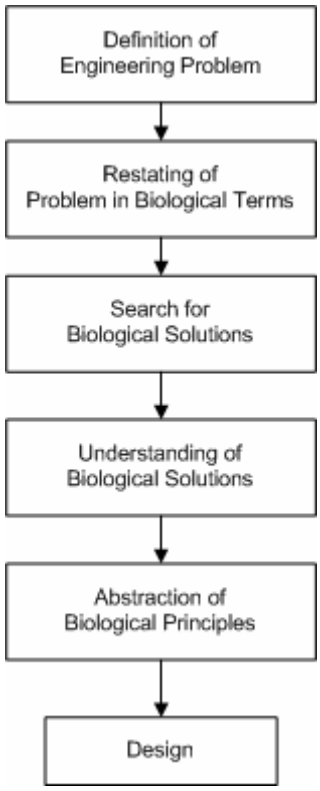

Figure 1.2: Problem driven biologically inspired design process.

A designer begins by defining an engineering problem in terms of the required functions the solution must fulfill. This is the "Definition of Engineering Problem" step. In the "Restating of Problem in Biological Terms" step, the designer begins to think about nature's solutions to his or her engineering problem. The engineer may ask himself or herself how animals or plants fulfill the function also required for his engineering problem. The function is now thought of in biological terms.

With the biological function in mind, the designer now begins to search the biological world to find organisms which perform the given function. This is the "Search for Biological Solutions" step of the process. After an appropriate biological system or

organism is found, the designer must find out how the function of interest is performed; this completes the "Understand of Biological Principles" step.

1.1.3 Biologically Inspired Design for Sustainability

Sustainable development is defined as "development that meets the needs of the present generation without compromising the needs of future generations" (UN 'Brundtland' Commission 1987). As sustainable development and sustainability gain more attention, engineers and designers continue to look for new and innovative ways to produce environmentally friendly products and processes.

Biologically inspired design is investigated as an approach to environmentally conscious or sustainable design. It has been suggested that engineers begin to look at how nature has become and remains sustainable (Benyus 1997; Beattie and Erhlich 2001). Principles of nature which all life follows and which results in sustainability can be abstracted, translated to engineering guidelines and used as a guiding process in engineering design. The Biomimicry Guild has already identified a number of "principles of life", many of which indicate the inherent sustainability of natural systems. These principles are shown in Figure 1.3; those principles dealing with specifically with sustainability are then listed below.

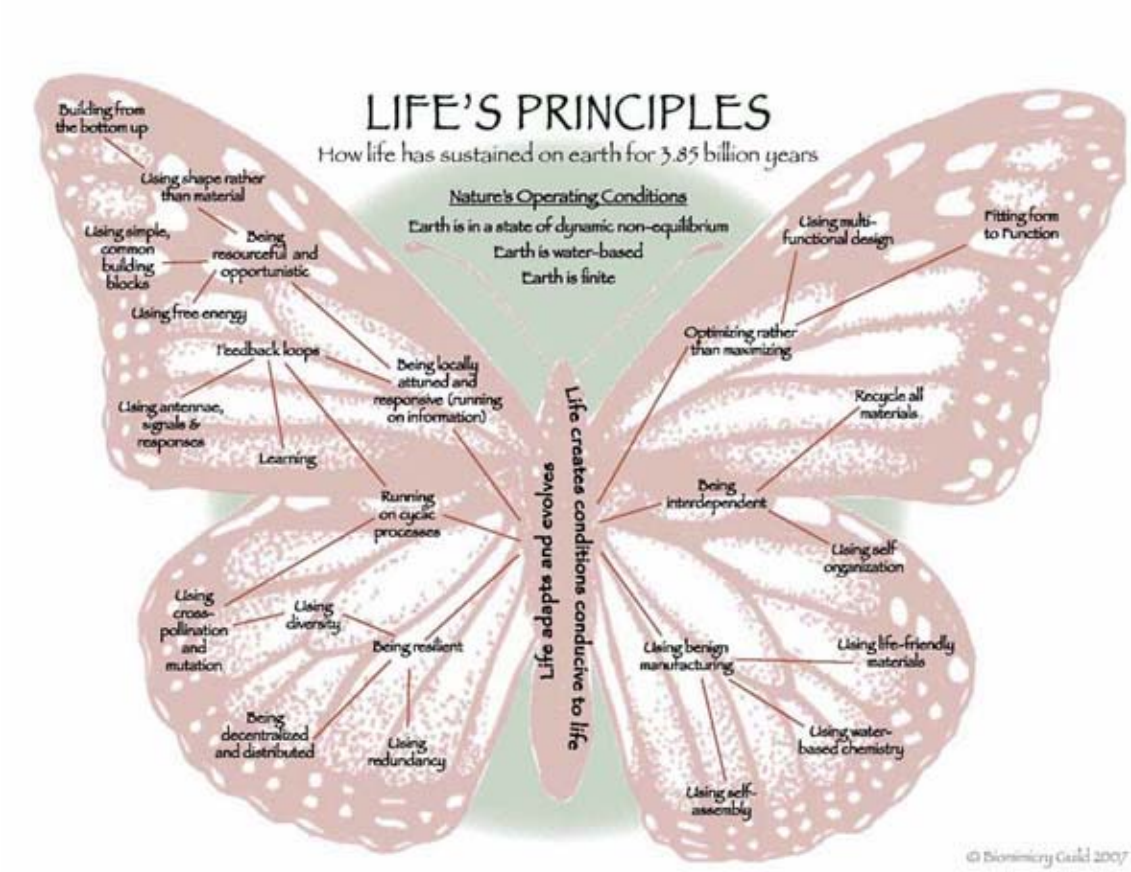

Figure 1.3: Principles of life developed by the Biomimicry Guild (Biomimicry Guild 2007).

- Life uses benign manufacturing.
    - Life uses water based chemistry.
    - Life uses "life-friendly" materials.
- Life recycles all materials.
- Life builds from the bottom up.
- Life uses free energy.
- Life is locally attuned and resourceful.

These are just a few of the identified principles of life, but they show that natural systems do in fact have governing principles to remain sustainable. It is assumed that if designers follow these same guidelines, their resulting products or processes will also be

sustainable. The challenge comes in translating these principles of life to engineering guidelines. Once these principles, along with other principles of nature, are identified, translated to engineering guidelines and put into place as a method of designing, a biologically inspired approach to sustainable design and manufacture will be able to be used.

Biologically inspired design is a new approach to sustainable design, different from previous sustainable design methods, such as Design for Environment, Environmentally Conscious Design and Manufacturing, and Environmentally Benign Design and Manufacturing. These other methods use information from case studies, policy and field observations, among other sources, to lead to environmentally conscious guidelines. Such a method of obtaining guidelines indicates that mistakes must be made before the environmentally superior path can be discovered. The biologically inspired sustainability approach hopes to avoid making engineering mistakes, by gathering information from a system which has already worked out the problems with regards to being sustainable: nature has learned "after 3.8 million years of evolution what works, what is appropriate, what lasts." (Benyus 1997).

A designer must be cautious about using principles and ideas from nature to produce environmentally superior designs. It is not guaranteed that a product or system with biological roots will be more sustainable than a more traditionally designed product or system, for example, something designed using EBDM. For this reason, an environmental analysis in the form of a life cycle assessment of a biologically inspired product is of interest; life cycle assessment is described in Section 1.3. An LCA is performed on self-cleaning technologies and compared to the environmental impacts of

industrial cleaning methods. If the results of the study indicate that the biologically inspired option is environmentally superior to the traditional option, more confidence will be given to the idea of biologically inspired sustainability. If the results indicate that the biologically concept has larger environmental impacts as compared to the traditionally designed option, it will show that designers must use caution when incorporating biologically inspired ideas into their design, perhaps coupling biologically inspired design with other environmentally conscious design methods.

1.2 Introduction to Self-Cleaning Surfaces

Self-cleaning surfaces are one such idea abstracted from nature. First observed on the lotus plant, researchers noticed that water beads up on the leaves. These drops of water roll off the surface of the leaf, taking dirt with it. A drop of water on a lotus leaf is shown in Figure 1.4.

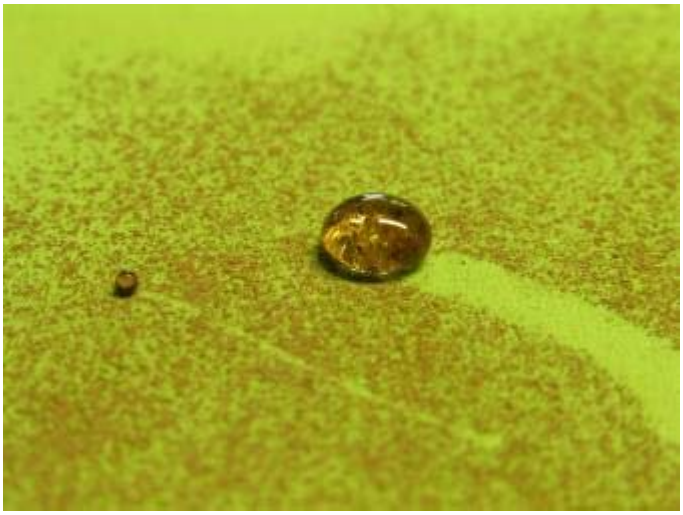

Figure 1.4: Lotus leaf with self-cleaning abilities (BIOPRO 2006).

Because the self-cleaning mechanism was first discovered on a lotus leaf, self-cleaning is sometimes referred to as the "Lotus Effect." Although the lotus leaf is the most popular

example of natural self-cleaning, these abilities appear on a number of organisms, as discussed in Chapter 2.

Self-cleaning surfaces are often used for the obvious purpose of keeping a surface clean. They can be used on the outside of houses or cars, for example, which are normally periodically cleaned. Self-cleaning surfaces have found other uses, though, such as for preventing oxidation, current conduction, snow adherence and scaling in pipes (Nakajima et al. 2001).

1.2.1 Potential Benefits of Use

A simple experiment can demonstrate the benefits of using a self-cleaning surface. One side of a piece of aluminum was divided in half; to one half a self-cleaning coating was applied, while the other half remained untreated. Next, the aluminum was soiled, and the piece of aluminum was placed on an incline. Equal amounts of water were then applied with a dropper to both the untreated and self-cleaning sides of the aluminum, in an attempt to remove the soil. The untreated side of the aluminum after cleaning is shown in Figure 1.5.

Figure 1.5: Soiled untreated aluminum exposed to water.

The self-cleaning side of the piece of aluminum after cleaning is shown in Figure 1.6.

Figure 1.6: Soiled self-cleaning aluminum exposed to water.

As shown in the figures above, the untreated aluminum is not effectively cleaned by water alone. The water runs over the contaminants, but it does not remove them. The self-cleaning surface, however, is effectively cleaned with just water. As the water travels down the inclined self-cleaning surface, it removes all contaminants it encounters, leaving behind a nearly perfectly clean trail. From this experiment, it is easy to see the potential environmental benefits of widespread use of self-cleaning experiments; less water will be needed to clean soiled surfaces, and the use of detergents may be completely avoided. It has been shown that self-cleaning surfaces are able to be nearly completely cleaned (99.7% of contaminants removed), simply by mist or fog cleaning, with no solvents or detergents (Fürstner and Barthlott 2005).

In conventional cleaning methods, more than just water is used for cleaning; detergents or solvents are added to the water, and additional energy is need to heat and/or agitate the cleaning water. Additional energy and resources also are needed to produce the solvents, which have associated environmental impacts. Often times a large volume of water is used to fill the tanks of cleaning machines, so additional water is needed.

With all of these added resources, it is clear that self-cleaning surfaces used in place of these traditional, aqueous cleaning methods will have less of an environmental impact.

1.2.2 Potential Burdens of Production

The "Lotus Effect" has inspired many different methods of producing a hydrophobic surface, as well as dozens of commercial products. The methods of producing self-cleaning surfaces are discussed in Chapter 2. When compared to an untreated surface, the self-cleaning surface will of course require more energy and resources to be consumed in production.

Many methods of producing self-cleaning surfaces involve a coating or film which provides surface roughness and hydrophobicity. The chemicals used in these coatings have the potential to have large environmental impacts, from materials acquisition and production. If toxic chemicals are used, adverse human health effects could be encountered. Many of the coatings use nanoparticles to provide roughness while remaining transparent (Nakajima et al. 2001); nanoparticles may also have adverse human health effects, as well as negative environmental effects (Oberdörster 2005). Will the environmental impacts of producing and using these chemicals and nanoparticles be much larger than the impacts of conventional cleaning?

Other methods of producing a self-cleaning surface, discussed in Chapter 2, include laser micromachining or growth of carbon nanotubes. These methods obviously require additional energy and resources. Some of the methods of manufacturing hydrophobic, self-cleaning surfaces require nanostructured templates. The templates are then repeatedly used, with heat and pressure, to structure polymeric surfaces. Although this method may initially appear to perhaps be more sustainable than a chemical coating, one must consider the amount of energy required to produce the materials for the template and for manufacturing the nanoscale structured surface. The resource consumption and emissions of producing a hydrophobic surface with this method may

heavily outweigh the benefits of using the surface, and may prove to be larger than simply using current industrial cleaning methods.

1.3 Life Cycle Assessment

Life cycle assessment (LCA) is a systematic method of quantifying the environmental impact of a system over its entire life cycle. LCA uses a "cradle to grave" perspective when analyzing a system (SAIC 2006). In the "cradle to grave" approach, assessment starts with the acquisition of materials from nature and considers all parts of a product's or system's life until the materials are returned to nature. The assessment works by summing all resource consumption and environmental release, then determining the environmental impact of this consumption and waste. Because all parts of the life cycle are considered, a more complete assessment of environmental impacts is obtained with a LCA.

A life cycle assessment has four stages. The stages of the life cycle assessment are shown in Figure 1.7.

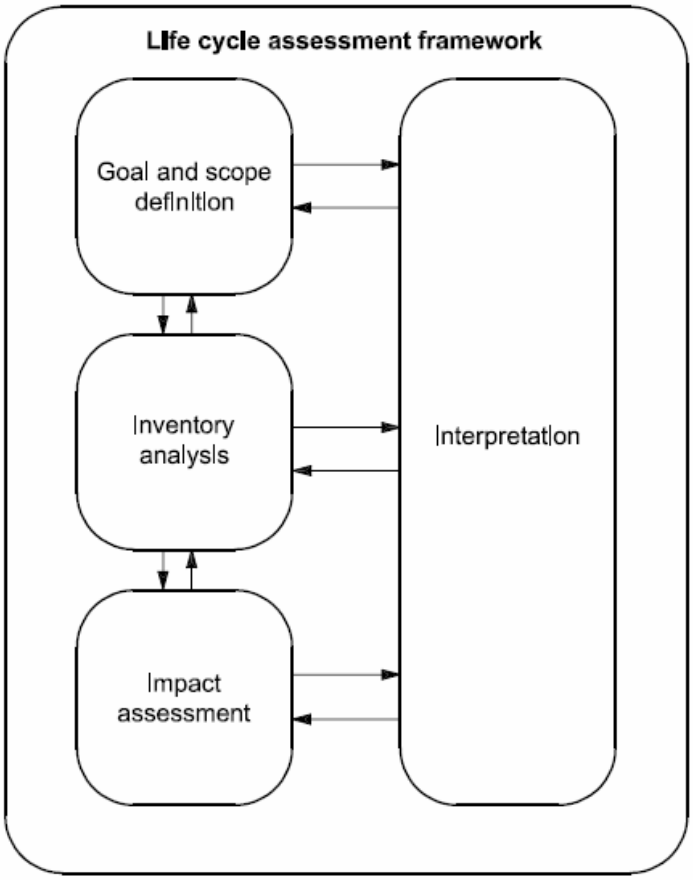

Figure 1.7: Stages of life cycle assessment (International Standards Organization 2006).

The four stages are described as (SAIC 2006):

- Goal and scope definition: Goals and objectives are set for the analysis. The system to be analysis is described, and the boundary is set.
- Inventory analysis: The resource consumption and emissions for the system are summed for each part of the life cycle.
- Impact assessment: The environmental impact of the inventory from the previous step is determined.
- Interpretation: The results of the inventory analysis and impact assessment are analyzed to identify problems, completeness and sensitivity. Recommendations for the preferred system are given.

Life cycle assessment will be used to determine the environmental impacts of self-cleaning surfaces and industrial cleaning methods. The results of the LCA will be used to determine whether self-cleaning surfaces are environmentally superior to more traditional methods of cleaning.

1.4 Research Objectives, Questions and Hypotheses

As discussed in the previous two sections, there are obvious benefits associated with using a self-cleaning surface, but additional resources are needed to produce the surface. The objective of this research is to quantify both the benefits of use and the burdens of production of the biologically inspired design over its entire life cycle. These results then will be compared to the burdens associated with the life cycle of conventional methods of cleaning a surface, particularly aqueous cleaning methods involving detergents or solvents.

Once these benefits and burdens are quantified, the first research question associated with this work will be addressed. This first question is:

- What overall benefits are associated with using biologically inspired self-cleaning surfaces when cleaning, as compared to current cleaning methods?

This research question can be broken up into two parts:

- What environmental burdens are associated with producing hydrophobic surfaces?
- What environmental benefits are associated with cleaning hydrophobic surfaces?

These questions lead to a hypothesis.

- From a life cycle perspective, self-cleaning surfaces have smaller environmental impacts than traditional aqueous cleaning methods.

The answers to the previous research questions serve as a case study for determining if biologically inspired designs lead to environmentally superior designs. This leads to a more broad research question involving biologically inspired design as a whole. The next research question is:

- Do biologically inspired designs produce environmentally superior products or systems, as compared to conventionally designed products or systems?

The hypothesis drawn from this question is:

- Biologically inspired designs lead to products or systems which are environmentally superior to products or systems designed by conventional means.

With biologically inspired design as an approach to sustainable design, and with a emphasis on "principles of life", used as a focus of this work, one many wonder what sort of principle of life/sustainability could be formed from the results of research. A far broader, more abstract research question then may be:

- Can a "principle of life" or a "principle of sustainability" be formed in relation to self-cleaning surfaces, or more generally to how nature cleans or how nature uses surfaces?

1.5 Organization of Thesis

Having described the problem to be addressed with this research, the entire thesis is laid out as follows:

- **Chapter 1** – In this chapter, the problem to be addressed by this research is described: determining if biologically inspired designs, specifically self-cleaning

surfaces, are environmentally superior to conventionally produced designs. This chapter contains the research objectives, questions and hypotheses.

- **Chapter 2** – In this chapter, the previous work in related areas is reviewed. In particular, the following topics are reviewed:
    - modeling and optimization of hydrophobic surfaces
    - biological occurrences of self-cleaning hydrophobic surfaces
    - methods of producing self-cleaning surfaces
    - commercial products featuring self-cleaning surfaces
    - current industrial methods of cleaning
- **Chapter 3** – In Chapter 3, the environmental impacts of self-cleaning surfaces are modeled, through a Life Cycle Assessment of a self-cleaning coating. The system includes materials acquisition and production of chemicals, manufacture and use of a self-cleaning coating.
- **Chapter 4** - A life cycle assessment also is performed of two methods of manufacturing a template to be used to produce self-cleaning surfaces. The first method involves a steel template with a laser micromachined pattern. The life cycle inventory of materials acquisition and production of such a template is determined in this chapter.
- **Chapter 5** – In this chapter, the third method of producing a self-cleaning surface is analyzed. This method uses an aluminum template chemically anodized to have nano-scale features. The materials acquisition and production of this type of template is analyzed, and a life cycle inventory is formed.

- **Chapter 6** – Life cycle inventories for the use phase, or cleaning, are developed in this chapter. The life cycle inventory associated with cleaning the self-cleaning surface is estimated. The life cycle of a system which includes the materials acquisition and production of a solvent, as well as the use of industrial cleaning machines also is developed in this chapter. Spray and ultrasonic cleaning are considered, with a range of part sizes, cleaning times, solvent concentrations, and solvent recycling scenarios.
- **Chapter 7** – In this chapter, the results of the Life Cycle Assessment are discussed. Significant issues are addressed, and the completeness, sensitivity and consistency of the life cycle assessment are analyzed.
- **Chapter 8** – This chapter concludes the thesis with a summary of the answers to the research questions above. The contributions of the research are discussed, and areas of future work are indicated.

CHAPTER 2

LITERATURE REVIEW

In this literature review, previous work concerning natural self-cleaning surfaces, methods of producing artificial self-cleaning surfaces, modeling and optimization of hydrophobic surfaces and current cleaning technology are analyzed. Models of hydrophobic surfaces are analyzed to understand the underlying physics of self-cleaning. Naturally occurring self-cleaning surfaces are reviewed to understand what type of surface features are required for hydrophobicity, and for what purposes these surfaces serve on the organisms on which they appear. Methods of producing artificial self-cleaning surfaces are reviewed to identify the large range of technologies employed in manufacturing, and also to identify methods which can be environmentally analyzed. Finally, current cleaning technology is analyzed to determine environmental issues which perhaps can be improved upon with the introduction of biologically inspired technologies.

2.1 Modeling and Optimization of Self-Cleaning Surfaces

The wetting or non-wetting properties of a surface are commonly measured by the static contact angle a liquid forms with the surface. The measurement of a contact angle for a static drop is shown in Figure 2.1.

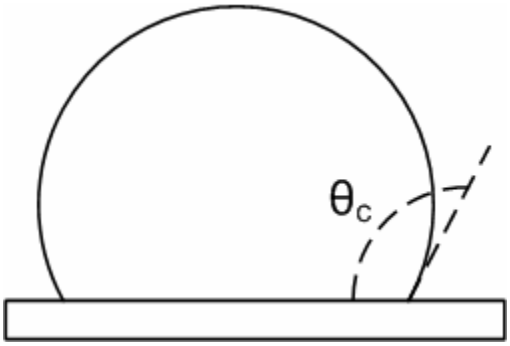

Figure 2.1: Measurement of the contact angle of a static drop.

When a drop of water forms a contact angle of less than 90º, the surface wets and is said to be hydrophilic. An example a drop with a low contact angle wetting a surface is shown in Figure 2.2.

Figure 2.2: Drop of water on a hydrophilic surface.

When a drop of water forms a contact angle of greater than 90º, the surface is said to be hydrophobic. Surfaces with contact angles above 150º are called superhydrophobic, and sometimes ultraphobic. An example of a drop with a high contact angle which does not wet a surface is shown in Figure 2.3.

Figure 2.3: Drop of water on a hydrophobic surface.

Young studied the behavior of liquids on heterogeneous, flat surfaces, and proposed this model for the contact angle of the liquid

$$\cos\theta_y = \frac{\sigma_{sf} - \sigma_{sl}}{\sigma_{lf}}$$

where σ_{sf}, σ_{sl} and σ_{lf} are the solid-fluid, solid-liquid and liquid-fluid interfacial tensions, respectively.

Wenzel expanded upon Young's equation for the case of a rough surface (Wenzel 1936)

$$\cos\theta_c = r\cos\theta_y$$

where θ_c is the apparent contact angle, and r is a roughness factor defined as

$$r = \frac{actual\ surface\ area}{geometric\ surface\ area}$$

A perfectly flat surface will have a roughness factor of 1; all real surfaces will be greater than 1. In Wenzel's model, it is assumed that the liquid will fill in the spaces between the surface roughness features.

For increasing values of the surface roughness factor, a Young's angle of greater than 90º will have an increasing apparent contact angle, and a Young's angle of less than 90º will have a decreasing apparent contact angle. Therefore, the addition of roughness features makes already hydrophobic surfaces more hydrophobic and hydrophilic surfaces more hydrophilic.

Cassie and Baxter expanded Wenzel's model to applicable to rough and porous surfaces:

$$\cos\theta_c = \phi_s\cos\theta_y + \phi_a$$

where ϕ_s is the area fraction of liquid-solid contact, and ϕ_a is the area fraction of liquid-air contact (Cassie and Baxter 1944). In this model, the liquid does not fill in the area

between roughness features, thereby forming a solid-liquid-gas composite surface. When a surface is rough and not porous, ϕ_a is 0 and Wenzel's model remains.

2.1.1 Determining the correct model

It is not certain when Wenzel's equation applies, or when the Cassie-Baxter model is appropriate. Lafuma and Quere suggest that the Cassie-Baxter model is valid for high contact angles or very rough surfaces; the Wenzel model is appropriate for hydrophobic surfaces with contact angles close to 90º (Lafuma and Quere 2003). Experiments performed by Yoshimitsu and coauthors showed that the Cassie-Baxter model is indeed appropriate for higher roughness values (Yoshimitsu 2002). Marmur found that for most surface structures, the Cassie-Baxter contact angle is higher than the Wenzel contact angle, and that for equal contact angles, less of the surface is wet with the Cassie-Baxter model (Marmur 2004).

Patankar found the both the Wenzel and Cassie-Baxter models are equilibrium states, and which model a drop will follow depends on how the drop was formed (Patankar 2003). It also was determined that the state with a lower contact angle is the lower energy state. Bico and coauthors found that a drop forming a composite surface (Cassie-Baxter model) will, when pressed, form a homogeneous surface (Wenzel model) (Bico et al. 1999). Zheng and coauthors determined the critical pressure that a drop in the Cassie-Baxter mode can withstand before transitioning to the Wenzel model to be 296 kPa (Zheng 2005). For short surface roughness features (>12 μm), the critical pressure may be less. The critical pressure can be increased by having surface asperities which are closer together.

Bico and coauthors derived an expression for an angle, θ_c, above which measured contact angle indicate the Cassie-Baxter model is correct (Bico et al. 2002); this angle is

$$\cos\theta_c = \frac{\phi_s - 1}{r - \phi_s}$$

Extrand derived an expression for the critical value of the contact line density by equating body and surfaces forces for a drop on a rough surface (Extrand 2002). Drops with a contact line density higher than the critical value will remain on top of surface roughness features (Cassie-Baxter model), while drops with a contact line density less than the critical value will fill in the areas between the surface features (Wenzel's model). Marmur analyzed the Gibb's energy of a drop of liquid to determine that a local minimum indicates the Cassie-Baxter is applicable, while a border minimum of the Gibb's energy represents the Wenzel model (Marmur 2004).

2.1.2 Behavior on Hydrophobic Surfaces

Richard and Quere studied the behavior of liquid drops on tilted hydrophobic surfaces. By tracking a small bubble inserted into a drop of glycerol, they found that drops will roll off of the surface, instead of sliding in the case of hydrophilic surfaces (Richard and Quéré 1999). They also found that the velocity of the drop tends to increase as the radius of the drop decreases.

2.1.3 Optimal Hydrophobic Surfaces

Studies and optimizations have been completed to determine the size, shape and density of surface roughness features which will maximize the contact angle of a liquid. Bico and coauthors found that the most important parameter in hydrophobicity is the area

fraction of liquid-solid contact (ϕ_s), and therefore spikes are the ideal surface roughness features (Bico et al. 1999). Marmur found that the contact angle predicted by the Cassie-Baxter model is not affected by the height of surface features, and only slightly affected by the slope of the features (Marmur 2004).

Nosonovsky and Bhushan performed an optimization of contact angle for surfaces with sawtooth, periodic, rectangular, rounded-top cylindrical, conical and random surface features (Nosonovsky and Bhushan 2005). Taken into account for each type of surface was sharpness of features (which can pin the drop in place) and whether a composite or homogeneous contact is formed between the drop and the surface. The ideal surface was determined to have rounded-top cylindrical roughness features. The contact angle is maximized by increasing the aspect ratio (height to radius ratio of the features) and the density of the surface features.

2.1.4 Contact Angle Hysteresis

It is suggested that the static contact angle of a liquid is not enough to measure the hydrophobicity of a surface. The contact angle hysteresis,

$$\Delta\theta = \theta_a - \theta_r$$

is the difference between the advancing contact angle, θ_a, and the receding contact angle, θ_r. The angle at which a surface is tilted when drops roll off is suggested as another measure of hydrophobicity. Both the roll-off angle and the contact angle hysteresis should be small in an ideal hydrophobic surface.

Contact angle hysteresis can be caused by the surface roughness features, and therefore happens commonly in the Wenzel model (Extrand 2002). Joanny and de Gennes claim the hysteresis happens when surfaces features are sharp and pin the drop in place (Joanny

and Gennes 1984). They proposed a model to determine when hysteresis will occur, using a metric of "strength" for a surface feature. A drop will be pinned on the feature and hysteresis will occur, if the strength is above a critical value.

2.2 Natural Self-Cleaning Surfaces

Barthlott and Neinhuis, when investigating the surface structures of plants, noticed smooth leaves were usually contaminated, while plants with a wax coating were usually clean (Barthlott and Neinhuis 1997). This observation led them to perform experiments comparing smooth and rough surfaced plants. The smooth plants selected included two evergreen species, and the rough plants included the leaves of the lotus plant. The contact angle (CA) of drops of water on the surface were measured; it was found that the smooth leaves had CAs of less than 90º, while the rough plants had CAs of higher than 128º. The lotus plant had a CA of approximately 160º. This indicates superhydrophobic behavior. Under a SEM, it was found that the lotus and other hydrophobic leaves had rough surface features, along with a wax covering. The smooth leaves had no wax coating.

Next, experiments were performed to determine the cleaning abilities of hydrophilic and hydrophobic leaves (Barthlott and Neinhuis 1997). The leaves were soiled with contaminants ranging in size from 0.5 to 30 micrometers. The leaves were then subjected to artificial rain for 2 minutes. After the rain, the rough surfaces leaves contained virtually none of the contaminants, while up to 80% of the contaminants remained on the smooth leaves. After re-contamination, the leaves were cleaned with artificial fog. The results of the fog cleaning were similar to that of rain; a large percent

of the particles remained on the smooth leaves, while few remained on the rough surfaced leaves.

Some potential benefits of this self-cleaning ability is that it helps to control the leaf temperature (Barthlott and Neinhuis 1997). Also, it is a possible barrier against pathogens and spores. Barthlott and Neinhuis call this self-cleaning ability the "Lotus Effect" and suggest that the surface features which lead to self-cleaning could be used in technological applications (Barthlott and Neinhuis 1997).

Bhusan and Jung studied the individual effect of micro- and nano-scale features on the hydrophobicity of plants (Bhushan and Jung 2006). Hydrophilic leaves were used as a comparison to understand the effect surface roughness and the wax coatings have on hydrophobicity. Lotus and colocasia were used as the hydrophobic plants; fagus and magnolia were the representative hydrophilic plants.

The contact angle of water on the surface of the leaves was measured. Acetone was then applied to the plants to remove any wax coating, and the CA was measured again. It was found that the hydrophobic plants were no longer hydrophobic (CA of less than 70º in this case), and the CA of the hydrophilic leaves stayed the same.

The contact angle was measured for all leaves while fresh, then again after drying. In the hydrophobic leaves, drying reduces the height of the microbumps on the surfaces, from approximately 7 micrometers to 3. For both the hydrophobic and hydrophilic leaves, this reduced the CA, though not significantly.

Bhusan and Jung concluded from these experiments that nano-scale roughness of the wax contributes more to the hydrophobicity of the leaves than the micro-scale bumps

(Bhushan and Jung 2006). They suggest that nanoscale roughness will be important in developing hydrophobic surfaces for technological applications.

Cheng and coauthors performed a similar experiment on lotus leaves (Cheng et al. 2006). In their experiment, they heated the leaves to 150ºC, which melted the nanoscale hairs on the leaf, but did not affect the surface chemistry. They then measured the contact angles of water on carnauba wax (similar to wax on lotus leaves), on the heat treated leaves which no longer had nanoscale features, and on untreated leaves. The found the contact angle on the wax to be 74º, on the leaves without nanofeatures to be 126º and the untreated leaves to be 142º. They also found that although the heat treated leaves were hydrophobic, drops stuck to the surface and did not roll off easily.

Cheng and coauthors concluded from these experiments that microscale bumps are responsible for the transition from hydrophilicity to hydrophobicity of the wax (Cheng et al. 2006). They also concluded that the large contact angle is a result of both the micro- and nanoscale features. Finally, they deduced that the nanoscale features are responsible for the self-cleaning abilities of the lotus leaf (Cheng et al. 2006).

Other organisms exhibit self-cleaning abilities. An example of a natural microroughed surface and the various organisms on which it has been found to appear is shown in Figure 2.4.

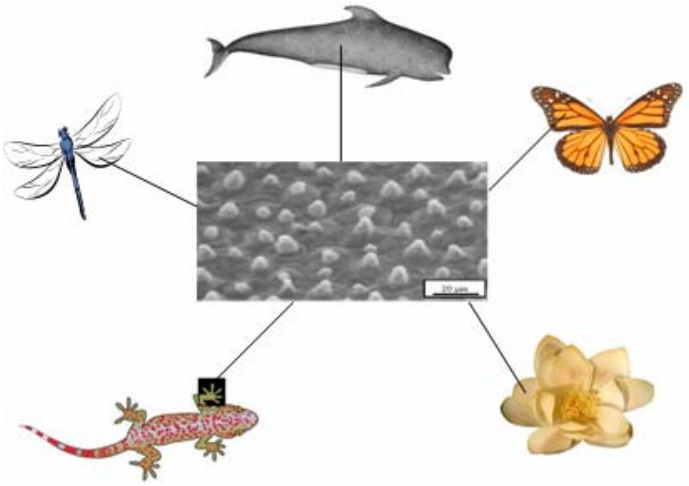

Figure 2.4: Variety of organisms identified as having self-cleaning properties.

Neinhuis and Barthlott measured the contact angle and used scanning electron microscopy (SEM) to characterize the surfaces of 200 species of plants (Neinhuis and Barthlott 1997). The majority of the 200 plants were found to be superhydrophobic, and the remaining plants were hydrophobic. On all water repellent leaves, wax crystalloids were found which measured 0.5 to 20 micrometers. The wax along with any surface features work together to increase the water repellency of the leaves.

Different reasons for the water repellency/hydrophobicity of the leaves are speculated depending on the geographic location of the plants (Neinhuis and Barthlott 1997). Hydrophobicity can be used to control the temperature of the leaves in semi-arid conditions. In wetlands, many pathogens are present, and the self-cleaning ability may be used to prevent these pathogens from infecting the plants. In open areas, the surface features may be used to reflect light. The self-cleaning ability may help to protect plants from salt damage when growing on beaches. Because CO_2 diffuses faster through air than through water, the hydrophobicity of the plant can aid in plant growth in humid areas.

The self-cleaning ability and hydrophobicity is not found only on plants. Wagner and coauthors investigated the surfaces of the wings of 97 species of insects (Wagner et al. 1996). The contact angle of water on each wing was measured. For each insect, the surface area to body mass index (SM) was measured, where

$$SM = \frac{wing\ surface}{body\ mass^{0.67}}$$

The contact angles measured ranged from 31.6º to 155.5º, and the SM index varied from 2.42 to 57. A positive correlation was found between the SM and CA; as the SM increases, the CA increases.

The wings of each species of insect were contaminated with silica dust and cleaned with artificial fog. After cleaning, the wings were examined with a SEM to determine the amount of particles remaining. In some species of insects, up to 99.59% of the particles were removed, while in other species 100% of the contaminants remained. A negative correlation was found between the SM index and the percentage of contaminants removed during fog cleaning (Wagner et al. 1996).

It is suggested that the insects with small wings, and therefore low SM indexes, are able to reach all parts of their wings with their legs. They are able to clean the the entire surface of their wings and have no need for self cleaning abilities (Wagner et al. 1996). Insects with large wings (and a large SM index) can not clean their entire wings and need the hydrophobic surface to aid in removing contaminants. Without the self-cleaning property, particles which adhere to the wings could affect flight.

Pilot whales have micro- and nano-scale surface features which aid in self cleaning (Baum et al. 2002). Cryo-scanning microscopy (C-SEM) was used to examine the surface structures on the skin of the pilot whale; nano-ridges of 100 nm depth were

found. The C-SEM also revealed that the skin had a very low amount of bio-foulers and other contaminants, considering the contaminant concentration of the pilot whale's environment. The self-cleaning ability of the pilot whale helps to reduce drag and improve hydrodynamics (Baum et al. 2002).

Self-cleaning properties are present on the feet of geckos (Hansen and Autumn 2005). The foot of the gecko is covered with million of setae which branch out into many spatulae. This structure provides dry adhesive abilities. Adhesive forces of the foot were measured while clean and after soiling; up to 60% of the force was lost when the foot was soiled. The gecko's feet were then able to be cleaned with air or a gentle flushing of water. The self-cleaning ability on the feet of the gecko is necessary for maintaining high adhesive forces (Hansen and Autumn 2005).

2.3 Artificial Self-Cleaning Surfaces

2.3.1 Methods of Manufacture

The water repellent and self-cleaning behavior of the lotus plant has inspired much research in fabricating artificial hydrophobic surfaces. Nakajima and coauthors conducted a review of advances in superhydrophobic film technologies (Nakajima et al. 2001). Research on producing hydrophobic films started in the 1950s and again became popular in the 1990s. The 21 methods of producing a hydrophobic film cited in this review can be group into 11 categories: addition of fillers, etching, plasma polymerization, plating with fluoride particles, wax solidification, anode oxidation, solution-precipitation, reaction, chemical vapour deposition, addition of sublimation material, phase separation, and molding.

The addition of a hydrophobic film to a surface limits the contact area of water or other contaminants. Besides the biologically inspired use for self-cleaning, a hydrophobic film can be useful in technological applications in which chemical reactions, bond formation, oxidation or current conduction need to be limited (Nakajima et al. 2001). Hydrophobic films haven even been applied to satellite dishes to reduce the adherence of snow (Nakajima et al. 2001).

One major problem associated with using these hydrophobic films is degradation (Nakajima et al. 2001). When used outdoors, the films can break down and stains begin to form. Another problem of hydrophobic films is a lack of transparency. The addition of surface features can scatter light. Because the visible wavelengths of light are between 400 and 750 nm, it is suggested that the surface features for transparency be less than 100 nm (Nakajima et al. 2001). Only 4 of the 21 methods of producing hydrophobic films result in transparent films.

One method for producing a transparent hydrophobic film was investigated by Nakajima and coauthors (Nakajima et al. 1999). In this method, boehmite or silica is used as the hydrophobic film material. They are sublimated in aluminum acetylacetonate and coated with fluoroalkysilane. This produced surface features in the form of pores which range between 100 and 300 nm, which are acceptable for transparency. The film produced with boehmite had a contact angle of 152.5º, and the film produced with silica had a CA of 150.4º; both films are superhydrophobic.

While these boehmite and silica films addressed the problem of transparency, they still faced the problem of degradation and stain accumulation when left outdoors (Nakajima et al. 1999). This problem was fixed by Nakajima and coauthors (Nakajima et

al. 2000). Titanium dioxide photocatalysts were added to the films in various concentrations; these photocatalysts are able to oxidize organic stains under UV light. Contact angles were measured on surfaces under UV illumination for 800 hours. For small concentrations of titanium dioxide, the surfaces remain superhydrophobic all 800 hours, with contact angles of over 140º for the entire period. The surfaces with superhydrophobic films were also observed under prolonged outdoor exposure. After 1800 hours, the film with 2 wt% titanium dioxide was clean and still had superhydrophobic water contact angles. It is suggested that a superhydrophobic film with such durability could be useful in many technical applications (Nakajima et al. 2000).

Aside from applying a film composed of hydrophobic materials, superhydrophobic surfaces have been produced by structuring or adding roughness to already hydrophobic materials. One such method to rough a surface is with nanostructured templates. Lee and coauthors electrochemically prepared templates of nano-patterned aluminum sheets and of nano-porous aluminum oxide (AAO) (Lee et al. 2004). Once the template is prepared, it is placed on polymeric sheets, heated to approximately 130ºC, and the pattern is transferred. Surfaces features (pores) of both 40 nm and 71 nm were produced from the template. Advancing and receding contacts angles as high as 155.5º and 147.6º, respectively, were produced from this method.

Guo and coauthors also were successful in the development of a template process for producing superhydrophobic surfaces (Guo et al. 2004). In this "template-rolling process," an alumina tube is anodized to produce a surface structure of nanopillar arrays. The alumina tube then is rolled over a polycarbonate sheet at a temperature higher than that of the glass transition temperature of the polycarbonate, and at high pressure.

Because the alumina tube is rolled over the polycarbonate sheet, a template removal step is not necessary, as opposed to other template methods.

In this template rolling process, surface features as small as 30 nm have been produced (Guo et al. 2004). Contact angles were measured for this surface, as well as surfaces produced with larger nanopillars. It was found that increasing nanopillar sizes decreases the contact angle. The maximum CA achieved with this method is 145.6º. This method can be used for large scale areas.

Lasers have also been used to produce microstructured templates to make hydrophobic surfaces. Groenendijk and Meijer investigated using femtosecond pulsed laser ablation on steel to produced a template (Groenendijk and Meijer 2006). This template is also intended to be used to structure polymeric surfaces. In this process, 200 femtosecond pulses are fired at the steel surface, either in one spot, scanning along a line, or scanning in a hatch pattern over the entire surface. During ablation, a "chaotic" roughness appears over the entire ablated area. This roughness depends on various properties of the laser and how many pulses hit one spot. This method successfully produced surface roughness which could be tailored for specific needs by adjusting laser parameters.

Zorba and coauthors used lasers to directly structure the surface of silicon, without a template (Zorba et al. 2006). In this method, laser irradiation produces microscale features on the silicon. Laser pulses of 150 femtoseconds at various fluences (energy densities) are directed at the surfaces. As the fluence of the laser is increased, surface structures change from ripples to cones, with the largest cone produced being 15 micrometers tall. These cones had nanoscale features. It was found that with increasing

laser fluence, the contact angle increased. Contact angles as high as 160º were produced with this method.

Another way to produce a superhydrophobic surface is with carbon nanotubes. Lau and coauthors produced vertically aligned carbon nanotubes using plasma enhanced chemical vapour deposition (PECVD) (Lau et al. 2003). The nanotubes can then be coated with polytetrafluoroethylene (PTFE) through hot filament chemical vapour deposition (HFCVD). The height and diameter of the nanotubes can be controlled in this process, and heights between 2 and 15 micrometers were produced.

The contact angle of water was measured on the coated and uncoated nanotubes or various heights (Lau et al. 2003). Ten to 15 micrometer high uncoated nanotubes are superhydrophobic, with a contact angle of 161º. However, this hydrophobicity does not last, and water will eventually be absorbed into the nanotube forest. The PTFE coated nanotubes are superhydrophobic, with contact angles as high as 170º. Both untreated and treated carbon nanotube forests were subjected to fog. Drops as small as 3 to 4 micrometers beaded up on the surface and were nearly spherical. On the untreated surface, water which has seeped in the nanotube forest will cause the nanotubes to bundle together. Advancing and receding contact angles were measured on surfaces with varying carbon nanotube height. The nanotube height has a large effect on the receding contact angle; taller nanotubes had less contact angle hysteresis.

Li and coauthors used aligned carbon nanotubes (ACNT) to produce a surface which is both hydrophobic and lipophobic (oil repellent) (Li et al. 2001). The nanotubes, grown on glass plates, were 60 nm in diameter and 3 micrometers in length. These as-grown nanotubes were hydrophobic but lipophilic. The nanotubes were oxidized with

sulphuric acid (H_2SO_4) and nitric acid (HNO_3), and water then formed a contact angle of 128º with the nanotubes. The oxidized nanotubes were then treated with fluoroalkylsilane; contact angles of water and oil were then 171 and 161 degrees, respectively. A surface which is both superhydrophobic and superlipophobic, or "amphiphobic," could have many useful industrial applications.

The minimum features sizes of which these methods of producing self-cleaning surfaces are capable are shown in Figure 2.5, for all methods which list a feature size.

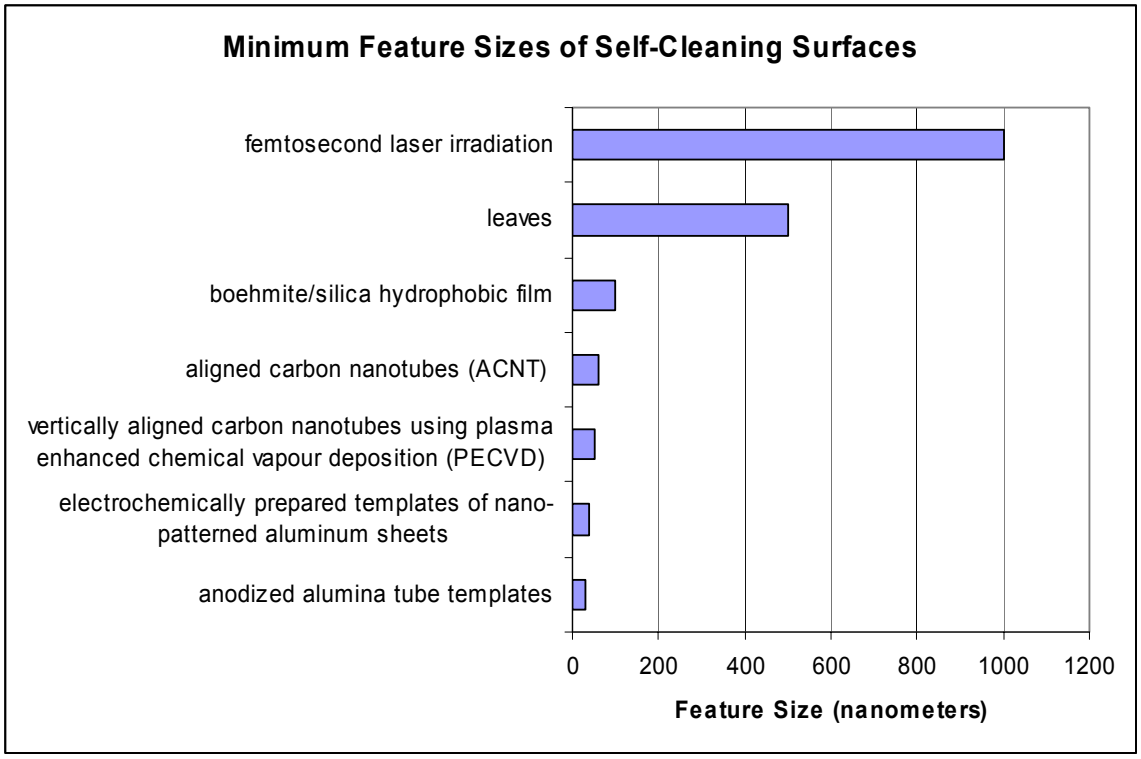

Figure 2.5: Minimum features sizes of self-cleaning surfaces created by various means of production.

The actual cleaning abilities of these artificial self-cleaning surfaces were investigated by Fürstner and Barthlott (Fürstner and Barthlott 2005). The cleaning properties of three types of surfaces were tested: silicon wafers with various surface structures, polymer replicates of hydrophobic leaves made from molds, and metals foils made hydrophobic with fluorinated chemicals. The surfaces were contaminated and then

cleaned with an artificial fog. After the fog cleaning, all surfaces had at least 87% of contaminants removed. In a second experiment, the surfaces were cleaned with an artificial rain. The higher kinetic energy of the rain drops completely cleaned all surfaces. These experiments show that hydrophobic surfaces can be cleaned with water alone.

2.3.2 Commercial Self-Cleaning Products

A number of commercially available products utilize the biologically inspired self-cleaning mechanism. Here are just a few of the current products:

- Procachem Corporation produces an Anti-Graffiti Coating Additive which is hydrophobic (Procachem).
- Nano-X GmbH produces a fabric coating (x-clean®) which uses nanometer sized features to repel water (Nano-X).
- Ecological Coatings, LLC, produces a range of hydrophobic coating products (Ecological Coatings 2008).
- Brombach-Gess GMBH has a marine glass coating called E2C-121 which uses nanoparticles of silicon and titanium to achieve hydrophobicity (Brombach Gess 2007).
- Sandtex® produces a paint which uses self-cleaning to keep the outside of buildings clean (Sandtex 2006).
- Stainmaster® Carpet uses a hydrophobic coating on their carpets to repel dirt (Stainmaster Carpet 2003).
- Erlus AG manufactures clay roof tiles which utilize the Lotus Effect to remain clean (Erlus).

- Eisch Glaskultur makes all of their glass products with the No Drop Effekt®, modeled after the lotus plant (Eisch Glaskultur).
- Schoeller Textiles AG uses 3XDRY®, a lotus inspired technology, to repel water on fabrics (Schoelle Textiles).
- Sto Corp. produces Lotusan paint, another water and dirt repelling paint for buildings (Sto Corp. 2007).
- Nanosphere is a textile coating with the Lotus Effect (Schoelle Textiles). The Nanosphere coating is shown in Figure 2.6.

Figure 2.6: Nanosphere coating prevents wine from wetting fabric (Schoelle Textiles).

These are just a small sample of the commercial self-cleaning products. A list of over 130 self-cleaning technologies, in the forms of research, patents of products, is available from the Biomimicry Guild. The self-cleaning surface appears on metals, glass, plastic, fabrics and many other types of surfaces. Clearly, the self-cleaning mechanism from nature has gained widespread popularity and for more than simply cleaning or for environmental benefits.

2.3.3 Claimed Environmental Benefits

It has been claimed that self-cleaning surfaces will have environmental benefits associated with their use (Thieme et al. 2001; Rickerby and Morrison 2007). Because these surfaces can be successfully cleaned with low intensity methods such as mist or

fog, it would seem that self-cleaning surfaces are a useful technology for sustainable design and manufacture. However, use is just one part of the life cycle. The environmental impact of acquiring the materials and producing the surface must also be taken into account. No publicly available work is available which quantifies the life cycle inventory of producing a self-cleaning surface. Furthermore, no data exists which quantifies the burdens of cleaning these surfaces. For any claims of environmental benefits of self-cleaning surfaces to be valid, the environmental impact of the entire life cycle will need to be lower than that of other methods of cleaning. The environmental impact of self-cleaning surfaces and for industrial cleaning methods will be determined with a life cycle assessment and then compared to each other.

2.4 Industrial Cleaning

Cleaning, "the removal of unwanted matter" (Murphy 2000), is the first step in any treatment of metal. Cleaning is achieved by one of the following mechanisms (Quitmeyer 1995):

- Solubilization – when the contaminants become dissolved in the cleaning solution.
- Emulsification – "Mutually immiscible components" become distributed uniformly in the cleaning solution.
- Wetting – liquids and surface active agents are used to weaken the bonds between the contaminants and the surface.
- Saponification – when fatty acids react with alkalis and produce soaps.
- Sequestration (chelation) – ions of the contaminants are deactiaveted to prevent reactions that created other contaminants, for example soap scum.

- Displacement – force is used to move the contaminants.
- Deflocculation – contaminants are divided into smaller parts which are then removed by the cleaning liquid.

Contaminants can be grouped into six categories (ASM International 1996): pigmented drawing compounds, unpigmented oil and grease, chips and cutting fluids, polishing buffing compounds, rust and scale, miscellaneous surface contaminants, and residue from magnetic particle inspection. Cleaners have three categories: organic solvents, semiaqueous or emulsion cleaners and aqueous based products (Quitmeyer 1995).

Contaminants can form two classes of bonds with the surface: chemical and physical (Kern 1993). When a chemical bond is formed between the contaminant and the surface, it is called chemical absorption or chemisorption. Chemical bonds include ionic, covalent and metallic. When a chemical bond is formed, rinsing or solvents may not be enough to remove the contaminant. Physical absorption occurs when intermolecular forces occur between the contaminants and the surface, such as dipole-dipole or London dispersion forces. Aqueous cleaning is very suitable for removing physically absorbed contaminants, because hydrogen bonds from the cleaning solution are stronger the intermolecular forces holding the contaminants on the surface. Gravity and electrostatic forces may also hold contaminants on a surface.

2.4.1 Solvent Cleaning

Solvent cleaning is "the dissolution of contaminants by an organic solvent" (ASM International 1996). Solvent cleaning is used to remove oils and greases. There are eight main methods of solvent cleaning (ASM International 1996):

- Static immersion
- Immersion with agitation of parts
- Immersion with agitation of both the solvent and the parts
- Immersion with scrubbing
- Pressure spraying in a spray booth
- Immersion scrubbing, followed by spraying
- Multistage washing
- Hand application with wiper

Solvent cleaning is achieved through the chemical action of the solvent, and not with mechanical force such as agitation (Pacific Northwest Pollution Prevention Resource Center 1996). Methyl chloroform and CFC-113 were the most commonly used solvents in the metal cleaning industry in the 1980s, with most solvent cleaning being done in the Fabricated Metal Product Manufacturing sector (US EPA 2004). Methyl chloroform was slowly replaced by chlorinated solvents, such as perchloroethylene (PCE), trichloroethylene (TCE), and methylene chloride (MC), in the metal cleaning industry (US EPA 2004). These chlorinated solvents, however, have health, safety and environmental problems, and demand for these solvents dropped.

In the 1990s, solvent cleaning began to replaced by aqueous based cleaning due to environmental concerns, specifically the ozone depleting nature of many of the solvents (US EPA 2004). Some manufacturers were unsatisfied with the results of aqueous cleaning and have switched back to solvent based cleaning. Of users in the metal cleaning industry who previously used ozone depleting solvents, 66% currently employ solvent based cleaning, while 25% use aqueous cleaning (US EPA 2004). In the solvent

cleaning sector, chlorinated solvents are the most popular, with tricholoethylene being used most frequently (US EPA 2004).

2.4.2 Semi Aqueous Cleaning

Semi-aqueous cleaning is another cleaning method which has started to replace solvent and vapor degreasing (Pacific Northwest Pollution Prevention Resource Center 1996). In this method, a cleaning solution, typically a combination of hydrocarbons and surfactants, is used to clean a part, and then the part is rinsed in water. Although this method consumes less water than aqueous cleaning, equipment costs are higher, and this method has not gained popularity in the U.S. metal cleaning industry.

2.4.3 Aqueous Cleaning

An aqueous cleaning system can be defined as a system which uses a cleaning solution that is at least 95% water (Pacific Northwest Pollution Prevention Resource Center 1996). Aqueous cleaning began replacing solvent vapor degreasing in the early 1990s (US EPA 2004).

Aqueous cleaners can utilize any of the seven cleaning mechanisms mentioned above (Quitmeyer 1995). The type of cleaning solution and contaminant determine which mechanism is used.

The following components usually make up aqueous cleaners (Quitmeyer 1995):

- alkalinity builders
- water conditioners, used to deactivate ions and prevent reactions in the cleaning solutions
- surface active agents (surfactants), used to reduce surface tensions

- corrosion inhibitors, sometimes found in alkaline cleaners

Other components are added to change the appearance or smell of the cleaner, such as in the use of fragrances or dyes. Deionized water is often used in place of tap water to prevent contaminants from salts in the water (Quitmeyer 1995).

Aqueous cleaning can have stages of washing, water rinsing and drying. This is more complex than the solvent cleaning methods they often replace, due to increased number of stages (US EPA 2004). Drying is an important step; if all of the cleaning solution is not removed, problems of rust, corrosion or contamination of other cleaning or rinsing fluids can occur (Pacific Northwest Pollution Prevention Resource Center 1996).

Temperature is an important factor of the effectiveness of aqueous cleaning (Kern 1993). Raising the temperature of the cleaning solution will cause reactions to occur faster. Generally, raising the temperature will also raise the solubility of the contaminants, which means cleaning will occur faster (Kern 1993). Cleaning time, concentration of the cleaning solution, and amount of mechanical action also affect the cleaning efficiency (Quitmeyer 1995).

Aqueous cleaning is not without disadvantages. Large volumes of water are used during cleaning, and after cleaning, the resulting waste water must be treated (US EPA 2004). Because the aqueous cleaning solution is not as effective as the ozone depleting solvents it has replaced, additional mechanical force is needed to remove contaminants, through agitation or ultrasonic cleaning (U.S. EPA 2004). Rinsing and drying are now added to the process, which consumes more energy (US EPA 2004).

There are a variety of aqueous cleaning systems, including immersion cleaning, spray washing, and ultrasonic cleaning. Spray cleaning is the most often used cleaning

system in manufacturing (Pacific Northwest Pollution Prevention Resource Center 1996). Immersion and spray cleaning are the two most commonly used methods to clean metal (Murphy 2000).

2.4.3.1 Immersion Cleaning

Immersion cleaning is placing the part to be cleaned in a solution of water and cleaner and allowing it to sit for a period of time. Immersion cleaning may also include recirculating the cleaner, electrocleaning or ultrasonic cleaning. Immersion cleaning is also called soak cleaning (Murphy 2000). Immersion cleaning can be both the simplest and least expensive (equipment wise) method of cleaning. A typical immersion cleaning process has a cleaner concentration of 75 g/L, a solution temperature of 77ºC and a run time of 5 minutes (Murphy 2000). Typically, high pH detergents will be used in immersion cleaning (Durkee 2002).

Immersion cleaning should be used for parts where spray cleaning cannot reach all surfaces, such as tubing or other complicated geometries, and it should be used for dried or rusty soils (Durkee 2002). One common type of industrial immersion cleaning is a belt conveyor machine; pins hold the parts to be cleaned on a conveyor belt which is run through an immersion tank (Durkee 2002). Belt conveyor machines have maximum belt velocities between 5 and 10 ft/min. Commonly, belts are 12 in wide; the belt then flows between 5 to 10 ft^2/min (Durkee 2002).

2.4.3.2 Electrocleaning

Electrocleaning is a type of immersion cleaning. In electrocleaning, similar cleaners to those of immersion cleaning are used, although they are altered to produce less foam (Murphy 2000). A direct current is produced in the cleaner bath, with the tank

carrying a negative charge and the part carrying a positive charge. Oxygen bubbles at the surface of the part then help to remove contaminants. The part may first be cleaned with a spray or immersion cleaning to remove most of the contaminants. The concentration of the cleaner is the water is slightly high, at 75 – 120 g/L and the solution is usually heated to 77-99ºC. The current used in cleaning falls in the range of 27 to 160 mA/cm^2 (Murphy 2000).

2.4.3.3 Spray Cleaning

Belt conveyors, described above, can also be configured to clean parts with spray only and no immersion step (Durkee 2002). Another common spray cleaning machine is the cabinet spray washer. In this machine, nozzles which produce flat or sheet sprays of cleaning solution are set to hit the part from all directions, while the part rests on a turntable and is rotated to ensure the entire surface is sprayed (Durkee 2002). Because parts are not soaked and only sprayed, mechanical force is the main mechanism to remove contaminants. Cabinet spray washers are advantageous because they do not require as much floor space as belt conveyor machines (Durkee 2002). The belt conveyor machines are often used to clean a series of small parts, while the cabinet spray washer is suitable for large parts (Pacific Northwest Pollution Prevention Resource Center 1996).

When performing spray cleaning, the cleaning solution is typically pressurized to 70-275 kPa, and the cleaning solution concentration falls in the range of 4 – 30 g/L. The cleaning solution will be heated to anywhere between 21 and 88 degrees C (Murphy 2000). Cleaning time in a cabinet spray machine ranges from 1 to 10 minutes, and typically, neutral pH detergents will be used (Durkee 2002). In a spray cabinet machine,

one must be concerned with reinfection – soil from dirty parts being sprayed onto clean parts (Durkee 2002).

2.4.3.4 Ultrasonic Cleaning

Ultrasonic cleaning is a method in which sound waves travel though the cleaning solution to create bubbles. These bubbles act as "scrubbers" and remove contaminants stuck to the parts. It is considered an efficient method of cleaning and is applicable for parts with complicated surfaces, which cannot all be reached by traditional sprayers (ASM International 1996). In ultrasonic cleaning, the same typical concentration of cleaner for immersion cleaning is used. Less cleaning time is need due to the added agitation of the bubbles (Murphy 2000).

Ultrasonic cleaning is not often used for large parts due to the high amount of energy needed to produce the sound waves for cleaning (Pacific Northwest Pollution Prevention Resource Center 1996).

2.5 Summary

As discussed in Section 2.3, self-cleaning surfaces are gaining popularity, with many commercial products available and many new technologies for their manufacture being developed. Environmental benefits are claimed for their use, as they have potential water and energy savings. However, the resources of producing the self-cleaning surfaces have not been considered in any published literature.

Common industrial cleaning methods have been reviewed, and it is shown that these processes have had many environmentally related problems. Solvents commonly used in cleaning have negative impacts on the environment, and many solvents have been phased out and banned. More environmentally friendly solvents used as replacements

have been found to be less effective, and many industries have reverted back to more harmful solvents.

Self-cleaning surfaces represent a possible solution to these problems with the cleaning industry. Self-cleaning surfaces could remove the need for any sort of solvent or detergent in cleaning, as they can be successfully cleaned with water alone. Before the use of self-cleaning surfaces become any more widespread, it should be determined if the burdens of manufacturing them outweigh the benefits gained from avoiding solvents or detergents. A life cycle assessment will help to determine if the claim of environmental benefits of self-cleaning surfaces are justified.

CHAPTER 3

MODELING ENVIRONMENTAL IMPACTS OF CHEMICAL SELF-CLEANING COATING

Although many of the researchers responsible for the self-cleaning surfaces discussed in Chapter 2 claim potential environmental benefits in the use of their technologies**,** no scientific data exists which quantifies the benefits of use or the burdens of production. Production burdens may outweigh benefits of use, if these hydrophobic surfaces consume large amounts of resources, produce emissions, or use toxic materials. Several of these self-cleaning technologies use nanomaterials, which have possible negative impacts on the environment and human health. For example, nanoparticles of titanium dioxide, which are used in some self-cleaning coatings (Nakajima et al. 2000), are more toxic than the same mass of larger diameter particles (Oberdörster 2005).

To fully quantify the environmental benefits of using a self-cleaning surface, one must consider both the benefits associated with cleaning the surface and the burdens associated with producing the surface. This will be determined by performing a Life Cycle Assessment (LCA) of the self-cleaning surface.

3.1 Goal and Scope of LCA

The ultimate goal of this study is to compare the life cycle of self-cleaning surfaces to more conventional methods of cleaning a surface. This includes the materials acquisition, production, use and disposal phases of the self-cleaning surface, as compared

to the use, in this case cleaning, phase of a non-self cleaning surface. This research will focus on the life cycle of three different self-cleaning surfaces and the life cycle of spray and ultrasonic aqueous cleaning methods.

The **functional unit** for this study is 1 m^2 of a surface. The size has been selected as a representative surface area which can be easily scaled. In this project, the materials acquisition, manufacture and use of a self-cleaning surface will be considered as the scope of the study.

A chemical self-cleaning coating (Nakajima et al. 2000) has been selected as one self-cleaning technology to be analyzed. This particular method of production has been selected for a few reasons:

- Data are available about the lifetime of the coating.
- Coatings can be used on many surfaces (plastics, metals, etc.).
- A similar self-cleaning coating is available to be used for experimentation

For all three methods of producing a self-cleaning surface, only the actual self-cleaning surface will be considered. This means that the material on which the self-cleaning surface is applied will not be considered. This system boundary has been selected because the self-cleaning surface can be used on a variety of different parts and materials.

3.2 Data Collection

3.2.1 Data Sources

Information about chemical reactions, process and toxicities were obtained from the following sources:

- Kirk-Othmer Encyclopedia of Chemical Technology
- Hawley's Condensed Chemical Dictionary, 14th edition

Life cycle inventory data was collected from:

- SimaPro 7.1 Software – EcoInvent Database.
- National Renewable Energy Laboratory (NREL) U.S. Life-Cycle Inventory Database
- Scientific journals

3.3 Chemical Components of Self-Cleaning Coating

The self-cleaning coating under assessment is produced with 5 main chemicals (Nakajima et al. 2000):

- Titanium Acetylacetonate ($TiO(C_5H_7O_2)_2$), abbreviated TACA
- Aluminum Acetylacetonate ($Al(C_5H_7O_2)_3$), abbreviated AACA
- Boehmite (AlOOH)
- Ethanol (C_2H_5OH)
- (Heptadecafluorodecyl)trimethoxysilane - a water repellent agent

Because information is not readily available about complex compounds such as titanium acetylacetonate and aluminum acetylacetonate, information must be gathered about how these chemicals are made. The individual chemical components used to produce these chemicals must be traced back to components which come from natural resources, such as those mined from ores, or at least as far back as to reactants for which life cycle inventory data are available.

3.3.1 Titanium Acetylacetonate

Titanium acetylacetonate is a product of the reaction of titanium oxychloride ($TiOCl_2$), acetylacetone ($C_5H_8O_2$) and sodium carbonate (Na_2CO_3) (Lewis 2002).

$$TiOCl_2 + 2C_5H_8O_2 + Na_2CO_3 \rightarrow TiO(C_5H_7O_2)_2 + 2NaCl + H_2CO_3$$

The life cycle process of titanium acetylacetonate production is shown in Figure 3.1.

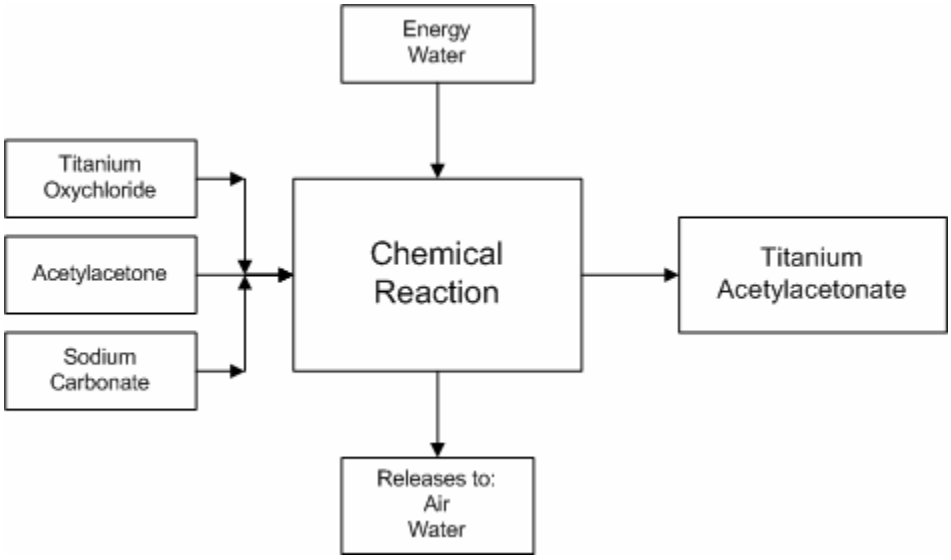

Figure 3.1: Unit process to produce titanium acetylacetonate.

The life cycle inventory data of both titanium oxychloride and acetylacetone will be determined by estimating resource consumption and emissions of previous chemical reactions. Sodium carbonate, or soda ash, is a mined material for which life cycle data are available; the life cycle inventory data for sodium carbonate is obtained from the Ecoinvent database (Althaus et al. 2004). The total life cycle inventory data for titanium acetylacetonate will be determined by making further assumptions about the resource consumption and emissions associated with the reaction of titanium oxychloride, acetylacetone and sodium carbonate.

Titanium oxychloride is formed in a reaction between titanium chloride ($TiCl_4$) and water (Fisher and Egerton 2001).

$$TiCl_4 + H_2O \rightarrow TiOCl_2 + 2HCl$$

The life cycle unit process diagram of the production of titanium oxychloride is shown in Figure 3.2.

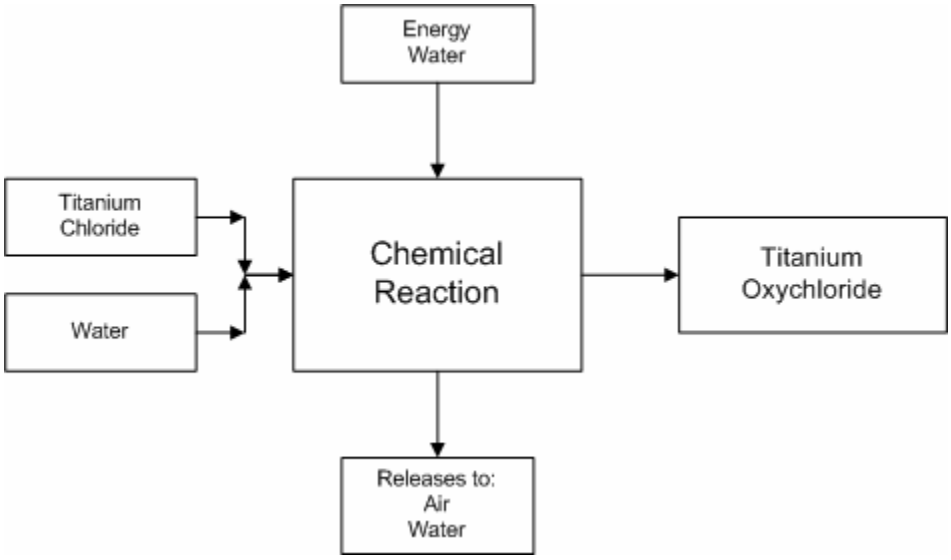

Figure 3.2: Unit process to produce titanium oxychloride.

The life cycle inventory data for titanium chloride will be determined by making assumptions about the resource consumption and emissions of the previous reaction. Assumptions will need to be made about the reaction of titanium chloride and water, in order to determine a life cycle inventory data set for titanium oxychloride.

A reaction of rutile (TiO_2), chlorine (Cl_2) and carbon produces titanium chloride in the following reaction: (Fisher and Egerton 2001):

$$TiO_2 + 2Cl_2 + 2C \rightarrow TiCl_4 + 2CO$$

The unit process of the production of titanium chloride is shown in Figure 3.3.

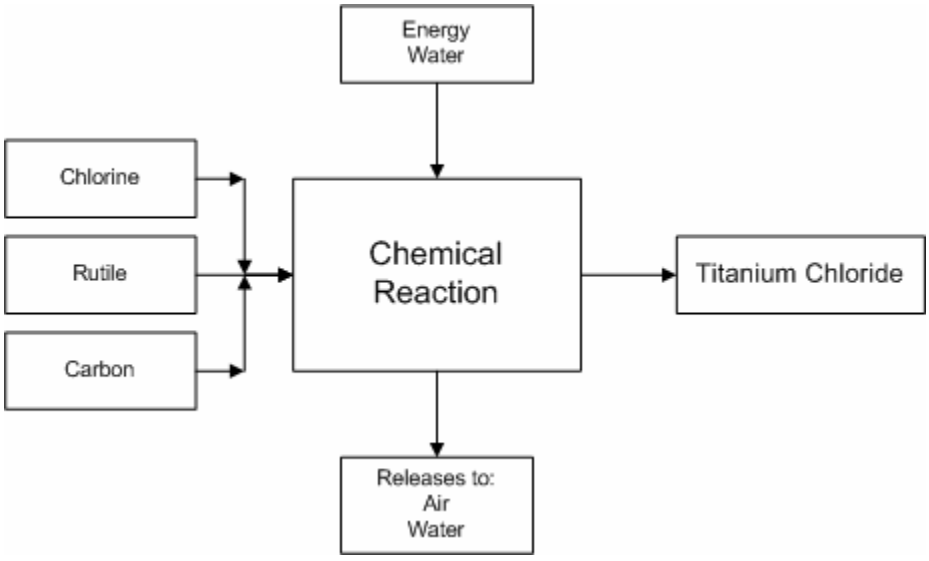

Figure 3.3: Unit process to produce titanium chloride.

Rutile is a mined material, carbon comes from mined natural resources and chlorine is produced as a co-product, along with caustic soda, from brine. Chlorine, rutile (titanium dioxide) and carbon life cycle inventory data are all obtained from the Ecoinvent database (Althaus et al. 2004). Assumptions will need to be made about the resource consumption and emissions associated with the reaction of these three chemicals to form titanium chloride.

Acetylacetone ($C_5H_8O_2$) is rearranged from isopropenyl acetate with a catalyst. Isopropenyl acetate is formed from the reaction of acetone ($CH_3C(O)CH_3$) and acetic anhydride ($(CH_3CO)_2O$) (Wagner 2002).

$$(CH_3CO)_2O + CH_3C(O)CH_3 \rightarrow C_5H_8O_2$$

The life cycle unit process diagram of acetylacetone production is shown in Figure 3.4.

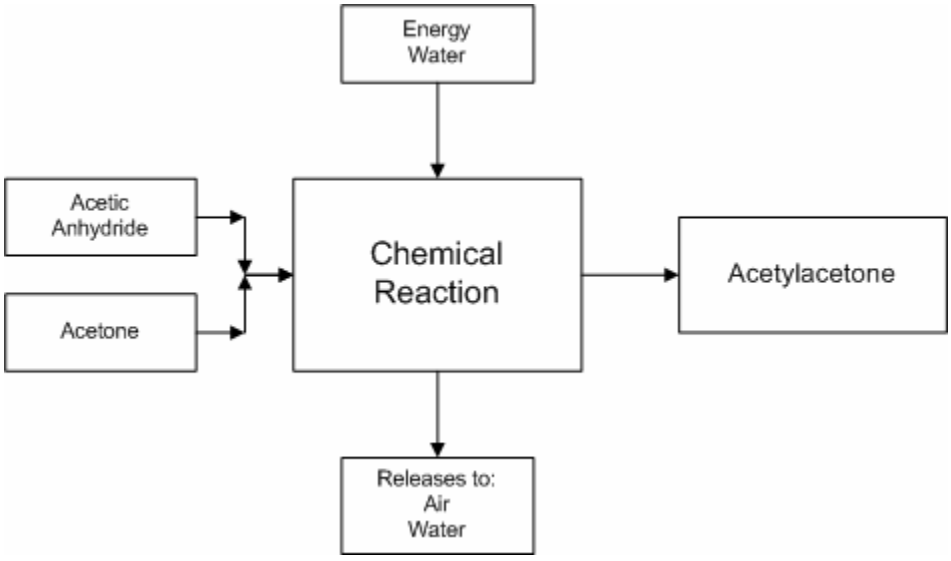

Figure 3.4: Unit process to produce acetylacetone.

Life cycle inventory data for both acetic anhydride and acetone are available from the Ecoinvent database (Althaus et al. 2004). Assumptions will need to be made about the reaction of these two chemicals, to determine the resource consumption and emissions of forming acetylacetone.

The chemicals necessary to produce titanium acetylacetonate are summarized in Figure 3.5.

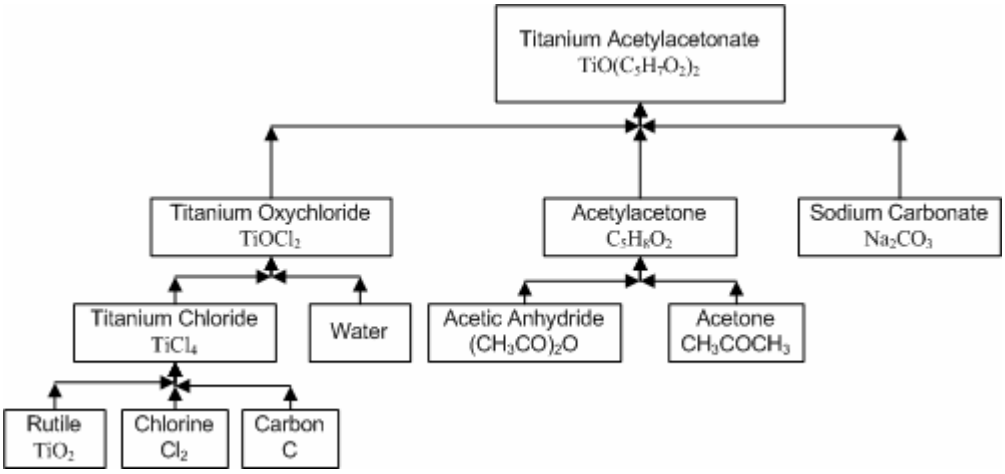

Figure 3.5: Chemical Components of Titanium Acetylacetonate.

3.3.2 Aluminum Acetylacetonate

Aluminum acetylacetonate can be produced by a reaction of aluminum sulphate ($Al_2(SO_4)_3$*nH_2O) and acetylacetone (Katakura and Koide 2005).

$$6C_5H_8O_2 + Al_2(SO_4)_3*17H_2O \rightarrow 2Al(C_5H_7O_2)_3 + 3H_2SO_4 + 17H_2O$$

Life cycle inventory data for aluminum sulphate is obtained from the EcoInvent database (Althaus et al. 2004), and acetylacetone data will be obtained as described above.

The chemicals necessary to produce aluminum acetylacetonate are summarized in Figure 3.6.

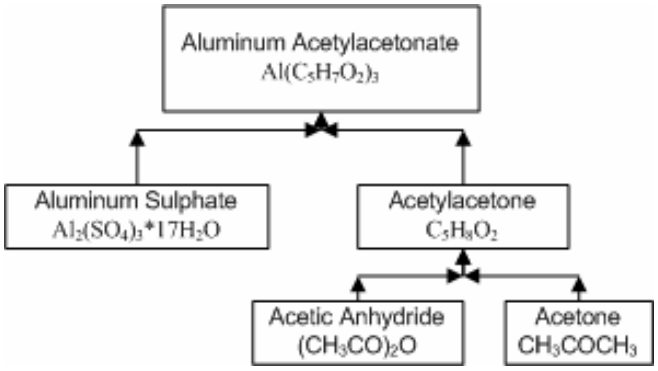

Figure 3.6: Chemical components of aluminum acetylacetonate.

3.3.4 Ethanol

Life cycle inventory data for the production of ethanol was obtained from (Kim and Dale 2005). Kim and Dale first considered the growth and harvest of the corn; the energy and emissions of the production of corn are shown in Table 3.1.

Table 3.1: Energy consumption and emissions from the production of 1 kg of corn.

Production of 1 kg of Corn		
Energy	1.4	MJ
Water	unknown	m^3
CO_2	-0.222	kg
CH_4	0	kg
N_2O	0.0988	kg
Total Emissions	unknown	kg

They next considered the production of one kilogram of ethanol. The energy and emissions of the production of ethanol are shown in Table 3.2 (Kim and Dale 2005).

Table 3.2: Energy and emission from production of ethanol from corn

Production of 1 kg of Ethanol		
Energy	16.1	MJ
Water	unknown	m^3
CO_2	0.914	kg
Total Emissions	unknown	kg

For this scenario, 3.26 kg of corn is required to produce 1 kg of ethanol (Kim and Dale 2005). Water consumption is reported as 38-46 kg of water per kg of ethanol produced (Patzek 2004). An average value of 0.042 m^3 of water per kg of ethanol produced will be used in this inventory. The total resource consumption and emissions of producing 3.26 kg of corn and then producing 1 kg of ethanol is shown in Table 3.3.

Table 3.3: Total energy consumption and emissions for ethanol production.

Production of 1 kg of Ethanol and corn		
Energy	20.664	MJ
Water	0.042	m^3
CO_2	0.248	kg
N_2O	0.322088	kg
Total Emissions	unknown	kg

3.3.5 Water Repellent Chemical

The particular water repellent chemical used is a methanol solution of (heptadecafluorodecyl)trimethoxysilane ($CF_3(CF_2)_7CH_2CH_2Si(OCH_3)_3$) (Nakajima et al. 2000). This water repellent chemical is a fluorosilicone, which indicates it is resistant to oil while having high resilience (Romenesko et al. 2005). This chemical is also called (1H,1H,2H,2H-heptadecafluorodecyl)trimethoxysilane. The water repellent chemical is produced with the following chemicals (Yoshino et al. 1993):

- trichlorosilane – $HSiCl_3$
- methanolic 0.1M hydrogen hexachloroplatinate (also called chloroplatinic acid) – H_2PtCl_6
- methanolic 3.6M sodium methoxide – $Na(CH_3O)$
- 1H,1H,2H-heptadecafluoro-1-decene – $C_{10}H_3F_{17}$

To produce the water repellent chemical, 25grams of trichlorosilane, 67.2 grams of 1H,1H,2H-heptadecafluoro-1-decene and 0.20cm^3 of chloroplatinic acid are combined and heated to 100ºC for 70 hours (Yoshino et al. 1993). After performing fractional distillation, a product of trichloro(1H,1H,2H,2H-henicosafluorododecylsilane) is formed. From this product, 35 grams are added to 30 cm^3 of 1,1,2-trichloro-1,2,2-trifluoroethane and then mixed with 65.0cm^3 sodium methoxide solution (Yoshino et al. 1993).

(Heptadecafluorodecyl)trimethoxysilane is then obtained by fractional distillation, with a yield of 59.4%. For this yield, a total of 20.37g is produced (Yoshino et al. 1993). The process is scaled up for the production of 1kg of (Heptadecafluorodecyl)trimethoxysilane and is shown in Figure 3.7.

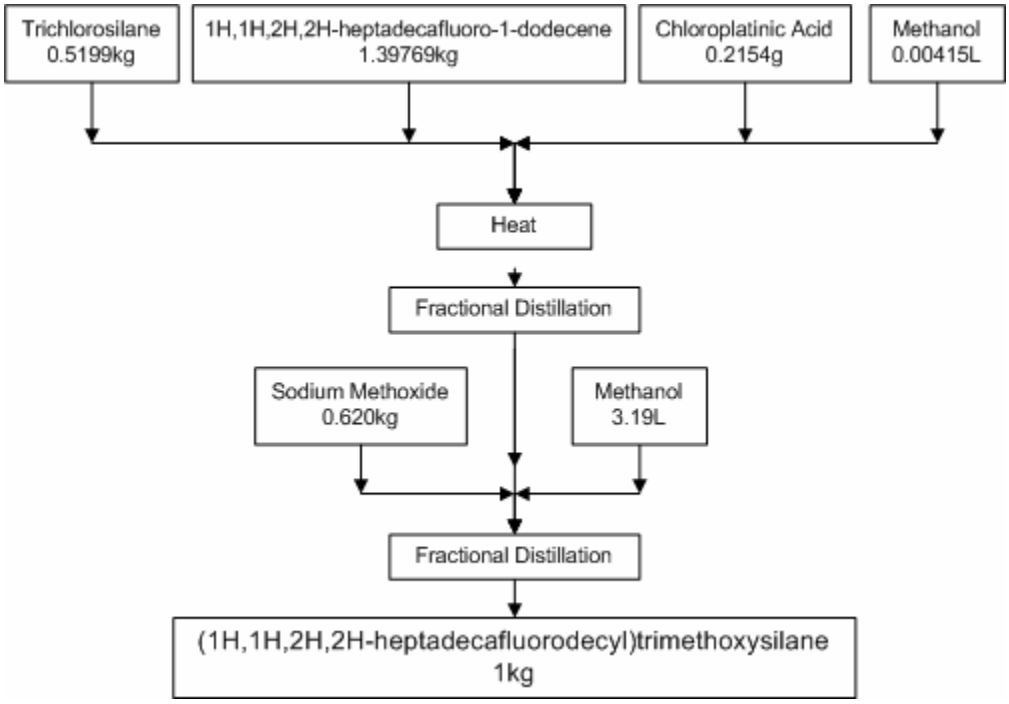

Figure 3.7: Process to produce (Heptadecafluorodecyl)trimethoxysilane.

The chemical reaction that occurs is shown in Figure 3.8 (Yoshino et al. 1993).

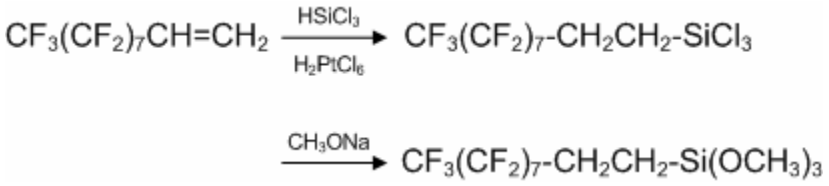

Figure 3.8: Chemical reaction which produces the water repellent chemical.

1H,1H,2H-heptadecafluro-1-decene ($C_{10}H_3F_{17}$), the main chemical used in the production of the water repellent chemical, is produced in a reaction of iodoperfluorooctane and ethylene, with a base reaction to remove HI:

$C_8F_{17}I + C_2H_4 \rightarrow C_{10}H_4F_{17}I$

$\rightarrow C_{10}H_3F_{17} + HI$

Life cycle inventory data for ethylene is obtained from the EcoInvent database (Althaus et al. 2004).

Iodoperfluorooctane is produced in a reaction of pentafluoroethyl iodide and tetrafluoroethylene (Smart and Fernandez 2000):

$$CF_3CF_2I + 3C_2F_4 \rightarrow C_8F_{17}I$$

Pentafluoroethyl iodide is produced with tetrafluoroethylene, iodine pentafluoride and iodine (Smart and Fernandez 2000):

$$5C_2F_4 + IF_5 + 2I_2 \rightarrow 5CF_3CF_2I$$

Iodine pentafluoride is produced with iodine and fluorine (Bailey and Woytek 2004):

$$I_2 + 5F_5 \rightarrow 2IF_5$$

Life cycle data are obtained for both iodine and fluorine (Althaus et al. 2004). The chemicals needed to produce 1H,1H,2H-heptadecafluro-1-decene are summarized in Figure 3.9.

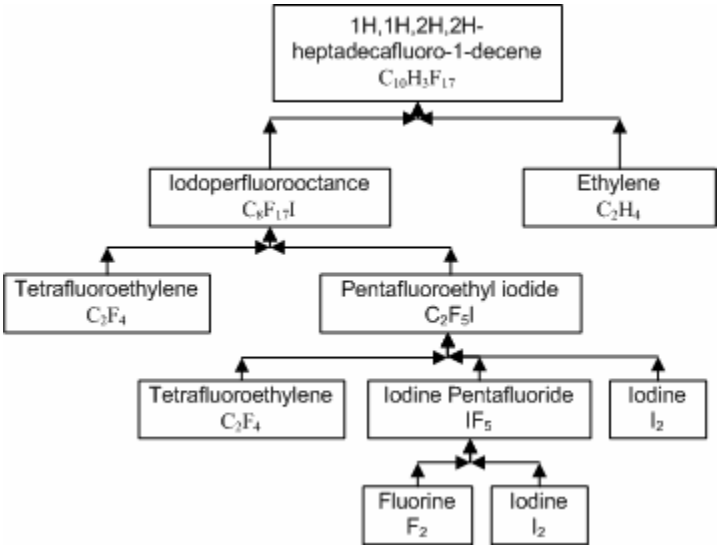

Figure 3.9: Chemicals used in the production of 1H,1H,2H-heptadecafluro-1-decene.

Life cycle inventory data are also needed for the three catalysts. Trichlorosilane is produced in a reaction of silicon and hydrochloric acid (Arkles 2000):

$$Si + 3HCl \rightarrow HSiCl_3 + H_2$$

Gate to gate life cycle inventory data are obtained for trichlorosilane (Overcash 2008), and cradle to gate data are obtained for both silicon and hydrochloric acid (Althaus et al. 2004).

Chloroplatinic acid is produced in a reaction of platinum, nitric acid and hydrochloric acid (Lewis 2002):

$$Pt + 4HNO_3 + 6HCl \rightarrow H_2PtCl_6 + 4NO_2 + 4H_2O$$

Gate to gate life cycle inventory data are obtained for chloroplatinic acid (Overcash 2008), and cradle to gate life cycle inventory data are obtained for platinum (Overcash 2008), nitric acid and hydrochloric acid (Althaus et al. 2004).

Sodium methoxide, CH_3ONa, is created in a reaction between sodium chloride and methanol (Horn and Horns 2000):

$$2CH_3OH + 2NaCl \text{ -> } Cl_2 + H_2 + 2NaOCH_3$$

Gate to gate life cycle data are obtained for sodium methoxide (Overcash 2008). Life cycle data for the production of methanol and sodium are taken from the EcoInvent database (Althaus et al. 2004).

3.3.6 Masses of Chemicals

The mass ratios of the main chemicals used in this coating were given: boehmite, aluminum acetylacetonate, and titanium acetylacetonate to ethanol as 0.0024, 0.024 and 0.0002, respectively (Nakajima et al. 2000). A spreadsheet was created to determine the masses of each of these chemicals, as well as the chemicals which make up aluminum acetylacetonate and titanium acetylacetonate, for a given total mass of coating. The

reactants of equations for which no LCI data were available were multiplied by 1.05263 (1/95%) to account for the assumption of 95% yield in the reaction.

Experimentation gives a rough estimate of 0.125 kg of coating to completely cover 1 m^2 of surface. Because the surface is coated five times (Nakajima et al. 2000), a total of approximately 0.60 kg of coating will be used. The chemicals and their masses for 0.60 kg of coating material are shown in Table 3.4.

Table 3.4: Masses of chemicals needed to produce 0.60kg of self-cleaning coating.

Chemical Name	Molecular Formula	Mass (g)
Titanium Acetylacetonate	$TiO(C_5H_7O_2)_2$	0.113
Titanium Oxychloride	$TiOCl_2$	0.0610
Titanium Chloride	$TiCl_4$	0.0903
Rutile	TiO_2	0.0400
Chlorine	Cl_2	0.0710
Carbon	C	0.0120
Water	H_2O	0.00857
Acetylacetone	$C_5H_8O_2$	0.0905
Acetone	CH_3COCH_3	0.0553
Acetic Anhydride	$C_4H_6O_3$	0.0972
Sodium Carbonate	Na_2CO_3	0.0479
Aluminum Acetylacetonate	$Al(C_5H_7O_2)_3$	13.6
Aluminum Sulphate	$Al_2(SO_4)_3*17H_2O$	14.3
Acetylacetone	$C_5H_8O_2$	13.2
Acetone	CH_3COCH_3	8.08
Acetic Anhydride	$C_4H_6O_3$	14.2
Boehmite	AlOOH	1.36
Ethanol	C_2H_5OH	565

It is assumed that a larger mass of the water repellent will be used for one coating, than for each of the coatings of the chemicals above, because the surface to be coated is submerged in the solution (Nakajima et al. 2000). For this reason, 0.25kg of the water repellent solution will be included in the inventory. The water repellent chemical is

hydrolyzed with a 3 fold molar excess of water (Yoshino et al. 1993). Converted to a mass basis, this means that for every kilogram of the water/water repellent solution, approximately 988.9 g will be water, and 11.1 g will be the water repellent chemical. The masses of the chemicals used for the water repellent solution are shown in Table 3.5.

Table 3.5: Masses of chemicals used in water repellent chemical solution.

Hydrophobic Coating with FAS			
Total mass of covering		0.25	kg
Total mass of water	H_2O	0.247232	kg
Total mass of FAS	$CF_3(CF_2)_7CH_2CH_2Si(OCH_3)_3$	0.002768	kg
Sodium Methoxide	CH_3ONa	0.001716	kg
Methanol	CH_3OH	0.001031	kg
Sodium Chloride	NaCl	0.001819	kg
Methanol	CH_3OH	0.008831	L
Trichlorosilane	$HSiCl_3$	0.001439	kg
Silicon	Si	0.000822	kg
Hydrochloric acid	HCl	0.003589	kg
Chloroplatinic acid	H_2PtCl_6	5.96E-06	kg
Platinum	Pt	2.99E-06	kg
Nitric acid	HNO_3	3.86E-06	kg
Hydrochloric acid	HCl	2.17E-06	kg
Methanol	CH_3OH	1.15E-05	L
1H,1H,2H,2H-heptadecafluoro-1-decene	$C_{10}H_3F_{17}$	0.003869	kg
Ethylene	C_2H_4	0.000256	kg
Iodoperfluorooctane	$C_8F_{17}I$	0.004985	kg
Tetrafluoroethylene	C_2F_4	0.002886	kg
Pentafluoroethyl Iodide	C_2F_5I	0.002361	kg
Tetrafluoroethylene	C_2F_4	0.001012	kg
Iodine	I_2	0.001027	kg
Iodine Pentafluoride	IF_5	0.000447	kg
Iodine	I_2	0.00041	kg
Fluorine	F_2	6.12E-05	kg

3.4 Compiling Life Cycle Inventory Data for Chemicals

Although many data are available about the production of these chemicals, only energy consumption, water consumption, greenhouse gases (carbon dioxide, methane and nitrous oxide), and air, water and soil emissions were recorded from the databases. The

water consumption included in the total life cycle inventory represents the amount of water throughput in each life cycle stage. The water has the potential to be recycled and reused after being included in the inventory.

For the case of life cycle inventory data obtained from the EcoInvent database, a total energy consumption is not given. Instead, masses of fuel used are given. Energy consumed was determined by summing the energy content of inputs such as coal, natural gas, crude oil and uranium. The following energy content values were used (PRé Consultants 1996):

- Coal, Brown (Lignite) - $8\frac{MJ}{kg}$
- Coal, Hard (Anthracite)- $18\frac{MJ}{kg}$
- Natural Gas - $36.6\frac{MJ}{m^3}$
- Oil, Crude - $42.6\frac{MJ}{kg}$
- Uranium - $451\frac{GJ}{kg}$

These fuel sources emit greenhouse gasses when combusted, which are not otherwise included in the life cycle inventory data of the EcoInvent database. The amount of carbon dioxide emitted for the combustion of natural gas is $0.120\frac{lb\,CO_2}{ft^3}$ (US EPA 1995). Converted to SI units,

$$0.120\frac{lb\,CO_2}{ft^3}\cdot\frac{0.45339kg\,CO_2}{lb\,CO_2}\cdot\frac{1ft^3}{0.2083m^3}=1.92\frac{kg\,CO_2}{m^3}$$

The methane emissions for combustion of natural gas are $\frac{2.3 lb\, CH_4}{10^6\, scf}$ (US EPA 1995), converted to SI units:

$$\frac{2.3 lb\, CH_4}{10^6\, scf} \cdot \frac{16 \frac{kg\, CH_4}{10^6\, m^3}}{\frac{lb\, CH_4}{10^6\, scf}} = 3.68 \times 10^{-5} \frac{kg\, CH_4}{m^3}$$

The emissions factor of lignite, also called brown coal is given as $2991.33 \frac{lb\, CO_2}{short\ ton}$ (EIA). Converted to SI units, the emission factor is:

$$2991.33 \frac{lb\, CO_2}{short\ ton} \cdot \frac{0.45359 kg\, CO_2}{lb\, CO_2} \cdot \frac{short\ ton}{0.9072 metric\ ton} \cdot \frac{metric\ ton}{1000 kg} = 1.50 \frac{kg\, CO_2}{kg\, coal}$$

The emissions factor of anthracite, also called hard coal, is given as $5675.29 \frac{lb\, CO_2}{short\ ton}$ (EIA). Converted to SI units, the emission factor is:

$$5675.29 \frac{lb\, CO_2}{short\ ton} \cdot \frac{0.45359 kg\, CO_2}{lb\, CO_2} \cdot \frac{short\ ton}{0.9072 metric\ ton} \cdot \frac{metric\ ton}{1000 kg} = 2.84 \frac{kg\, CO_2}{kg\, coal}$$

The methane emissions of coal are $1.54 \frac{g\, CH_4}{kWh}$ (Govetto 2008). Converted to a mass basis, the emissions of lignite coal are:

$$1.54 \frac{g\, CH_4}{kWh} \cdot \frac{kg\, CH_4}{1000 g\, CH_4} \cdot \frac{kWh}{3.6 MJ} \cdot 8 \frac{MJ}{kg} = 0.0034 \frac{kg\, CH_4}{kg\, coal}$$

The methane emissions of anthracite coal are:

$$1.54 \frac{g\, CH_4}{kWh} \cdot \frac{kg\, CH_4}{1000 g\, CH_4} \cdot \frac{kWh}{3.6 MJ} \cdot 18 \frac{MJ}{kg} = 0.0077 \frac{kg\, CH_4}{kg\, coal}$$

Nitrous oxide emissions of combusting coal are $0.0052\frac{g\,N_2O}{kWh}$ (Govetto 2008).

Converted to a mass basis, the nitrous oxide emissions of lignite coal are:

$$0.0052\frac{g\,N_2O}{kWh}\cdot\frac{kg\,N_2O}{1000g\,N_2O}\cdot\frac{kWh}{3.6MJ}\cdot 8\frac{MJ}{kg}=1.16\times10^{-5}\frac{kg\,N_2O}{kg\,coal}$$

The nitrous oxide emissions of anthracite coal are:

$$0.0052\frac{g\,N_2O}{kWh}\cdot\frac{kg\,N_2O}{1000g\,N_2O}\cdot\frac{kWh}{3.6MJ}\cdot 18\frac{MJ}{kg}=2.6\times10^{-5}\frac{kg\,N_2O}{kg\,coal}$$

Crude oil greenhouse gas emissions from combustion are determined from total US consumption, $13.7TBtu$, and total emissions, $1.0Tg\,CO_{2eq}$ (US EPA 2004). On a mass basis, the greenhouse gas emissions of crude oil are:

$$\frac{1.0Tg\,CO_{2eq}}{13.7TBTU}\cdot\frac{1BTU}{1055.06J}\cdot\frac{10^6J}{MJ}\cdot\frac{42.6MJ}{kg\,crude\,oil}\cdot\frac{kg\,CO_{2eq}}{1000g\,CO_{2eq}}=2.95\frac{kg\,CO_{2eq}}{kg\,crude\,oil}$$

The greenhouse gas emissions of these fuels are summarized in Table 3.6.

Table 3.6: Greenhouse gas emissions from various fuel sources.

	Greenhouse Gas			
Fuel	**CO_2**	**CH_4**	**N_2O**	
Natural Gas	1.92	3.68E-05	0	kg/m^3
Coal, Brown	1.5	0.0034	1.16E-05	kg/kg coal
Coal, Hard	2.84	0.0052	2.60E-05	kg/kg coal
Crude Oil	2.95	-	-	kg/kg oil

For each chemical input into titanium acetylacetonate and aluminum acetylacetonate, life cycle inventory data are gathered. The energy contents of the fuel inputs are used to calculate the total energy requirements of production of each chemical. The total green house gas emissions of production of each fuel type are calculated and are added to the life cycle inventory, which normally do not contain emissions from fuel

combustion (Althaus et al. 2004). The energy and emissions calculations and total life cycle inventory data for these chemicals are shown in Appendix A.

For chemicals which have no publicly available life cycle data, guidelines are proposed (Hischier et al. 2005) to determine total resource consumption and emissions for production:

- 95% efficiency of reaction
- energy consumption even in exothermic reactions
- energy and water consumption are average values for chemical plants
    - Averaging the energy input from the LCI data of chemicals which make up both titanium acetylacetonate and aluminum acetylacetonate gives approximately 30 MJ/kg of chemical. This will be used as the average energy consumption for chemicals which have no LCI data.
    - The average value of water consumed for these same chemicals is calculated to 6 m^3/kg chemical. This will be used as the average water consumption for chemicals which have no LCI data.
    - These average values are an estimation and will be replaced if and when more industry data are available about the production of these chemicals.
- 0.2% of input materials are emitted to air
- water emissions are the difference between the extra input materials and the air emissions
- no solid wastes

These guidelines were used to estimate data for the following reactions:

- Acetic anhydride ($C_4H_6O_3$) and acetone (CH_3COCH_3) to form acetylacetone ($C_5H_8O_2$), for both titanium acetylacetonate and aluminum acetylacetonate production.
- Rutile (TiO_2), carbon (C) and chlorine (Cl_2) to form titanium chloride ($TiCl_4$).
- Titanium chloride ($TiCl_4$) and water to form titanium oxychloride ($TiOCl_2$).
- Titanium oxychloride ($TiOCl_2$), acetylacetone ($C_5H_8O_2$) and sodium carbonate (Na_2CO_3) to form titanium acetylacetonate ($TiO(C_5H_7O_2)_2$).
- Aluminum sulphate ($Al_2(SO_4)_3*17H_2O$) and acetylacetone ($C_5H_8O_2$) to form aluminum acetylacetonate ($Al(C_5H_7O_2)_3$).
- Iodine (I_2) and fluorine (F_2) to produce iodine pentafluoride (IF_5).
- Iodine (I_2), iodine pentafluoride (IF_5) and tetrafluoroethylene (C_2F_4) to produce pentafluoroethyl iodide (C_2F_5I).
- Tetrafluoroethylene (C_2F_4) and pentafluoroethyl iodide (C_2F_5I) to produce idoperfluorooctane ($C_8F_{17}I$).
- Ethylene (C_2H_4) and iodoperfluorooctane ($C_8F_{17}I$) to produce 1H,1H,2H,2H,-heptadecafluoro-1-decene ($C_{10}H_3F_{17}$).

3.5 Complied Inventory Data for Materials Acquisition

With the mass of each chemical calculated, the appropriate energy consumption, water consumption, greenhouse gasses and air, water and soil emissions are determined. The complied life cycle inventory data for 0.60 kg total coating material (AACA, TACA, boehmite and ethanol) is shown in Table 3.7. The life cycle inventory for this mixture per chemical is given in Appendix A.

Table 3.7: Summary of compiled life cycle inventory data for production of 0.60kg of self-cleaning coating.

Production of 0.6kg of Self-Cleaning Coating		
Energy	14.47	MJ
Water	0.4063	m^3
CO_2	0.450	kg
CH_4	0.00028	kg
N_2O	0.1882	kg
Air Emissions	0.061	kg
Water Emissions	0.119	kg
Soil Emissions	4.88E-5	kg

The life cycle inventory data for 0.25kg of the water repellent chemical solution are given in Table 3.8. The inventory per chemical of the water repellent is given in Appendix A.

Table 3.8: Life cycle inventory of water repellent chemical solution.

Water Repellent Solution		
Energy	1.11	MJ
Water	0.119	m^3
CO_2	0.126	kg
CH_4	6.7E-05	kg
N_2O	0.00045	kg
Air Emissions	0.0140	kg
Water Emissions	1.39E-03	kg
Soil Emissions	1.02E-04	kg

The total life cycle inventory for all parts of chemical production is shown in Table 3.9.

Table 3.9: Total inventory of chemical production for self-cleaning coating.

Total Chemical Production		
Energy	15.6	MJ
Water	0.525	m^3
CO_2	0.576	kg
CH_4	0.000343	kg
N_2O	0.189	kg
Air Emissions	0.0751	kg
Water Emissions	0.121	kg
Soil Emissions	0.000151	kg

3.6 Inventory Data of Production

The production of the self-cleaning surface involves taking the chemicals listed above, mixing them, applying them to a surface, and heating (Nakajima et al. 2000). A flow diagram for the production process is shown in Figure 3.10.

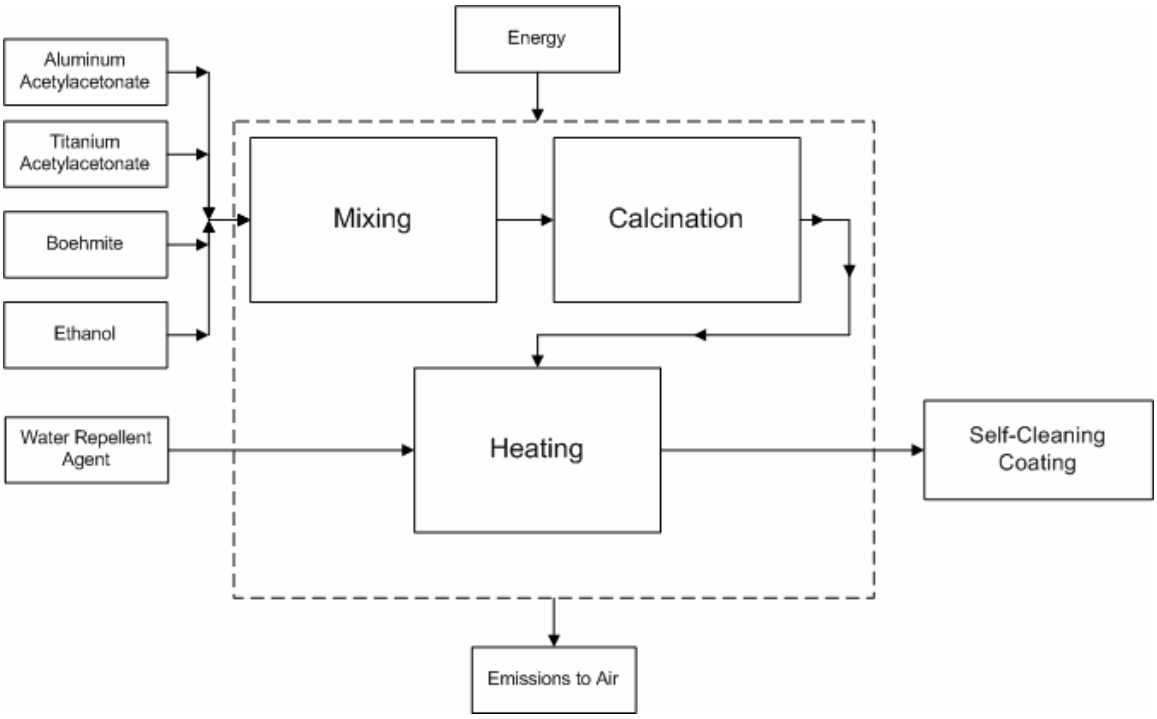

Figure 3.10: Process for application of self-cleaning coating to surface.

Calcination is "heating of a solid to a temperature below its melting point to bring about a state of thermal decomposition or a phase transition other than melting" (Lewis 2002). In the preparation of this self-cleaning coating, once the coating is mixed, it is applied to a surface and calcinated at 500ºC (Nakajima et al. 2000).

Because the coating is mostly ethanol, one can assume the amount of energy required for calcination is simply the amount of energy required to heat the total mass of ethanol. The energy can be calculated from the specific heat of ethanol. The temperature

dependent specific heat of ethanol for the range of 273K to 1500K has an equation of the form (Kyle 1984):

$$\overline{C_p} = a + bT + cT^2 + dT^3$$

where $\overline{C_p}$ has units of $\frac{kJ}{kmolK}$, T has units of K, and

$a = 19.9$

$b = 0.2096$

$c = -10.38 \times 10^{-5}$

$d = 20.05 \times 10^{-9}$

The maximum error in this temperature dependent specific heat is 0.22%, with a maximum of 0.40% (Kyle 1984).

The ethanol is assumed to be heated from room temperature (293K) to 500ºC (773K) and a total mass of $m = 600g$ will need to be heated. The energy required to heat the ethanol is

$$E = \left(C_{p,2}T_2 - C_{p,1}T_1\right)m$$

where $T_1 = 293K$ and $T_2 = 773K$.

$\overline{C_{p,1}}$ is calculated at $T_1 = 293K$ and is:

$$\overline{C_{p,1}} = 19.9 + 0.2096 \cdot 293 + \left(-10.38 \times 10^{-5}\right) \cdot 293^2 + \left(20.05 \times 10^{-9}\right) \cdot 293^3 = 72.906 \frac{kJ}{kmolK}$$

$\overline{C_{p,2}}$ is calculated at $T_2 = 773K$ and is:

$$C_{p,2} = 19.9 + 0.2096 \cdot 773 + \left(-10.38 \times 10^{-5}\right) \cdot 773^2 + \left(20.05 \times 10^{-9}\right) \cdot 773^3 = 129.158 \frac{kJ}{kmolK}$$

As an intermediate step:

$$\overline{C_{p,2}}T_2 - \overline{C_{p,1}}T_1 = 129.158\frac{kJ}{kmolK}\cdot 773k - 72.906\frac{kJ}{kmolK}\cdot 293k = 99839\frac{kJ}{kmol}$$

Using the molar mass of ethanol ($\frac{46.06844kg}{kmol}$) and total mass of ethanol, the total energy used to heat the coating is:

$$E = 99839\frac{kJ}{kmol}\cdot\frac{kmol}{46.06844kg}\cdot 0.6kg = 1300kJ = 1.3MJ$$

Therefore, approximately 1.3MJ is required to heat 0.6kg of ethanol from room temperature to 500ºC

In the following steps, a water repellent agent is applied to the surface, and it again heated, this time to only 140ºC (Nakajima et al. 2000). Assuming that most of the ethanol evaporated during calcination, only the water repellent again remains on the surface to be heated. The water repellent solution is 98% water, so the energy required for heating will be approximated as the energy necessary to heat only water. To heat this volume of water from room temperature to 140ºC is a temperature difference of

$$\Delta T = 140 - 20 = 120^{\circ}\mathrm{C} = 120K$$

With the fact that specific heat of water is $c_p = 4.1855\frac{kJ}{kgK}$, the total energy used to heat the coating is

$$E = 4.1855\frac{kJ}{kgK}\cdot 120K\cdot 0.125kg = 62.7825kJ$$

The total energy used in these two steps is:

$$E = 1300kJ + 62.78kJ = 1.362MJ$$

A total of 1.362MJ is consumed in the calcination and baking of the self-cleaning coating.

The carbon dioxide emissions can be estimated by the amount of energy consumed (Thomas 2000):

$$E_{CO_2} = CF_e\left(P_e + P_c\right) + CF_g\left(P_g\right) + CF_s P_s$$

This equation accounts for electricity, steam and natural gas energy sources. It is assumed that the energy required to calcinate and then heat the self-cleaning coating comes completely from electricity. Simplifying the equation for just electricity, the equation reduces to:

$$E_{CO_2} = CF_e\left(P_e\right)$$

In the previous equation, CF_e is 1.40x10^{-7} tons CO_2/kJ (Thomas 2000). The carbon dioxide emissions of the calcinating and heating the coating are:

$$E_{CO_2} = 1.4\times10^{-7}\,\frac{tons\,CO_2}{kJ}\left(1362kJ\right) = 1.91\times10^{-4}\,tons\,CO_2 = 0.191kg\,CO_2$$

The methane emissions for electricity in Georgia are given as $\frac{1.235\times10^{-9}\,kg\,CH_4}{kJe}$ (Thomas 2000). The methane emissions of the electricity to power the calcination and heating process are

$$\frac{1.235\times10^{-9}\,kg\,CH_4}{kJe}\cdot 1400kJe = 1.682\times10^{-6}\,kg\,CH_4$$

The nitrous oxide emissions for electricity used in Georgia are $\frac{2.81\times10^{-9}\,kg\,N_2O}{kJe}$ (Thomas 2000). The nitrous oxide emissions of calcinating and heating the self-cleaning coating are:

$$\frac{2.81\times10^{-9}\,kg\,N_2O}{kJe}\cdot 1400kJe = 3.827\times10^{-6}\,kg\,N_2O$$

The life cycle inventory data for calcinating and heating the self-cleaning coating are summarized in Table 3.10.

Table 3.10: Energy consumption and emissions from the application of the self-cleaning coating.

Application of 1m^2 of coating		
Energy	1.362	MJ
CO_2	0.191	kg
CH_4	1.682E-6	kg
N_2O	3.827E-6	kg

The machines used to calcinate and heat the coating will not be 100% efficient. The device used to calcinate and heat, however, will be less efficient. The energy consumption and emissions calculated above therefore represent a minimum. The actual total energy consumption will be higher. The total energy consumption will be

$$E = \frac{1.362MJ}{\eta}$$

where η is the efficiency of the heater. The associated greenhouse gas emissions can be calculated from the energy consumption including an efficiency.

3.7 Total Life Cycle Inventory of Production of Self-Cleaning Coating

By summing the resource consumption and emissions of producing the chemicals for the coating with that of heating and calcinating the coating on the surface, one obtains the total data for production of the coating. These data are shown in Table 3.11.

Table 3.11: Total life cycle inventory data for production and application of the self-cleaning coating.

Total Inventory of Chemical Coating		
Energy	16.9	MJ
Water	0.525	m^3
CO_2	0.767	kg
CH_4	3.45E-04	kg
N_2O	1.89E-01	kg
Air Emissions	0.0750	kg
Water Emissions	0.121	kg
Soil Emissions	1.5E-04	kg

3.8 Summary

In this chapter, the life cycle inventory for the production of a chemical self-cleaning coating was determined. The life cycle of the coating includes materials acquisition and production of chemicals, and calcination and heating of chemicals to apply the coating. The inventory by life cycle stage is shown in Table 3.12.

Table 3.12: Life cycle inventory for chemical coating by stage.

Production and Application of Self-Cleaning Coating			
	Chemical Production	**Application**	
Energy	15.6	1.362	MJ
Water	0.525	0	m^3
CO_2	0.576	0.191	kg
CH_4	0.00034	1.68E-06	kg
N_2O	0.189	3.83E-06	kg
Air Emissions	0.0751	0	kg
Water Emissions	0.121	0	kg
Soil Emissions	0.00015	0	kg

This life cycle inventory data will be compared to inventory of two other methods of producing a self-cleaning surface, and to two methods of industrially cleaning.

CHAPTER 4

LIFE CYCLE INVENTORY OF LASER MACHINING TO PRODUCE SELF-CLEANING TEMPLATES

Two template methods of producing a self-cleaning surface have also been selected to be analyzed with a life cycle assessment. The first template is a flat plate made of steel and machined to have a nanorough surface via laser ablation (Groenendijk and Meijer 2006). A $1m^2$ template will be the system to be analyzed. This system has been selected because it is another, different method of producing a self-cleaning surface, Because it is a template method, it is reusable and has the potential to be more environmentally friendly than the chemical coating.

4.1 Laser Ablation Machining

One method to produce micro- and nanoscale structures is through laser machining. Laser machining typically uses one of three types of laser modes: short, ultrashort or continuous wave (Madou 2002). In ultrashort laser mode, pulses of lasers last less then 10 picoseconds. When such short laser pulses are used, energy is imparted onto the material at a high rate; because so much energy is present, even extremely hard materials can be easily laser machined.

The large amount of energy per laser pulse also causes the solid material to change state directly to a gas or plasma (Madou 2002). The plasma carries the excess heat away from the material, although at a slower rate than the repetition of the laser

pulses. Because the energy is not quickly diffused, the temperature of the material where the laser is aimed quickly rises and remains above the melting point of the material. This increase in temperature makes the laser machining process very efficient. With the temperature high enough to convert the material from solid to gas, no liquid material is present to spread or condense on other parts of the materials. Ultrashort laser pulses create a very clean machining process, with no metal debris accumulating on the surface around the laser's path and no damage caused to the surrounding area. The ultrashort laser machining process is shown in Figure 4.1.

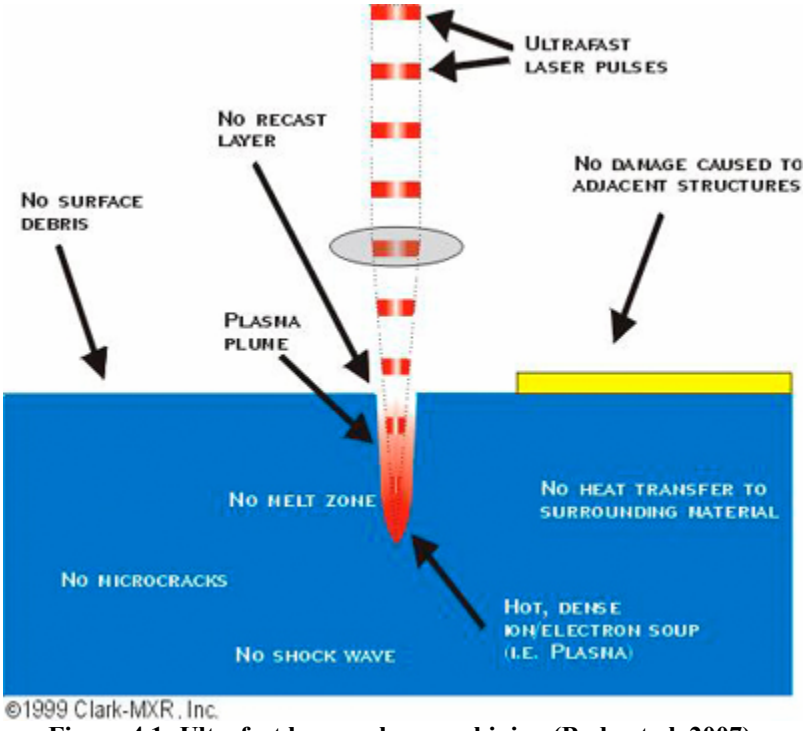

Figure 4.1: Ultrafast laser pulses machining (Bado et al. 2007).

Because ultrashort laser pulses can create nanoscale features, laser machining is a candidate for creating self-cleaning surfaces. Laser pulses with lengths of 200 femtoseconds have been used to created nanorough surfaces on steel (Groenendijk and Meijer 2006). The steel is nanoroughed with the intention of becoming a mold or

template for producing self-cleaning surfaces on polymers. The pattern will be transferred from the metal mold to a polymeric surface with heat and pressure.

To determine the life cycle inventory for this method of manufacturing a self-cleaning surface, one must consider the materials acquisition and production of the steel for the mold, the laser machining process, the surface transfer process, and the cleaning of the self-cleaning surface. In this chapter, the inventory of the materials acquisition, machining and pattern transfer will be determined.

4.2 Energy Consumption of Laser Ablation

In one experiment of machining a steel surface as a template for producing a self-cleaning surface, a titanium sapphire laser system was used. The Coherent Vitesse™ Duo was used for the laser and power supply, and the Coherent RegA9000 was used as the amplifier (Groenendijk and Meijer 2006). For the purposes of laser machining, the laser pulse length was set to 200 femtoseconds (Groenendijk and Meijer 2006). The repetition rate was 250kHz, which is the number of emitted pulses per second. The average power of this laser is 0.3 W (Coherent Inc. 2000).

The pulse energy of the laser is given in the laser specifications as $3\mu J$ (Coherent Inc. 2000); this simply means that each pulse of the laser will consume that much energy. The pulse energy is often calculated by dividing the average power of the laser by the repetition rate; this calculation is accurate as long as the power used between pulses is negligible. Therefore, to use the pulse energy as an accurate measure of energy consumption, it must be assumed that no power is used between pulses.

In producing the steel template with laser ablation, various scan speeds were used by the laser to cover the surface (Groenendijk and Meijer 2006). If $1m^2$ is again used as

the functional unit for this life cycle study, it is necessary to determine how long it will take for the laser to move 1 m. Using this time and the repetition rate of the laser, it is determined how many pulses of the laser will be emitted. Using the pulse energy of the laser, the total energy consumption of the laser for machining can be determined.

The fastest laser scan speed used to produce the template was $2000\frac{mm}{s}$ (Groenendijk and Meijer 2006). At this speed, it will take 0.5 second to cover 1 m. Therefore, the number of pulses the laser will emit while scanning a 1 m line is

$$\frac{s}{2000mm}\cdot 1000mm = 0.5s\cdot\frac{250000\,pulses}{s} = 125000\,pulses$$

For the scan speed of $1000\frac{mm}{s}$, it will take 1 second to cover 1 m; therefore 250,000 pulses of the laser will be emitted in that time. Similarly, for a scan speed of $500\frac{mm}{s}$, it will take the laser 2 seconds to cover 1m, while emitting 500,000 pulses. With a scan speed of $250\frac{mm}{s}$, it will take the laser 4 seconds to move 1 m, while 1,000,000 pulses are emitted; for the scan speed of $16\frac{mm}{s}$, the laser will take 62.5 s to move 1 m, while emitting 15,625,000 pulses.

The laser was used to scan lines 15 μm apart (Groenendijk and Meijer 2006). Therefore, for a 1m of width, 66,667 lines will have to be made. Using the pulse energy of the laser, the amount of pulses per 1m long line scanned, and the total number of lines the laser must scan, the energy consumption of the laser to cover $1m^2$ of surface can be determined. The energy consumption for the 2000mm/s scan speed is:

$$\frac{3\times10^{-6}J}{pulse}\cdot 125000\,pulses\cdot 66667 lines = 25000J = 25kJ$$

The energy consumptions of the laser pulses to structure $1m^2$ of surface for various scan speeds are summarized in Table 4.1.

Table 4.1: Energy consumption of laser to structure $1m^2$ of surface for various scan speeds.

Scan Speed (mm/s)	Energy Consumption (kJ)
2000	25
1000	50
500	100
250	200

The energy consumption of the laser has been calculated, but one must also consider the energy required to move the laser as it scans over the surface. Specifications were found for a laser micromachining system which uses ablation. This particular system, the Picomaster Picosecond laser machining workstation, has a maximum scan speed of 2000mm/s, so it will able to scan surfaces as fast as performed in the laser ablation experiments by Groenendijk and Meijer (EKSPLA). This machine has a minimum laser spot size of 5μm, which means it will be able to produce surface features small enough to produce the self-cleaning effect (EKSPLA). This particular machine, however, only has a repetition rate of 100kHz, which is less then 250kHz used by Groenendijk and Meijer. Also, the pulse duration of laser is at minimum 10 picoseconds, while the laser used by Groenendijk and Meijer was capable of pulses of 200 femtoseconds (EKSPLA).

Because this laser machining workstation is not capable of exactly the same performance as the laser used by Groenendijk and Meijer, its power consumption specifications will used to obtain an estimate of the total energy used to produce $1m^2$ of a self-cleaning surface template. Email correspondence with Ekspla, the company which

produces the Picomaster laser machining workstation, revealed that the machine may require up to 5kW of power when the machine is operating at full workload. It is assumed that machine will be at full workload the entire time the template is being ablated, so that a maximum power required will be calculated.

With the power consumption of the machine known, the total energy consumption to produce the template can be determined, if the time needed to machine the template is known. The time needed to cover $1m^2$ of a surface can be calculated from the scan speeds of the laser and the fact that 66,667 lines must be scanned by the laser when they are 15 um apart. The times needed to cover $1m^2$ for various laser scan speed are shown in Table 4.2.

Table 4.2: Time for laser to cover $1m^2$ for various scan speeds.

Scan Speed (mm/s)	Time to Cover $1m^2$ (s)	Time to Cover $1m^2$ (hr)
2000	33333.5	9.26
1000	66667	18.52
500	133334	37.037
250	266668	74.074

The energy consumption of the machine can be calculated for each of these scan speeds, using the power consumption mentioned above (5kW). The energy consumed for each scan speed is shown in Table 4.3.

Table 4.3: Energy consumption for various scan speeds.

Scan Speed (mm/s)	Energy Consumed (MJ)
2000	166.6675
1000	333.335
500	666.67
250	1333.34

The greenhouse gas emissions of the laser ablation of the surface can be calculated, assuming all electricity (Thomas 2000). The total energy and associated greenhouse gas emissions for each scan speed are shown in Table 4.4.

Table 4.4: Greenhouse gas emissions of laser ablation, for various scan speeds.

Scan Speed (mm/s)	Energy (MJ)	CO_2 (kg)	CH_4 (kg)	NO_2 (kg)
2000	166.67	23.33345	0.000205834	0.000468336
1000	333.34	46.6669	0.000411669	0.000936671
500	666.67	93.3338	0.000823337	0.001873343
250	1333.34	186.6676	0.001646675	0.003746685

4.3 Life Cycle Inventory of Steel Production

Cold rolled stainless steel 304 with bright annealed finish is used as the template material (Groenendijk and Meijer 2006). The template was made of 2mm thick cold rolled stainless steel 304 (austenitic). For $1m^2$ of surface this is a total volume of $0.002m^3$ of steel. The density of this steel is $\rho = \frac{7.93g}{cm^3}$. Therefore, the total mass of steel used for the template is

$$\frac{7.93g}{cm^3} \cdot \left(\frac{100cm}{1m}\right)^3 \cdot \frac{1kg}{1000g} \cdot 0.002m^3 = 15.86kg$$

The life cycle inventory data for the production of stainless steel 304 bright annealed was obtained from the International Stainless Steel Forum (ISSF). This life cycle inventory data are cradle to gate. The life cycle data includes two scenarios: one with credit and one without. The scenario without credit is the case where all new material is used to produce the stainless steel. The scenario with credit is when some proportion of the material used to produce the steel is recycled scrap (Fujii et al. 2005).

The world average for recycled scrap used in the production of stainless steel is 60% (Terörde 2006). The life cycle data for the with credit scenario is deteremined with

$$X = Xprimary + \left(Xrecycled - Xprimary\right) \cdot RR \cdot Y$$

where X is the life cycle scenario "with credit", $Xprimary$ is the life cycle data from the scenario where 100% new material is used, $Xrecycled$ is the life cycle data from the scenario with 100% recycled scrap, RR is the recycling ratio, and Y is the percentage yield of the scrap input (Fujii et al. 2005). The "with credit" scenario assumes a recycling ratio of 80% and yield of 0.91.

For this life cycle inventory study, the two sets of data are averaged. The average data for the production of 1 kg of steel are shown in Table 4.5.

Table 4.5: Life cycle inventory data for the production of stainless steel 304 bright annealed (ISSF 2006).

Production of 1 kg S.S. 304 BA		
Energy	45.304	MJ
Water	0.05805	m^3
CO_2	5.8	kg
CH_4	0	kg
N_2O	0.012405	kg
Air Emissions	5.8791	kg
Water Emissions	0.01601	kg
Soil Emissions	2.32988	kg

Inventory data from the ISSF for the production of 15.86kg of stainless steel 304 BA are shown in Table 4.6.

Table 4.6: Life cycle inventory data for the production of 15.86kg of stainless steel 304 BA for the template.

Production of 15.86 kg Stainless Steel 304 BA		
Energy	718.5214	MJ
Water	0.920673	m^3
CO_2	91.988	kg
CH_4	0	kg
N_2O	0.196743	kg
Air Emissions	93.24253	kg
Water Emissions	0.253919	kg
Soil Emissions	36.9519	kg

4.4 Life Cycle Inventory of Transferring the Pattern

With the steel template prepared, the nanoscale surface pattern can be transferred to a polymeric surface. In other methods of producing a nanostructed polymeric surface from a template, the polymer is heated to above its glass transition temperature (Lee et al. 2004). In this case the template and material (polystyrene) was heated to 130ºC, while the glass transition temperature is only 101ºC (Lee et al. 2004). In another template method, the polymer material used was polycarbonate, and the template and material were heated to between 150 and 170ºC, with an applied pressured of 2.1×10^5 to 3.3×10^5 Pa (Guo et al. 2004).

The specific heat of the template material can be used to determine the amount of energy required to heat it. For stainless steel 304 which has been annealed, the specific heat is approximately $500\frac{J}{kgK}$ (Incropera and DeWitt 2002). Therefore, the energy needed to heat the template from room temperature to 101ºC is

$$500\frac{J}{kgK}\cdot(374-293K)\cdot15.86kg = 642330J = 642kJ$$

To heat the stainless steel template to 170ºC requires more energy:

$$500\frac{J}{kgK}\cdot(443-293K)\cdot 15.86kg = 1189500J = 1.189MJ$$

The steel template will lose some of its heat to the cooler surrounding air during the pattern transfer. Heat will be lost due to free convection from the top of the plate. The total heat lost can be estimated from

$$q = hA(T_s - T_\infty)$$

The temperature of the surface of the steel plate, T_s, is 170ºC. The temperature of the ambient air, T_∞, is assumed to be 20ºC. The properties of the air at 370K (T_f, the average of the surface and ambient temperatures) are shown in Table 4.7.

Table 4.7: Air properties at T_f=370K.

Property	**Symbol**	**Value**	**Unit**
Thermal Conductivity	k	0.0313	W/mK
Kinematic Viscosity	ν	22.8E-6	m^2/s
Thermal Diffusivity	α	32.8E-6	m^2/s
Prandtl Number	Pr	0.697	
Volumetric Thermal Expansion	β	2.725E-3	1/K

First, the characteristic length of the plate is determined with the following equation:

$$L \equiv \frac{A_s}{P}$$

The characteristic length of this plate is:

$$L = \frac{1m \times 1m}{4m} = 0.25m$$

Next the Rayleigh number is calculated with:

$$Ra_L = \frac{g\beta(T_s - T_\infty)L^3}{\nu\alpha}$$

The Rayleigh number for this plate is:

$$Ra_L = \frac{9.8\frac{m}{s^2} \cdot 2.725\times10^{-3}\left(170^\circ C - 20^\circ C\right)\left(0.25m\right)^3}{\left(22.8\times10^{-6}\frac{m}{s^2}\right)\left(32.8\times10^{-6}\frac{m}{s^2}\right)} = 8.3694\times10^7$$

The Nusselt number for the upper surface of heated flat plate with a Rayleigh number of greater than 10^7 is determined with (Incropera and DeWitt 2002):

$$Nu_L = 0.15Ra_L^{1/3}$$

The Nusselt number for the steel template is:

$$Nu_L = 0.15\left(8.3694\times10^7\right)^{1/3} = 65.6129$$

The Nusselt number is used to find the convection coefficient with

$$\overline{h} = \frac{k}{L}\overline{Nu}_L$$

The convection coefficient for the top of the steel plate is

$$\overline{h} = \frac{0.0313\frac{W}{mK}}{0.25m}\left(65.6129\right) = 8.2147\frac{W}{m^2K}$$

The rate of heat loss of the steel template from the top due to free convection is

$$q = 8.2147\frac{W}{m^2K} \cdot 1m^2 \cdot \left(170^\circ C - 20^\circ C\right) = 1232.21W$$

The total amount of heat lost after 5 minutes from the top of the template is:

$$1232.21W \cdot \frac{60s}{\min} \cdot 5\min = 369.663kJ$$

Heat is also lost from each side of the template from free convection. The amount of heat lost is estimated by modeling each side as a vertical plate. The characteristic length of a vertical plate is equal to its height; for the case of the template, this length is 2mm. The Rayleigh number is calculated as above, with the new characteristic length,

and is 42.85, indicating laminar flow. The Nusselt number for the side of the plate is determined with the following equation (Churchill and Chu 1975):

$$Nu_D = \left(0.68 + \frac{0.670 Ra_D^{1/4}}{\left[1 + \left(\frac{0.429}{\Pr} \right)^{9/16} \right]^{4/9}} \right)^2$$

The Nusselt number for the sides of template is 1.99297.

The convection coefficient for the side of template is determined with

$$\overline{h} = \frac{k}{H} \overline{Nu}_L$$

The convection coefficient for the side of the template is $31.19 \frac{W}{m^2 K}$. The heat transfer rate is

$$q = 31.19 \frac{W}{m^2 K} \cdot 0.002 m^2 \cdot \left(170^\circ C - 20^\circ C \right) = 9.357 W$$

After 5 minutes, the total amount of heat lost from the side is:

$$9.357 W \cdot \frac{60 s}{\min} \cdot 5 \min = 2.807 kJ$$

For all four sides, a total amount of 11.228kJ is lost through free convection.

Heat is lost from the steel template to the polycarbonate surface through conduction. The thermal conductivity of polycarbonate is $0.2 \frac{W}{mK}$ (Incropera and DeWitt 2002). The amount of heat flow through the polycarbonate is determined from Fourier's Law:

$$q = kA \frac{dT}{dx}$$

The amount of heat conducted through the polycarbonate is dependent on its thickness:

$$q = 0.2\frac{W}{mK}\cdot 1m^2 \cdot \frac{\left(170^\circ C - 20^\circ C\right)}{x} = \frac{30}{x}W$$

where x is the thickness of the polycarbonate, in meters. The heat transfer through conduction from the template to the polycarbonate for various thicknesses of the polycarbonate and the total heat lost over a period of 5 minutes is shown in Table 4.8.

Table 4.8: Heat transfer and heat loss for various thicknesses of polycarbonate.

Thickness (m)	Q (W)	Total Heat Loss (kJ)
0.005	6000	1800
0.01	3000	900
0.015	2000	600
0.02	1500	450
0.025	1200	360
0.03	1000	300
0.035	857.142	257.142
0.04	750	225
0.045	666.6667	200
0.05	600	180

Assuming the pattern is transferred from the steel template to a polycarbonate material with a thickness of at least 5mm, the total maximum heat lost over 5 minutes to both conduction and free convection is 2.169MJ. With the addition of the necessary energy to first heat the entire steel template to 170ºC, the total energy used to heat the template and keep it heated for 5 minutes is 3.370MJ.

The energy and greenhouse gas emissions of heating the template using electricity are summarized in Table 4.9.

Table 4.9: Energy and greenhouse gas emissions from heating the template.

	heated to 170°C	
Energy	3.370	MJ
Carbon Dioxide	0.4718	kg
Methane	4.16E-6	kg
Nitrous oxide	9.47E-6	kg

The energy calculated above represents the minimum theoretical energy consumption, for a 100% efficient heating device. The actual heating device used on the template will be less than 100%; the energy consumption of such a device will be:

$$E = \frac{3.37MJ}{\eta}$$

where η is the efficiency of the heater.

A pressure of in the range of 2.1E5 Pa to 3.3E5 Pa is applied while the heated steel template is in contact with the polymeric surface (Lee et al. 2004). To calculate the energy required to apply the pressure, one first calculates the necessary force:

$$2.1\times10^5\,Pa = 2.1\times10^5\,\frac{N}{m^2}\cdot 1m^2 = 2.1\times10^5\,N$$

To calculate the energy in Joules need to provide this force, one must also know the distance the template must travel. Since the template is transferring a nanoscale pattern, it must only move a few nanometers. Therefore the energy needed to apply the pressure is:

$$2.1\times10^5\,N\cdot\left(100\times10^{-9}\,m\right) = 0.021J$$

For the higher applied pressure, the energy needed is:

$$3.3\times10^5\,N\cdot\left(100\times10^{-9}\,m\right) = 0.033J$$

These energies represent the minimum energy it would take to apply the given pressure. A machine applying the pressure would consume more energy; however, it appears that in comparison to the amount of energy needed to heat the template, the amount of energy used to apply the pressure is negligible. Therefore the impact of applying the pressure will be ignored.

4.5 Total Life Cycle Inventory of Steel Template

The total resource consumption and emissions of producing the template is determined by summing the life cycle inventory data for the laser ablation of the nanoscale pattern with the data for the production of stainless steel for the template material.

Minimum inventory data are calculated for the case where a scan speed of $2000\frac{mm}{s}$ is used; with the highest scan speed the least amount of time is needed to structure $1m^2$. The maximum case is when a scan speed of $250\frac{mm}{s}$ is used. The life cycle inventory data for the production of the template are shown in Table 4.10.

Table 4.10: Life cycle inventory data for the production of a template.

	Minimum	Maximum	
Energy	885.1889	2051.8614	MJ
Water	0.920673	0.920673	m^3
CO_2	115.3215	278.6556	kg
CH_4	0.000206	0.0016466	kg
N_2O	0.197211	0.2004896	kg
Air Emissions	93.24253	93.24253	kg
Water Emissions	0.253919	0.253919	kg
Land Emissions	36.9519	36.9519	kg

The total energy consumption and emissions of the template per use of the template diminishes for increasing number of uses; the more times the template is used, the less energy used to produce the template that can be attributed to each use. The energy consumption of producing the template per use of the template is shown in Figure 4.2, for both the highest and lowest laser scan speed.

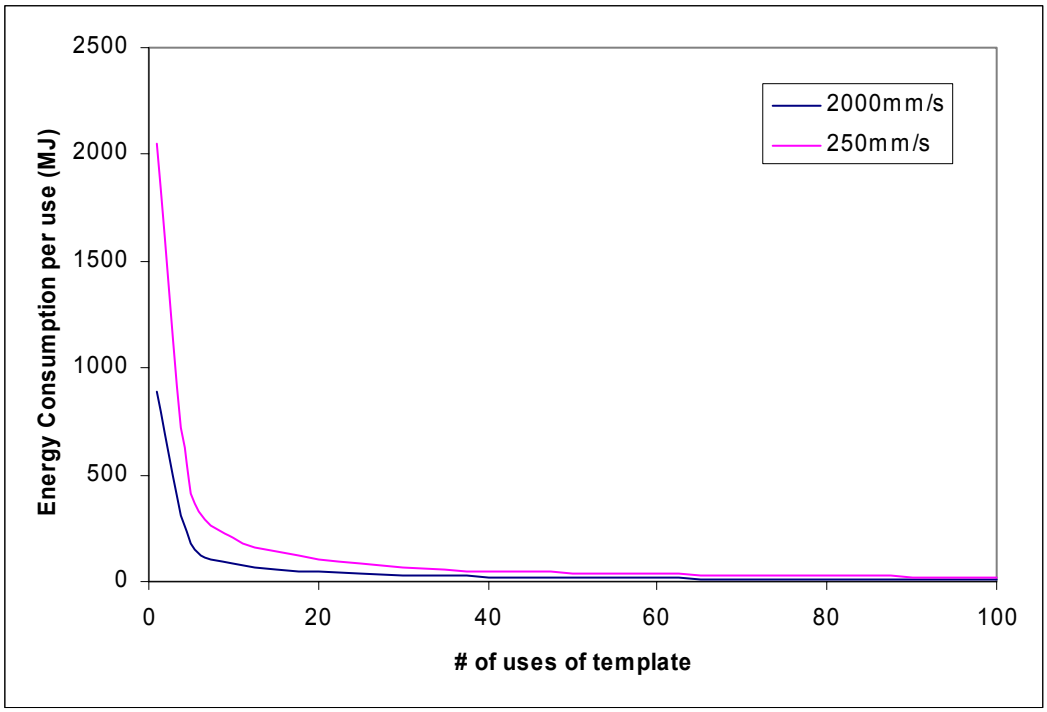

Figure 4.2: Energy consumption per use of template.

The carbon dioxide emissions per use of the template are shown in Figure 4.3.

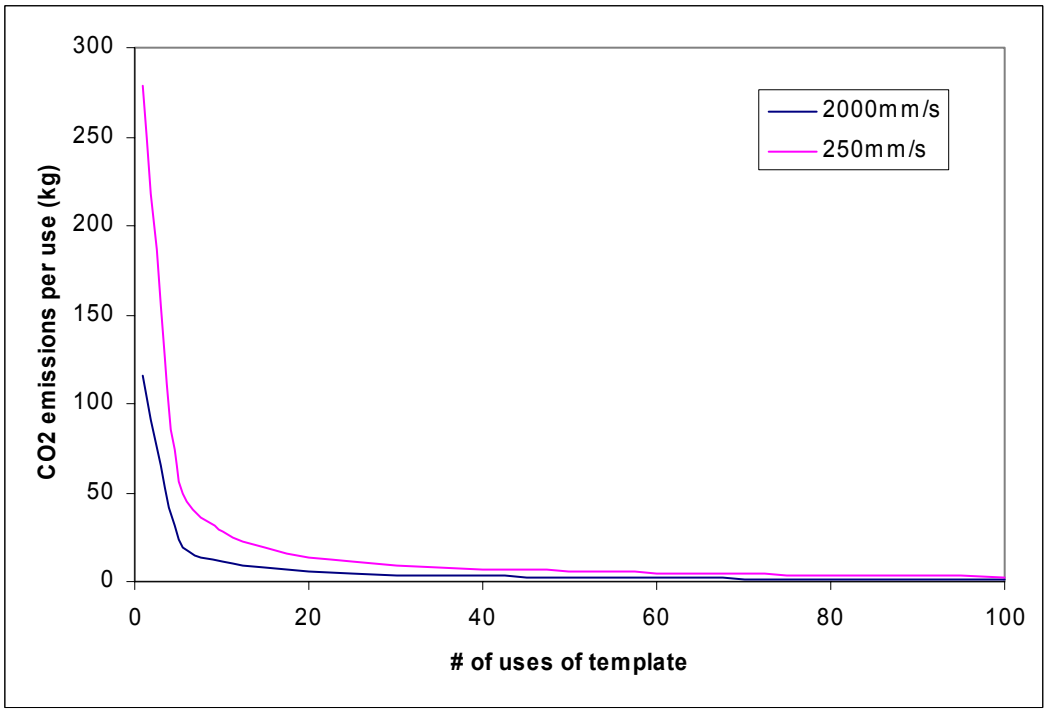

Figure 4.3: Carbon Dioxide emissions per use of the template.

The life cycle inventory data per use for increasing number of uses is shown in Table 4.11, for the case of laser scan speed of $2000\frac{mm}{s}$. These data also include the energy and emissions from heating the template to 170ºC to transfer the pattern from the template to a polycarbonate surface.

Table 4.11: Life cycle inventory data for production of template per use, for laser scan speed of 2000 mm/s.

# of Uses	Energy (MJ)	Water (m^3)	CO_2 (kg)	CH_4 (kg)	N_2O (kg)	Air Emissions	Water Emissions	Soil Emissions
1	889	0.921	116	2.10E-4	1.97E-1	93.2	0.254	37.0
10	88.9	0.092	11.6	2.10E-5	1.97E-2	9.32	0.025	3.70
25	35.5	0.037	4.63	8.40E-6	7.89E-3	3.73	0.010	1.48
50	17.8	0.018	2.32	4.20E-6	3.94E-3	1.87	0.005	0.739
75	11.8	0.012	1.54	2.80E-6	2.63E-3	1.24	0.003	0.493
100	8.89	0.009	1.16	2.10E-6	1.97E-3	0.932	0.003	0.370

The life cycle inventory data per use for the case of a laser scan speed of $250\frac{mm}{s}$ is shown in Table 4.12.

Table 4.12: Life cycle inventory data for production of template per use, for laser scan speed of 250mm/s.

# of Uses	Energy (MJ)	Water (m3)	CO_2 (kg)	CH_4 (kg)	N_2O (kg)	Air Emissions	Water Emissions	Soil Emissions
1	2060	0.921	279	1.65E-3	2.00E-1	93.2	0.254	37.0
10	206	0.092	27.9	1.65E-4	2.00E-2	9.32	0.025	3.70
25	82.2	0.037	11.2	6.60E-5	8.02E-3	3.73	0.010	1.48
50	41.1	0.018	5.58	3.30E-5	4.01E-3	1.87	0.005	0.739
75	27.4	0.012	3.72	2.20E-5	2.67E-3	1.24	0.003	0.493
100	20.6	0.009	2.79	1.65E-5	2.00E-3	0.932	0.003	0.370

4.6 Summary

The life cycle inventory has been complied for a steel template laser ablated to have a nanorough texture. The inventory includes materials acquisition and production of stainless steel, energy use and emissions for laser ablating machines, and energy and

emissions to heat the template and transfer the pattern to a polymeric surface. The inventory was complied for a range of laser scan speeds. The life cycle inventory data per stage of production is shown in Table 4.13

Table 4.13: Life cycle inventory data for laser ablated template for each stage of production.

	Steel Production	Ablation Min.	Ablation Max.	Pattern Transfer	
Energy	718.52	167	1333	3.37	MJ
Water	0.921	0	0	0	m^3
CO_2	92.0	23.3	186.7	0.472	kg
CH_4	0	2.06E-04	1.65E-03	4.16E-06	kg
N_2O	0.197	4.68E-04	0.00375	9.47E-06	kg
Air Emissions	93.2	0	0	0	kg
Water Emissions	0.254	0	0	0	kg
Land Emissions	36.9	0	0	0	kg

It is determined that for a high laser scan speed, majority of the energy consumption is attributed to steel production, while for low laser scan speeds, the majority of the energy is attributed to the ablation process. All waste produced in this inventory comes from the production of steel.

An uncertainty analysis was also performed to determine most likely values for the inventory, using randomly selected values from a distribution of the number of times the template can be used. This analysis is described in Appendix D.

CHAPTER 5

LIFE CYCLE INVENTORY OF ANODIZED ALUMINUM TEMPLATE

Anodizing is used to create nanostructures on the surface of aluminum; the aluminum then is used as a template which, when heated and applied to polymeric surfaces, can create a self-cleaning surface (Guo et al. 2004). Anodizing is used to structure the surface of an aluminum tube; the tube then is rolled over a polymeric surface while being heated and with applied pressure (Guo et al. 2004). This method has successfully created nanopillars on the surface of the polymer as small as 30nm in diameter. The process used to create the nanostructured aluminum tube template is shown in Figure 5.1.

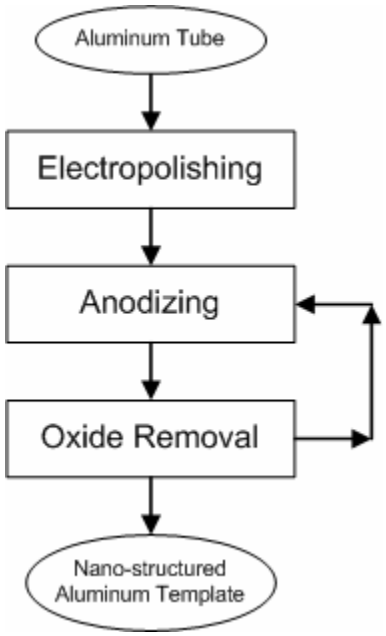

Figure 5.1: The process used to create a nanostructured aluminum tube for a template.

It has been suggested that a rolling template method of replicating a nanostructure is ideal for mass production (Abbott and Gaskell 2007); for this reason, this particular template method has been selected to be analyzed with a life cycle assessment.

5.1 Life Cycle Inventory of Aluminum Production

The aluminum tube on which Guo and coauthers created the nanostructured surface is 6 cm long, 5cm of which were anodized, and the diameter of the tube appears to be approximately 1cm (Guo et al. 2004). To scale this process up to provide the functional unit of $1m^2$ of a self-cleaning surface, the tube must be at least 1m long. The circumference of the aluminum tube must be 1m, to provide $1m^2$ of total surface area. The radius of such an aluminum tube is 0.159m. A thickness of 5mm is selected for this study, in order to have a similar thickness as that of the steel template. The total volume of the aluminum used for the tube is

$$V = \pi(1m)\left((0.159m)^2 - (0.154m)^2\right) = 0.0049166m^3 = 4916.6cm^3$$

With a density of $\rho = \frac{2.70g}{cm^3}$, the total mass of aluminum used in the tube is

$$m = \frac{2.70g}{cm^3} \cdot 4916.6cm^3 = 13274g = 13.274kg$$

Aluminum production data from new materials (primary production) were obtained from NREL and are shown in Table 5.1 (NREL 2007).

Table 5.1: Life cycle inventory data for primary production of aluminum.

Production of 1000lb Primary Aluminum		
Energy	49667	MJ
Water		m^3
CO_2	1698	lb
CH_4	6.22E-2	lb
N_2O	1.96E-3	lb
Air Emissions	1805.06	lb
Water Emissions	5.4232	lb
Land Emissions	2885	lb

The total resource consumption and emissions for the production of 13.27kg of aluminum are shown in Table 5.2.

Table 5.2: Life cycle inventory data for the production of 13.27kg of aluminum.

Production of 13.27kg Primary Aluminum		
Energy	1463.204	MJ
Water	0	m^3
CO_2	22.69019	kg
CH_4	0.000831	kg
N_2O	2.62E-05	kg
Air Emissions	24.12082	kg
Water Emissions	0.07247	kg
Land Emissions	38.55194	kg

Life cycle inventory data for the production of aluminum from recycled scrap (secondary production) were also obtained from NREL and are shown in Table 5.3 (NREL 2007).

Table 5.3: Life cycle inventory data for secondary production of aluminum.

Production of 1000lb Secondary Aluminum		
Energy	29543.47	MJ
Water		m^3
CO_2	28.3	lb
CH_4	0	lb
N_2O	0	lb
Air Emissions	50.493	lb
Water Emissions	0.593	lb
Land Emissions	161	lb

The life cycle inventory data for the production of 13.27kg of aluminum for the template tube are shown in Table 5.4.

Table 5.4: Life cycle inventory data for the production of 13.27 kg aluminum (secondary).

Production of 13.27kg Secondary Aluminum		
Energy	870.359	MJ
Water	0	m^3
CO_2	0.37817	kg
CH_4	0	kg
N_2O	0	kg
Air Emissions	0.674732	kg
Water Emissions	0.007924	kg
Land Emissions	2.151425	kg

5.2 Life Cycle Inventory of Electropolishing

The aluminum tube is first electropolished at 20V for 5 minutes in a solution of 70% perchloric acid and ethanol (Guo et al. 2004). The electrochemical unit process is shown in Figure 5.2.

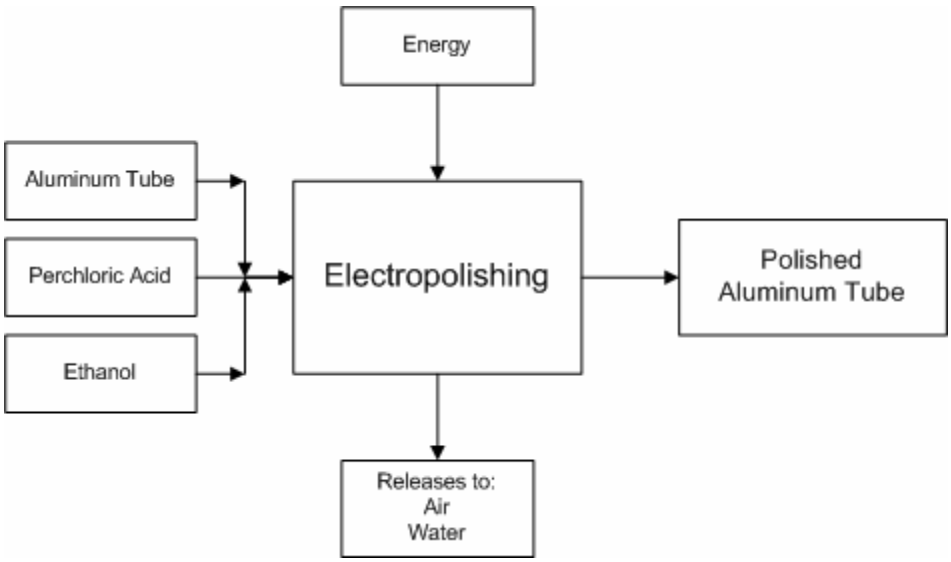

Figure 5.2: Unit process of electrochemical polishing.

Electropolishing, or electrochemical polishing, is an electrochemical machining process in which the part to be polished is placed in an electrolyte and a current is applied (Delstar Metal Finishing Inc. 2003). The electropolishing process removes metal from the surface of the part. During the process, a film forms on the surface of the metal; this film is at its thinnest over any protrusions in the metal. At the spots where this film is the thinnest, the electrical resistance is lowest. Therefore, at these spots, the rate of metal removal is at its highest. The finished electropolished part will be "microscopically smooth" (Delstar Metal Finishing Inc. 2003).

5.2.1 Electricity Consumption of Electropolishing

When electrochemically polishing a surface, a current density recommended for aluminum is $50\frac{A}{ft^2}$ (Electro Polish Systems Inc. 2006). This current density is equivalent to $0.0538\frac{A}{cm^2}$. The total surface area to be electrochemically polished is $1m^2$ or $10000cm^2$.

The total current needed to polish the aluminum tube is:

$$0.0538\frac{A}{cm^2}\cdot 10000cm^2 = 538A$$

The energy consumption of electrochemically polishing the aluminum, for a voltage of 20V used for 5 minutes is:

$$20V\left(538A\right)\cdot\frac{60s}{\min}\cdot 5\min = 3.2291MJ$$

The emissions of electrochemically polishing the aluminum are determined by assuming all energy used is electricity. The energy consumption and emissions of the applied voltage of the electrochemical polishing are summarized in Table 5.5.

Table 5.5: Life cycle inventory data for energy of electrochemical polishing of aluminum.

Electrochemical Polishing		
Energy	3.23	MJ
CO_2	0.452	kg
CH_4	3.99E-06	kg
NO_2	9.07E-06	kg

5.2.2 Chemical Production for Electropolishing

The current is applied while the aluminum tube rests in a solution of perchloric acid and ethanol (Guo et al. 2004). The minimum volume of liquid needed is estimated from a box which could encompass the tube. The volume of the box is:

$$V = 31.83cm \times 31.83cm \times 100cm = 101314.89cm^3 = 101.3L$$

However, the aluminum occupies 4.9L of space. The total amount of liquid needed to fill up the remaining space is

$$V = 101.314L - 4.9166L = 96.4L$$

The volume ratio of perchloric acid to ethanol is 1:5 (Guo et al. 2004). The total volumes of both the ethanol and the perchloric acid are determined by solving the following two equations:

$$V_{ethanol} = 5V_{perchloric\ acid}$$

$$V_{ethanol} + V_{perchloric\ acid} = 96.4L$$

Solving these equations yields a volume of 16.1L for the perchloric acid and 80.3L for ethanol.

The perchloric acid used in the mixture has a concentration of 70% (Guo et al. 2004). This concentration, for perchloric acid, is equivalent to a molarity of 11.6. The number of moles of perchloric acid used in the solution is:

$$11.6M = \frac{x\,mol}{16.066L} \rightarrow x = 186.3656mol$$

Using the molar mass of perchloric acid, the total mass used in this solution is:

$$186.3656mol \cdot \frac{100.46g}{mol} = 18722g = 18.722kg$$

Perchloric acid is produced by a reaction of sodium perchlorate and hydrochloric acid (Mendiratta et al. 2005):

$$NaClO_4 + HCl \rightarrow HClO_4 + NaCl$$

Sodium perchlorate is produced by the electrochemical oxidation of sodium chlorate (Mendiratta et al. 2005):

$$NaClO_3 + H_2O \rightarrow NaClO_4 + 2H^+ + 2e^-$$

The electrolysis of sodium chloride is used to produce sodium chlorate (Mendiratta and Duncan 2003):

$$NaCl + 3H_2O \rightarrow NaClO_3 + 3H_2$$

The production of sodium chlorate has six steps: brine treatment, electrolysis, crystallization and salt recovery, chromium removal, hydrogen purification and collection, and electrical distribution (Mendiratta and Duncan 2003). The six step process consumes 4950 to 6050 kWh per ton of sodium chlorate produced (Mendiratta and Duncan 2003). This is approximately 17.82 to 21.78 MJ per kg of sodium chlorate.

The chemical components of perchloric acid are shown in Figure 5.3.

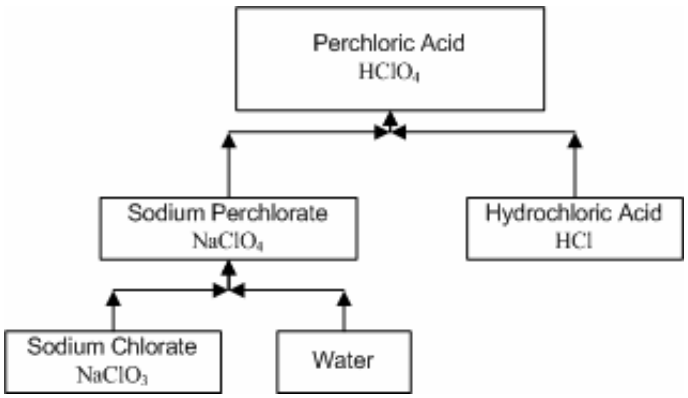

Figure 5.3: Chemical components of perchloric acid.

Life cycle inventory data for the production of sodium chlorate and hydrochloric acid were obtained from the EcoInvent database (Althaus et al. 2004). The complied life cycle inventory data for these chemicals can be found in Appendix A.

The life cycle inventory data for perchloric acid was calculated by making standard assumptions (Hischier et al. 2005) about the two chemical reactions: the reaction of sodium chlorate with water to form sodium perchlorate, and the reaction of sodium perchlorate with hydrochloric acid to form perchloric acid. The life cycle inventory data for the production of 18.722kg of perchloric acid are shown in Table 5.6.

Table 5.6: Life cycle inventory data for the production of 18.722 kg of perchloric acid.

Production of 18.722 kg perchloric acid		
Energy	1290	MJ
Water	628	m^3
CO_2	70.7	kg
CH_4	0.149	kg
N_2O	1.24E-04	kg
Air Emissions	66.5	kg
Water Emissions	6.19	kg
Soil Emissions	0.0214	kg

The ethanol used in this mixture is not diluted. The total mass of ethanol used in this solution is determined from its density:

$$\frac{0.789g}{cm^3}\cdot\left(\frac{100cm}{1m}\right)^3\cdot\frac{1m}{1000L}\cdot 80.3311L = 63381g = 63.381kg$$

The life cycle inventory data of ethanol (Kim and Dale 2005) (compiled in Chapter 3) for 63.381kg is shown in Table 5.7.

Table 5.7: Life cycle inventory data for the production of 63.381kg of ethanol from corn.

Production of 63.381 kg of Ethanol from Corn		
Energy Consumed	1310	MJ
Water Consumed	2.66	m^3
Carbon Dioxide Equivalent	15.7	kg
Nitrous oxide	20.4	kg

5.2.3 Total Life Cycle Inventory of Electropolishing Step

The total life cycle inventory data for the electrochemical polishing of the aluminum, including the energy to produce the applied voltage and the production of chemicals, are shown in Table 5.8.

Table 5.8: Total life cycle inventory for electrochemical polishing of aluminum.

Total of Electrochemical Polishing Step		
Energy	2600	MJ
Water	630	m^3
CO_2	86.7	kg
CH_4	1.48E-01	kg
N_2O	2.04E+01	kg
Air Emissions	66.4	kg
Water Emissions	6.18	kg
Soil Emissions	0.0214	kg

5.3 Life Cycle Inventory of Anodizing

After electropolishing, the aluminum tube is anodized in oxalic acid at 50V for 6 hours (Guo et al. 2004). The anodizing unit process is shown in Figure 5.4.

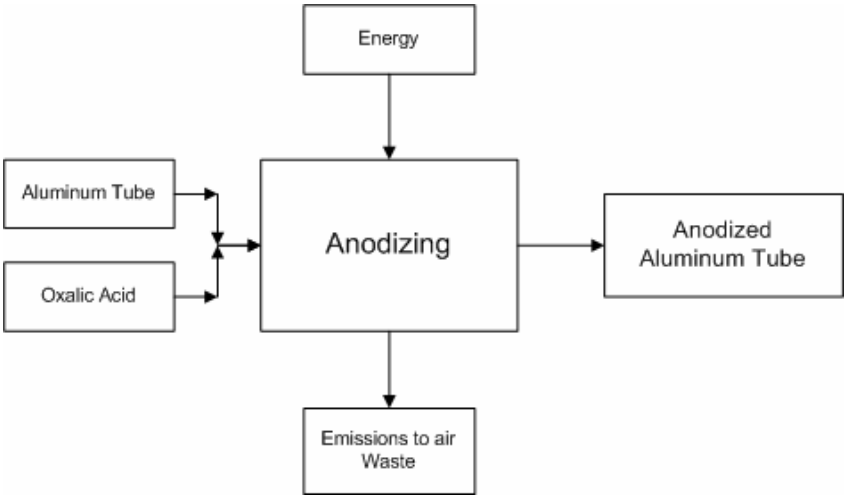

Figure 5.4: Anodizing unit process.

Anodizing occurs when a part is subjected to direct current, while the part rests in an acid bath (Petschel and Hart 2000). The part becomes the anode and oxidation occurs on the surface of the part. For the case of anodizing aluminum, aluminum oxide will form. Meanwhile, hydrogen ions are eventually released to the air. It is an electrolytic reaction.

A few factors influence the resulting surface structure of anodizing, including the current density and the type and temperature of the acid (Petschel and Hart 2000). The acid is normally chilled. A few different types of acid are commonly used, each with different results. Using oxalic acid when anodizing results in a "very hard, wear resistant coating" (Petschel and Hart 2000).

5.3.1 Electricity Consumption of Anodizing

First, the energy consumption of anodizing is considered. The voltage is given, but a current is also required to determine the total energy. The "Rule of 720" is often used to determine the appropriate anodizing time, for a given desired film thickness and applied current density (Couden 2008). The "Rule of 720" is

$$Anodizing\ Time(\min) = \frac{coating\ thickness(mil) \cdot 720}{current\ density\left(\frac{A}{ft^2}\right)}$$

The anodizing time is given as 6 hours, or 360 minutes (Guo et al. 2004). The coating thickness is estimated as the maximum height of surface features – 168.4nm, or approximately 0.010mils. The resulting current density is $0.02\frac{A}{ft^2}$, or $2.15278\times10^{-5}\frac{A}{cm^2}$.

The total energy consumption using this current density is:

$$50V \cdot 2.15278\times10^{-5}\frac{A}{cm^2} \cdot 10000cm^2 \cdot \frac{3600s}{hr} \cdot 6hr = 0.233042MJ$$

The emissions of the applied voltage of the anodizing process can be determined by assuming all energy used is supplied by electricity. The energy consumption and emissions from the applied voltage are summarized in Table 5.9.

Table 5.9: Energy consumption and emissions of applied voltage of anodizing process.

Anodizing		
Energy	0.233	MJ
CO_2	0.0326	kg
CH_4	2.88E-07	kg
N_2O	6.55E-07	kg

5.3.2 Chemical Production for Anodizing

Next, the resource consumption and emissions of producing oxalic acid and cooling it are calculated. The oxalic acid used is a 0.3M aqueous solution (Guo et al. 2004). Assuming that again 96.4L of liquid is used to completely submerge the aluminum tube, the moles of oxalic acid needed are:

$$0.3M = \frac{x\,mol}{96.3974L} \rightarrow x = 28.919mol$$

The molar mass of oxalic acid is used to determine the total mass:

$$28.919mol \cdot \frac{90.03g}{mol} = 2603.60g$$

Gate-to-gate life cycle data were obtained for the production of oxalic acid (Overcash 2008). Oxalic acid ($C_2H_2O_4$) is produced by a reaction of ethylene glycol ($C_2H_6O_2$) and oxygen:

$$C_2H_6O_2 + 2O_2 \text{ -> } C_2H_2O_4 + 2H_2O$$

Nitric acid (HNO_3) and sulfuric acid (H_2SO_4) are used as catalysts in the reaction. The inputs for the production of 1kg of oxalic acid are shown in Table 5.10.

Table 5.10: Inputs for production of oxalic acid (Overcash 2008).

Inputs to produce 1kg oxalic acid		
Ethylene glycol	0.92	kg
Oxygen	0.95	kg
Nitric Acid	0.35	kg
Sulfuric Acid	0.54	kg
Water	0.067	kg

Life cycle inventory data for nitric acid, sulfuric acid, ethylene glycol and oxygen were obtained from the EcoInvent database (Althaus et al. 2004). The life cycle inventory data for these chemicals can be found in Appendix A.

The life cycle inventory data for each of the input chemicals were summed, along with the gate-to-gate data of the oxalic acid. These life cycle inventory data, for the production of 2.603 kg of oxalic acid, are shown in Table 5.11.

Table 5.11: Life cycle inventory data of the production of 2.603 kg of oxalic acid.

Production of 2.603 kg oxalic acid		
Energy	222	MJ
Water	22.6	m^3
CO_2	5.68	kg
CH_4	0.0116	kg
N_2O	2.70E-06	kg
Air Emissions	19.2	kg
Water Emissions	0.824	kg
Soil Emissions	0.0264	kg

5.3.3 Energy Consumption of Cooling Chemicals for Anodizing

During anodizing, the oxalic acid is cooled to 8ºC (Guo et al. 2004). The energy consumption of cooling the oxalic acid is estimated from its specific heat. The specific heat of oxalic acid is $C_p = (1.084 + 0.0318t)\frac{J}{g}$ (Sawada and Murakami 2000). The amount of energy which must be removed from the oxalic acid to cool it from room temperature to 8ºC is:

$$E = (1.084 + 0.0318(20^\circ C)) - (1.084 + 0.0318(8^\circ C))\frac{J}{g} \cdot 2603g = 993.3048J$$

The amount of energy that must be removed to cool the remaining water is

$$4.184\frac{kJ}{kgK} \cdot 91.27kg \cdot (293K - 281K) = 4582kJ$$

The amount of heat gained by the oxalic acid from the warmer surrounding air by convection over the six hour period is estimated. It is assumed that heat is gained from the exposed top of the tank which contains the chemical mixture by free convection. The film temperature for convection (the average of the surface temperature and the ambient air temperature) is 287K. The properties of air at 287K are shown in Table 5.12 (Incropera and DeWitt 2002).

Table 5.12: Properties of air at T_f=287K.

Property	Symbol	Value	Unit
Thermal Conductivity	k	0.02526	W/mK
Kinematic Viscosity	ν	14.73E-6	m^2/s
Thermal Diffusivity	α	20.78E-6	m^2/s
Prandtl Number	Pr	0.71308	
Volumetric Thermal Expansion	β	3.484E-3	1/K

First, the characteristic length of the surface of the exposed oxalic acid solution is calculated:

$$L = \frac{A_s}{P} = \frac{0.3183m^2}{2 \cdot 0.3183m + 2 \cdot 1m} = 0.12072m$$

Next, the Rayleigh number is calculated:

$$Ra_L = \frac{9.8\frac{m}{s^2} \cdot 0.003484\frac{1}{K}(293K - 281K)(0.12072m)^3}{\left(14.733 \times 10^{-6}\frac{m}{s^2}\right)\left(20.784 \times 10^{-6}\frac{m}{s^2}\right)} = 2.354194 \times 10^6$$

The Nusselt number for the top of a cool surface is (Incropera and DeWitt 2002):

$$Nu_L = 0.27Ra_L^{1/4}$$

The Nusselt number for the surface of the chilled solution is:

$$Nu_L = 0.27\left(2.354194 \times 10^6\right)^{1/4} = 10.576$$

The convection coefficient is:

$$\bar{h} = \frac{0.02526\frac{W}{mK}}{0.12072m}(10.576) = 2.2130\frac{W}{m^2K}$$

The rate of heat gained from the surrounding air is:

$$q = 2.2130\frac{W}{m^2K} \cdot 0.3183m^2 \cdot \left(20^\circ C - 8^\circ C\right) = 8.4527W$$

The total heat gained from the surrounding air over 6 hours is:

$$8.4527W \cdot \frac{3600s}{hr} \cdot 6hr = 182.578kJ$$

Heat is also gained through the walls of the tank which contains the acid, by conduction. The rate of heat gain is determined with Fourier's Law:

$$q = kA\frac{dT}{dx}$$

The tank walls first gain heat by convection; this heat is then transferred to the solution by conduction. This heat transfer is illustrated in Figure 5.5.

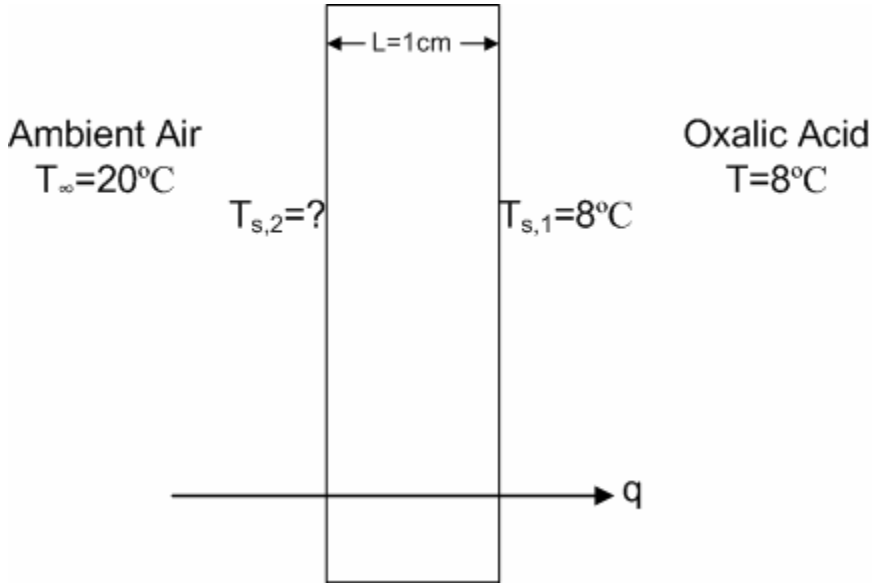

Figure 5.5: Heat transfer from convection and conduction through tank wall.

The total heat transfer rate is determined first by calculating the convection coefficient, the summing the convection thermal resistance with the conduction thermal resistance. The total thermal resistance is

$$U = \frac{1}{\frac{L}{k} + \frac{1}{h}}$$

The equivalent thermal circuit is shown in Figure 5.6.

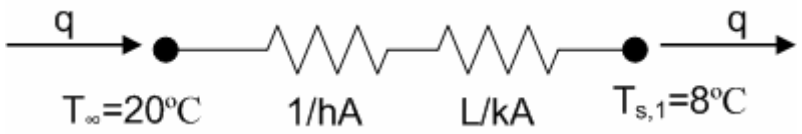

Figure 5.6: Equivalent thermal circuit for convection and conduction heat gain.

The overall heat transfer is determined with

$$q = UA\left(T_{s,1} - T_{\infty}\right)$$

Anodizing tanks are commonly made of polypropylene, which has a thermal conductivity of approximately $k = 0.12\frac{W}{mK}$ (Incropera and DeWitt 2002). From one manufacturer, polypropylene tanks for anodizing are available with wall thicknesses of 1cm (Plating Sales Inc. 2005). With this information, the heat transfer from the surrounding air to the oxalic acid due to conduction and convection is determined.

Determining the heat transfer from the surrounding air to the outside of the tank is not as straightforward as that of the exposed acid, because the conduction and convection occur in series. The ambient temperature, T_{∞}, is assumed to be 20ºC, and the surface temperature on the inside of the tank, $T_{s,1}$, is known to be 8ºC. The surface temperature on the outside of the tank, $T_{s,2}$, is not known, but is needed to determine the film temperature, which is used to determine the properties of air for convection. Because this temperature is not known, it must first be estimated, then the overall heat transfer can be calculated. Because the heat transfer occurs in series, the heat transfer rate of convection is equal to that of conduction, which are both equal to the overall heat transfer rate.

The actual surface temperature on the outside of the tank, $T_{s,2}$, can be calculated once the heat transfer is known

$$T_{s,2} = T_{s,1} - \frac{qL}{kA}$$

This actual $T_{s,2}$ is then used to determine an updated film temperature and updated properties of air for convection. This process is repeated until the estimated $T_{s,2}$ and the calculated $T_{s,2}$ converge.

$T_{s,2}$ is first estimated to be 14ºC; the film temperature is then 290K. The properties of air at 290K are shown in Table 5.13 (Incropera and DeWitt 2002).

Table 5.13: Properties of air at T_f=290K.

Property	**Symbol**	**Value**	**Unit**
Thermal Conductivity	k	0.0255	W/mK
Kinematic Viscosity	ν	15.50E-6	m^2/s
Thermal Diffusivity	α	21.18E-6	m^2/s
Prandtl Number	Pr	0.7096	
Volumetric Thermal Expansion	β	3.448E-3	1/K

The sides of the tank are modeled as vertical plates. The characteristic length for all sides of the tank is equal to the height, 0.3183m. The Rayleigh number of the plate is

$$Ra_L = \frac{9.8\frac{m}{s^2} \cdot 0.003448\frac{1}{K}(293K - 287K)(0.3183m)^3}{\left(15.50\times10^{-6}\frac{m}{s^2}\right)\left(21.18\times10^{-6}\frac{m}{s^2}\right)} = 2.0581\times10^7$$

The Nusselt number for a vertical plate in free convection is (Churchill and Chu 1975):

$$Nu_D = 0.68 + \frac{0.670Ra_D^{1/4}}{\left[1+\left(\frac{0.429}{\Pr}\right)^{9/16}\right]^{4/9}}$$

The Nusselt number for the sides of the tank which are 1m long by 0.3183m high is 35.314. This Nusselt number yields a convection coefficient of $h = 2.82917\frac{W}{m^2K}$. The overall heat transfer coefficient is

$$U = \frac{1}{\frac{0.01m}{0.12\frac{W}{mK}} + \frac{1}{2.829\frac{W}{m^2K}}} = 2.289\frac{W}{m^2K}$$

and the overall heat transfer rate for one of the longer sides of the tank is

$$q = 2.289\frac{W}{m^2K} \cdot 0.318m^2\left(20^\circ C - 8^\circ C\right) = 8.7446W$$

This heat transfer rate is used to calculate the actual $T_{s,2}$:

$$T_{s,2} = 281K - \frac{8.7446W \cdot 0.01m}{0.12\frac{W}{mK} \cdot 0.3183m^2} = 10.2894^\circ C$$

The previously calculated $T_{s,2}$ is used to calculate a new film temperature – 288.7026K. The properties of air at 288.1447K are shown in Table 5.14.

Table 5.14: Properties of air at T_f=288.7026K.

Property	**Symbol**	**Value**	**Unit**
Thermal Conductivity	k	0.025352	W/mK
Kinematic Viscosity	ν	14.83E-6	m^2/s
Thermal Diffusivity	α	21.94E-6	m^2/s
Prandtl Number	Pr	0.71008	
Volumetric Thermal Expansion	β	3.47E-3	1/K

The values of Rayleigh number, Nusselt number, convection coefficient, overall heat transfer coefficient and overall heat transfer for the updated $T_{s,2}$ are shown in Table 5.15.

Table 5.15: Heat transfer values for T_f=288.1447K.

Quantity	Value	Unit
Ra	3.43E+07	
Nu	40.03309	
h	3.18851	W/m^2K
U	2.51915	W/m^2K
q	-9.62214	W

The actual surface temperature on the outside of the tank is calculated from the heat transfer rate to be 10.51915ºC. Because the error between this temperature and the previous surface temperature is only 2.2%, the values for the properties of air and the overall heat transfer are accepted and the process is not repeated.

The heat transfer rate of 9.62W calculated above applies to the two sides of the tank with an area of $0.3183m^2$. The other two sides of the tank have an area of $0.1013m^2$. The heat transfer rate for one of these sides is 3.06W. The total heat transfer rate from all four sides of the tank is therefore 25.4W.

Next the heat transfer through the corners of the tank is considered. The heat transfer due to conduction for this scenario is calculated with (Incropera and DeWitt 2002):

$$q = Sk\Delta T$$

In the previous equation, S is the conduction shape factor (Incropera and DeWitt 2002). The shape factor for the edge of adjoining walls is

$$S = 0.54D$$

where D is the height of the tank. The shape factor for a corner of this tank is 0.171882. The thermal resistance of conduction through the corner of the tank is

$$R = \frac{1}{Sk}$$

Combining the thermal resistance of conduction with that of convection, one finds the over thermal resistances of the two modes of heat transfer in series:

$$R_{total} = \frac{1}{Sk} + \frac{1}{hA}$$

The heat transfer due to both conduction and convection through the corners of the tank is calculated with

$$q = \frac{\Delta T}{R_{total}}$$

Because the surface temperature of the outside of the tank, which is needed to determine the film temperature for convection, is not known, the same iterative approach as above will be used to determine overall heat transfer. Using the previously calculated $T_{s,2}$ of 10.2894ºC as an initial guess of the surface temperature of the outside of the tank, which gives a film temperature of 288.1447K, and the properties of air listed in Table 5.14, the same Rayleigh number, Nusselt number and convection coefficient are calculated as listed in Table 5.16. The thermal resistance is calculated to be 97.75K/W and the heat transfer is 0.123W. These heat transfer values yield an actual $T_{s,2}$ of 13.95ºC.

The calculated $T_{s,2}$ gives an updated film temperature of 289.976K. The properties of air at 289.976K are listed in Table 5.16.

Table 5.16: Properties of air at T_f=289.976K.

Property	**Symbol**	**Value**	**Unit**
Thermal Conductivity	k	0.025498	W/mK
Kinematic Viscosity	ν	14.99E-6	m^2/s
Thermal Diffusivity	α	21.18E-6	m^2/s
Prandtl Number	Pr	0.7096	
Volumetric Thermal Expansion	β	3.449E-3	1/K

The properties of air listed in Table 5.16 are used to calculate the heat transfer quantities shown in Table 5.17.

Table 5.17: Heat transfer values for corners of tank at T_f=289.976K.

Quantity	Value	Unit
Ra	2.59E6	
Nu	21.30236	
h	3.416159	W/m^2K
R	94.46566	K/W
q	-0.1270	W

The $T_{s,2}$ calculated from this heat transfer rate is 14.16ºC, which is a 1.4% error from the estimated $T_{s,2}$, so the heat transfer rate is accepted.

The total amount of heat gained by the oxalic acid from the four sides of the tank over a period of six hours is:

$$25.3697\frac{J}{s}\cdot\frac{3600s}{hr}\cdot 6hr = 547.9855kJ$$

The total amount of heat gained from the four corners of the tank is

$$0.1270\frac{J}{s}\cdot\frac{3600s}{hr}\cdot 6hr = 2.743kJ$$

The total amount of heat which must be removed from the oxalic acid solution to cool it and keep it cooled over 6 hours is 5505.3kJ.

The amount of energy used to cool the oxalic and remove the total heat calculated above is determined by assuming that the heat is removed by an ideal refrigeration cycle. The coefficient of performance for a refrigeration system is

$$COP_R = \frac{Cooling\ Effect}{Work\ input} = \frac{Q_L}{W_{net,in}}$$

The cooling effect, or Q_L, was determined to be 5505.3kJ. For a conservative coefficient of performance of 2, the required net input is 2752.65kJ. The energy and emissions of cooling the oxalic acid, assuming all electricity, are shown in Table 5.18.

Table 5.18: Energy and emissions of cooling oxalic acid for anodizing.

Cooling of Oxalic acid		
Energy	2.75	MJ
CO_2	0.385	kg
CH_4	3.40E-06	kg
N_2O	7.73E-06	kg

The cooling effect calculated above is the theoretical minimum amount of energy which will need to be removed. This cooling effect and the coefficient of performance selected above may not accurately represent an actual system being cooled. For this reason, smaller coefficients of performance should also be considered.

5.3.4 Total Life Cycle Inventory of Anodizing Step

The total life cycle inventory for the anodizing step is determined by summing the data for energy consumption of anodizing, oxalic acid production, and cooling the oxalic acid. The total life cycle inventory data for anodizing are shown in Table 5.19.

Table 5.19: Total life cycle inventory data for anodizing step of production of template.

Total of Anodizing Step		
Energy	224.6	MJ
Water	22.6	m^3
CO_2	6.104	kg
CH_4	0.0116	kg
N_2O	1.10E-05	kg
Air Emissions	19.2	kg
Water Emissions	0.823	kg
Soil Emissions	0.0264	kg

5.4 Life Cycle Inventory of Oxide Removal

The next step in producing the template, after anodizing, is removal of the oxide layer which is formed during anodizing (Guo et al. 2004). The unit process diagram for the oxide removal step is shown in Figure 5.7.

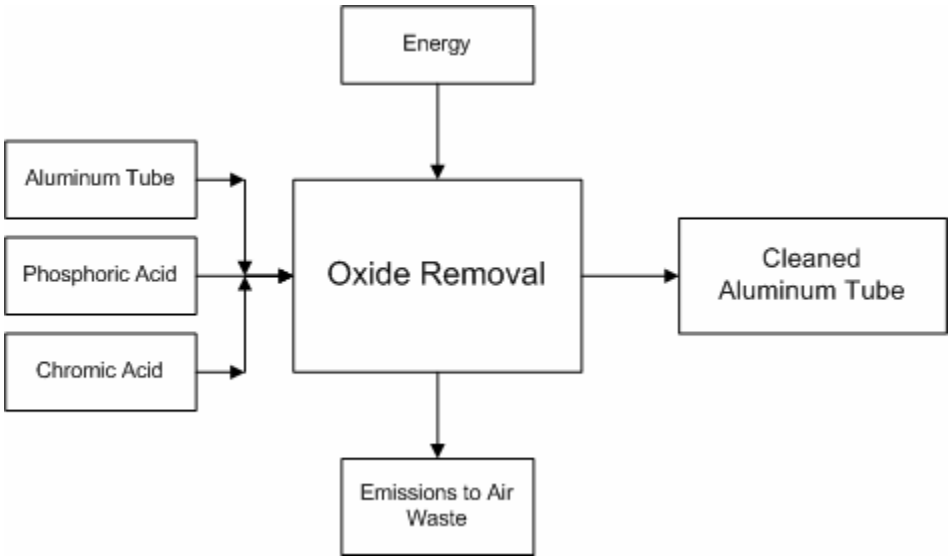

Figure 5.7: Unit process diagram for oxide removal.

5.4.1 Life Cycle Inventory of Chemical Production for Oxide Removal

Oxide removal is accomplished chemically; the template is placed in a mixture of phosphoric acid and chromic acid (Guo et al. 2004). The phosphoric acid has a concentration of 6% by weight, and the chromic acid has a concentration of 1.8% by weight (Guo et al. 2004). If the mixture of the acids is 1:1, each acid will require 48.2L. The amount of pure chromic acid needed for this concentration is determined from the following equations:

$$\frac{m_{acid}}{2.7\frac{g}{cm^3}} + m_{water} = 48.1987L$$

$$\frac{m_{acid}}{m_{acid} + m_{water}} = 0.018$$

Solving these two equations yields 0.878kg of 100% chromic acid.

Similarly, the amount of pure phosphoric acid necessary to produce the solution can be determined from the following equations:

$$\frac{m_{acid}}{1.685\frac{g}{cm^3}} + m_{water} = 48.1987L$$

$$\frac{m_{acid}}{m_{acid} + m_{water}} = 0.06$$

By solving these equations, it is determined that 2.96kg of 100% phosphoric acid is needed to produce 48.2L of 6% phosphoric acid.

Chromic acid (CrO_3) is produced in a reaction of chromium oxide, sodium carbonate, oxygen and sulphuric acid (Overcash 2008):

$$2Cr_2O_3 + 4Na_2CO_3 + 3O_2 + 6H_2SO_4 \rightarrow 4CrO_3 + 2Na_2SO_4 + 4NaHSO_4 + 4H_2O + 4CO_2$$

Gate-to-gate life cycle inventory data were obtained for the production of chromic acid (Overcash 2008). The inputs for the production of 1kg of chromic acid are shown in Table 5.20.

Table 5.20: Inputs for the production of 1 kg of chromic acid.

Inputs to produce 1kg chromic acid		
Chromium ore	2.452	kg
Sulfuric Acid	1.790	kg
Sodium Carbonate	1.710	kg
Water	15.627	kg
Air	1.838	kg

Life cycle inventory data for chromite (chromium ore), sulfuric acid and sodium carbonate were obtained from the EcoInvent LCI database (Althaus et al. 2004). The life cycle inventory data for these chemicals can be found in Appendix A.

The life cycle inventory data for each of the inputs and the data for production of chromic acid from these inputs were summed. Life cycle inventory data for the production of 48.1987L of chromic acid are shown in Table 5.21.

Table 5.21: Life cycle inventory data for the production of 48.1987L of 1.8% chromic acid.

Production of 48.1987L chromic acid		
Energy	57.5	MJ
Water	5.44	m^3
CO_2	1.59	kg
CH_4	0.00177	kg
N_2O	1.03E-08	kg
Air Emissions	0.931	kg
Water Emissions	0.248	kg
Soil Emissions	0.000517	kg

Phosphoric acid (H_3PO_4) is produced from a reaction of phosphate rock, sulfuric acid and water (Overcash 2008):

$$Ca_5(PO_4)_3F + 4H_2SO_4 + 10H_2O \rightarrow 5CaSO_4*2H_2O + 3H_3PO_4 + HF$$

Life cycle inventory data for phosphoric acid were obtained from the EcoInvent database (Althaus et al. 2004). The complied life cycle inventory data for phosphoric acid can be found in Appendix A. The inventory data for the production of 2.96kg of phosphoric acid and the water used to dilute it to 6% concentration are shown in Table 5.22.

Table 5.22: Life cycle inventory data for the production of 48.2L of 6% phosphoric acid.

Production of 48.2L of Phosphoric Acid - 6%		
Energy	58.8	MJ
Water	9.93	m^3
CO_2	3.61	kg
CH_4	0.00631	kg
N_2O	0	kg
Air Emissions	3.81	kg
Water Emissions	0.157	kg
Soil Emissions	0.0646	kg

5.4.2 Life Cycle Inventory of Heating Chemicals for Oxide Removal

The mixture of chemicals is heated to 60ºC for 10 hours. Because this mixture of acids is 95% water, the energy consumption of heating the mixture and keeping it heated for 10 hours will be approximated as that of water. The energy required to heat the water to 60ºC from room temperature is

$$4.184\frac{kJ}{kgK}\cdot 96.3874kg\cdot\left(333K-293K\right)=16.131MJ$$

The amount of heat lost from the exposed water to the surrounding air is again estimated assuming free convection. With a surface temperature of 60ºC and an assumed ambient temperature of 20ºC, the film temperature is 313K. The properties of air at 313K are shown in Table 5.23 (Incropera and DeWitt 2002).

Table 5.23: Properties of air at T_f=313K.

Property	**Symbol**	**Value**	**Unit**
Thermal Conductivity	k	0.027262	W/mK
Kinematic Viscosity	ν	17.19E-6	m^2/s
Thermal Diffusivity	α	24.4E-6	m^2/s
Prandtl Number	Pr	0.70518	
Volumetric Thermal Expansion	β	3.19E-3	1/K

The Rayleigh number for this scenario is:

$$Ra_L = \frac{9.8\frac{m}{s^2} \cdot 3.1949 \times 10^{-3} \left(60^\circ C - 20^\circ C\right)\left(0.12072m\right)^3}{\left(17.1978 \times 10^{-6}\ \frac{m}{s^2}\right)\left(24.424 \times 10^{-6}\ \frac{m}{s^2}\right)} = 5.24555 \times 10^6$$

The Nusselt number for a heated flat surface is calculated using the following equation (Incropera and DeWitt 2002):

$$Nu_L = 0.54 Ra_L^{1/4}$$

The Nusselt number in this case is:

$$Nu_L = 0.54\left(5.24555 \times 10^6\right)^{1/4} = 25.8429$$

The convection coefficient is:

$$\overline{h} = \frac{0.027262\frac{W}{mK}}{0.12072m}\left(25.8429\right) = 5.836\frac{W}{m^2 K}$$

The rate of heat lost to the surrounding air from the exposed water is:

$$q = 5.836\frac{W}{m^2 K} \cdot 0.3183m^2 \cdot \left(60^\circ C - 20^\circ C\right) = 74.304W$$

The amount of heat lost from the exposed water over a period of 10 hours is 2.6749MJ.

Heat is also lost through the tank walls through conduction and from the walls to the ambient air through free convection. The heat transfer scenario is shown in Figure 5.8.

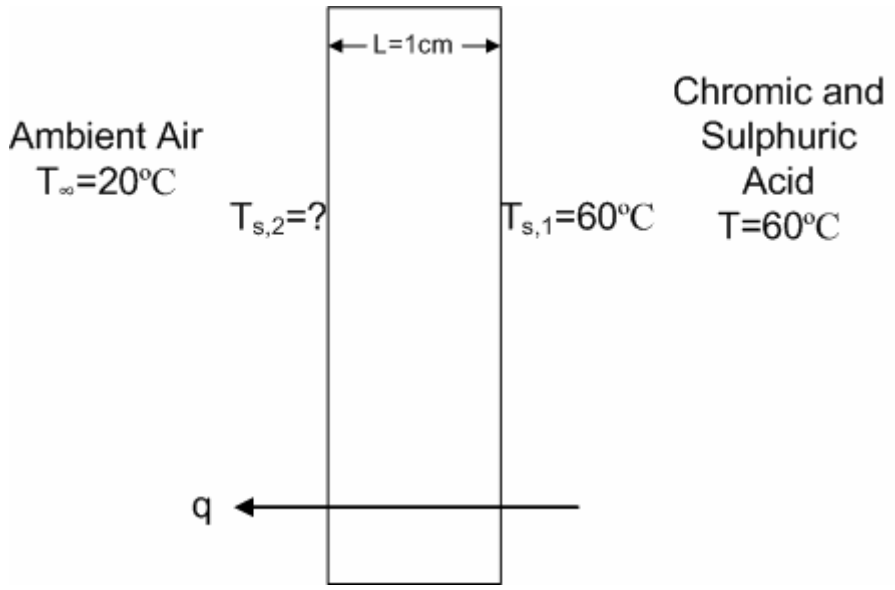

Figure 5.8: Heat transfer from acid solution due to conduction and convection.

The convection coefficient will be calculated in the same fashion as for the case of heat gained for the oxalic acid. The surface temperature on the outside of the tank is first guessed to be 34ºC, yielding a film temperature of 300K. The properties of air at 300K are shown in Table 5.24 (Incropera and DeWitt 2002).

Table 5.24: Properties of air at T_f=300K.

Property	**Symbol**	**Value**	**Unit**
Thermal Conductivity	k	0.0263	W/mK
Kinematic Viscosity	ν	15.89E-6	m^2/s
Thermal Diffusivity	α	22.5E-6	m^2/s
Prandtl Number	Pr	0.707	
Volumetric Thermal Expansion	β	3.33E-3	1/K

With these properties of air and information about the temperature difference of the height of the sides of the tank, heat transfer values are calculated are shown in Table 5.25.

Table 5.25: Heat transfer quantities for T_f=300K and A=0.3183m^2.

Quantity	Value	Unit
Ra	4.13E+07	
Nu	41.87295	
h	3.4598	W/m^{2}K
U	2.6855	W/m^{2}K
q	34.19214	W

This heat transfer rate means that the surface temperature on the outside of the tank is actually 51.04824ºC. This surface temperature is used to calculate a new film temperature of 308.5241K. The properties of air at 308.5241K are shown in Table 5.26 (Incropera and DeWitt 2002).

Table 5.26: Properties of air at T_f=308.5241K.

Property	Symbol	Value	Unit
Thermal Conductivity	k	0.026931	W/mK
Kinematic Viscosity	ν	16.75E-6	m^2/s
Thermal Diffusivity	α	23.76E-6	m^2/s
Prandtl Number	Pr	0.70581	
Volumetric Thermal Expansion	β	3.241E-3	1/K

The heat transfer values were calculated with these updated air properties and are shown in Table 5.27.

Table 5.27: Heat transfer quantities for T_f=306.5K and A=0.3183m^2.

Quantity	Value	Unit
Ra	7.99E+07	
Nu	49.2699	
h	4.1686	W/m^{2}K
U	3.0939	W/m^{2}K
q	39.39113	W

The heat transfer rate is used to calculate $T_{s,2}$, which is now 49.68ºC. The new film temperature is 307.8K, and the properties of air at this temperature are shown in Table 5.28.

Table 5.28: Properties of air at T_f=307.8436K.

Property	Symbol	Value	Unit
Thermal Conductivity	k	0.026880	W/mK
Kinematic Viscosity	ν	16.67E-6	m^2/s
Thermal Diffusivity	α	23.66E-6	m^2/s
Prandtl Number	Pr	0.70590	
Volumetric Thermal Expansion	β	3.25E-3	1/K

The heat transfer quantities are calculated with these properties of air and are shown in Table 5.29

Table 5.29: Heat transfer quantities for T_f=305.8445K and A=0.3183m^2.

Quantity	Value	Unit
Ra	7.72E+07	
Nu	48.856	
h	4.12589	W/m^2K
U	3.07026	W/m^2K
q	39.0905	W

The surface temperature of the outside of the tank is calculated with this heat transfer to be 49.7658ºC, which only represents 0.16% error. This heat transfer rate is accepted. The heat transfer rate is also calculated for the other sides of the tank, which have an area of 0.10131m^2. The heat transfer rate for these sides is 12.44W.

Heat is also lost through the corners of the tank. The same process is used to determine the heat transfer, as was used for the case of the cooled oxalic acid. The first estimated $T_{s,2}$ is selected as 49.69ºC, which is the final $T_{s,2}$ used to determine heat transfer from the walls of the tank. The properties of air listed in Table 5.28 are used to calculate heat transfer properties, which are the same as those listed in Table 5.29, with the exception of resistance of 86.55576K/W (calculated instead of U) and a heat transfer of $q = 0.4261W$. This heat transfer rate yields a $T_{s,2}$ of 37.59ºC.

The calculated $T_{s,2}$ gives a film temperature of 301.7973K. The properties of air at 301.7973K are shown in Table 5.30.

Table 5.30: Properties of air at T_f=301.7973K.

Property	Symbol	Value	Unit
Thermal Conductivity	k	0.026433	W/mK
Kinematic Viscosity	ν	16.07E-6	m^2/s
Thermal Diffusivity	α	22.76E-6	m^2/s
Prandtl Number	Pr	0.70675	
Volumetric Thermal Expansion	β	3.31E-3	1/K

The heat transfer values shown in Table 5.31 were calculated from the properties of air in Table 5.30.

Table 5.31: Heat transfer quantities for corners of tank at T_f=301.7973K.

Quantity	Value	Unit
Ra	5.04E+07	
Nu	43.97776	
h	3.65210	W/m^2K
R	91.49496	K/W
q	0.43718	W

The heat transfer rate shown in Table 5.31 gives a $T_{s,2}$ of 38.80413ºC, which is a film temperature of 302.4021K. The properties of air for 302.4021K are shown in Table 5.32.

Table 5.32: Properties of air at T_f= 302.4021K.

Property	Symbol	Value	Unit
Thermal Conductivity	k	0.026477	W/mK
Kinematic Viscosity	ν	16.13E-6	m^2/s
Thermal Diffusivity	α	22.85E-6	m^2/s
Prandtl Number	Pr	0.70666	
Volumetric Thermal Expansion	β	3.31E-3	1/K

The properties of air shown in Table 5.32 are used to calculated the heat transfer values in Table 5.33.

Table 5.33: Heat transfer quantities for corners of tank at T_f=302.4021K.

Quantity	Value	Unit
Ra	5.33E+07	
Nu	44.59615	
h	3.70973	W/m^2K
R	90.82683	K/W
q	0.44040	W

The heat transfer rate shown in Table 5.33 yields a T_s of 38.64822ºC, which is an error of 0.403% between this $T_{s,2}$ and the previous temperature used to calculate the heat transfer. Because the error is low, the process is not repeated.

The total heat transfer rate through all four sides of the tank is 103.0661W, and the total heat transfer rate through the four corners of the tank is 1.761594W. Over a period of 10 hours, the total heat lost through the four walls and the four corners of the anodizing tank is 3.773MJ. A total of 22.578944MJ is needed to heat the water and to replace the heat lost through conduction and convection. The life cycle inventory data for heating the acid solution for the oxide removal step are summarized in Table 5.34.

Table 5.34: Life cycle inventory data for heating of chemical solution.

Heating for oxide removal		
Energy	22.6	MJ
CO_2	3.16	kg
CH_4	2.79E-05	kg
N_2O	6.34E-05	kg

The energy consumption of heating the chemicals shown above represents the theoretical minimum amount of energy required. For a heater which is less than 100% efficient, the total energy consumption of heating will be

$$E = \frac{22.6MJ}{\eta}$$

where η is the efficiency of the heater. A range of efficiencies will be considered.

5.4.3 Total Life Cycle Inventory of Oxide Removal Step

The total life cycle inventory data for the oxide removal step are determined by summing the life cycle data from the production of the chemicals with the data of the heating of the chemicals. The total life cycle inventory data are shown in Table 5.35.

Table 5.35: Total life cycle inventory data for the oxide removal step.

Oxide Removal Step		
Energy Consumed	139	MJ
Water Consumed	15.4	m^3
Carbon Dioxide emitted	8.36	kg
Methane emitted	8.11E-03	kg
Nitrous oxide	6.35E-05	kg
Total Air Releases	4.75	kg
Total Water Releases	0.405	kg
Total Soil Releases	0.0651	kg

5.5 Life Cycle Inventory of Pattern Transfer

When transferring the nanostructured pattern from the template to the polymeric surface, it is suggested that the template be heated to at least the glass transition temperature of the polymeric surface (Guo et al. 2004). The best results occurred when the template was heated to 150 to 170ºC.

The specific heat of aluminum is approximately $900\frac{J}{kgK}$ (Incropera and DeWitt 2002). The energy required to heat the template to 170ºC from room temperature is:

$$900\frac{J}{kgK}\cdot 13.27kg\cdot\left(443K-293K\right)=1.791MJ$$

This amount of energy will be required to heat the template every time it is used to transfer the pattern to polymeric surface.

Heat is lost from the outside of the aluminum tube to the surrounding air through free convection. The average of the surface temperature and the ambient temperature is

the same for the case the steel template; therefore, the air properties listed in are again used to determine the heat transfer of the aluminum tube.

The Rayleigh number of a cylinder is determined with (Incropera and DeWitt 2002):

$$Ra_D = \frac{g\beta(T_s - T_\infty)D^3}{\nu\alpha}$$

The Rayleigh number for the aluminum template is:

$$Ra_L = \frac{9.8\frac{m}{s^2} \cdot 2.725\times10^{-3}\left(170^\circ C - 20^\circ C\right)(0.3183m)^3}{\left(22.8\times10^{-6}\frac{m}{s^2}\right)\left(32.8\times10^{-6}\frac{m}{s^2}\right)} = 1.727369\times10^8$$

The Rayleigh number is used to determine the Nusselt number. The Nusselt number for a long horizontal cylinder is determined with the following equation (Churchill and Chu 1975):

$$Nu_D = \left(0.60 + \frac{0.387Ra_D^{1/6}}{\left[1+\left(\frac{0.559}{\Pr}\right)^{9/16}\right]^{8/27}}\right)^2$$

The Nusselt number for the aluminum tube template is $Nu_D = 66.76486$. The convection coefficient for a horizontal cylinder is determined with (Incropera and DeWitt 2002)

$$\overline{h} = \frac{k}{D}\overline{Nu}_D$$

The convection coefficient for the aluminum tube is

$$\bar{h} = \frac{0.0313\frac{W}{mK}}{0.3183m}(66.76486) = 6.5653\frac{W}{m^2K}$$

The rate of heat transfer from the outside of the aluminum tube is:

$$q = 6.5653\frac{W}{m^2K}(\pi \cdot 0.3183m \cdot 1m)(170^\circ C - 20^\circ C) = 984.767W$$

The amount of heat lost from the aluminum tube to the surrounding area over 5 minutes is:

$$984.767W \cdot \frac{60s}{\min} \cdot 5\min = 295.43kJ$$

Because the surface of the aluminum tube rests tangent to the polycarbonate surface, the rate of conduction to the polycarbonate is not as easily calculated as for the case of the flat steel template. If a strip of width 1cm of contact is made between the tube and the polymeric surface, the heat transfer rate will be:

$$q = 0.2\frac{W}{mK} \cdot 0.01m^2 \cdot \frac{(170^\circ C - 20^\circ C)}{x} = \frac{0.3}{x}W$$

The heat transfer rate will again vary with the thickness of the polycarbonate material. Again assuming a minimum polycarbonate thickness of 5mm, the heat transfer rate from the aluminum tube to the polycarbonate is 60W. The amount of heat lost to polycarbonate through conduction over the course of 5 minutes is 18kJ.

The total amount of heat which will need to be added to the aluminum to keep it heated for the pattern transfer process is 313.43kJ. The emissions of 313.43kJ of electricity are shown in Table 5.36.

Table 5.36: Energy and emissions of heating template to transfer pattern.

Heating for Pattern Transfer		
Energy	0.313	MJ
CO_2	0.0439	kg
CH_4	3.87E-07	kg
N_2O	8.81E-07	kg

The energy and emissions shown above represent a heater efficiency of 100%. The energy consumption of transferring the pattern for a less efficient heater is

$$E = \frac{0.313MJ}{\eta}$$

where η is the efficient of the device used to heat the template.

5.6 Total Life Cycle Inventory for Production of Aluminum Template

The total life cycle inventory data for the production of the template, for the case of primary production of aluminum, are shown in Table 5.37.

Table 5.37: Total life cycle inventory data for the production of the template, with primary production for aluminum.

Total Inventory for Primary Aluminum		
Energy	4795	MJ
Water	707	m^3
CO_2	138	kg
CH_4	0.189	kg
N_2O	20.4	kg
Air Emissions	138	kg
Water Emissions	8.72	kg
Soil Emissions	38.8	kg

The total life cycle inventory data for the production of the template, with secondary production used for the aluminum, are shown in Table 5.38.

Table 5.38: Total life cycle inventory data for the production of the template, with secondary production for aluminum.

Total Inventory for Secondary Aluminum		
Energy	4202	MJ
Water	707	m^3
CO_2	116	kg
CH_4	0.188	kg
N_2O	20.4	kg
Air Emissions	115	kg
Water Emissions	8.66	kg
Soil Emissions	2.36	kg

The total energy used to produce the aluminum template is 4457MJ for primary aluminum and 3864MJ for secondary aluminum. The amount of energy used for the production of the template that can be attributed to each m^2 of self-cleaning surface produced decreases with increasing uses of the template. The energy per use of the template is shown in Figure 5.9, for both primary and secondary aluminum production.

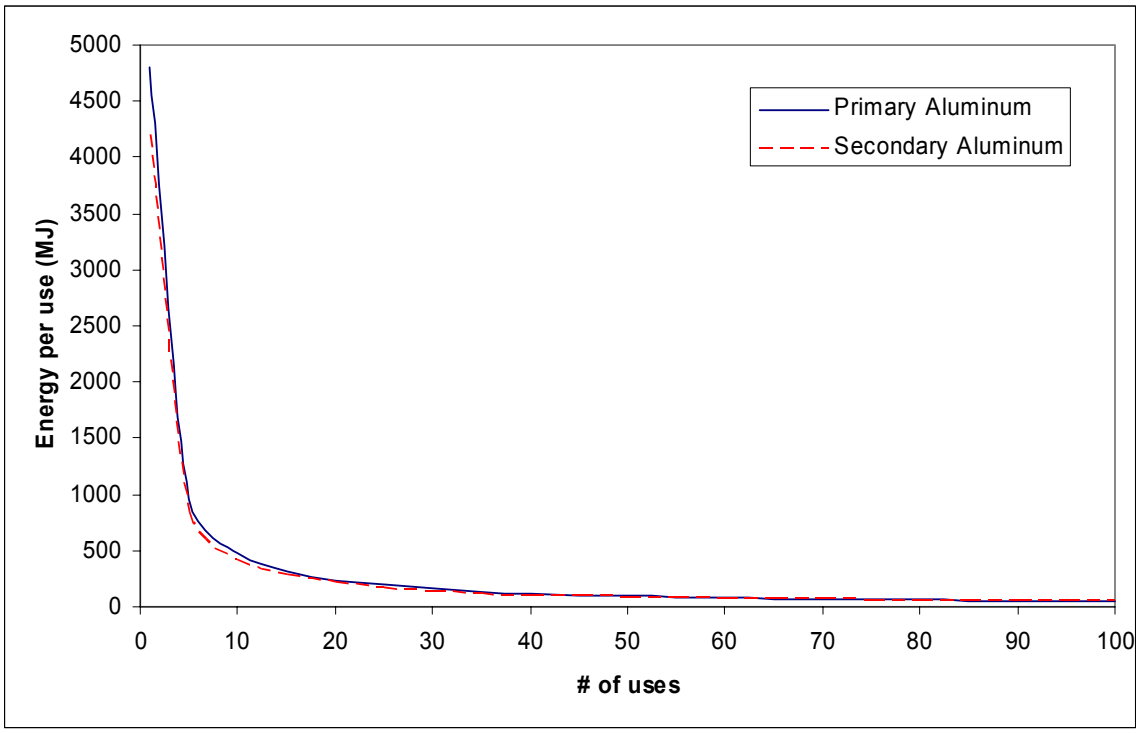

Figure 5.9: Energy consumption per use of the template.

The life cycle inventory data per use for increasing uses, including the energy and emissions associated with transferring the pattern to a polymeric surface, are shown in Table 5.39, for primary aluminum production.

Table 5.39: Life cycle inventory data per use for primary aluminum production.

# of Uses:	1	10	25	50	75	100	
Energy	5160	516	207	103	68.8	51.6	MJ
Water	707	70.7	28.3	14.1	9.43	7.07	m^3
CO_2	190	19.0	7.59	3.80	2.53	1.90	kg
CH_4	1.89E-01	1.89E-02	7.58E-03	3.79E-03	2.53E-03	1.89E-03	kg
N_2O	2.04E+01	2.04E+00	8.17E-01	4.08E-01	2.72E-01	2.04E-01	kg
Emissions:							
Air	139	13.9	5.54	2.77	1.85	1.39	kg
Water	8.72	0.872	0.349	0.174	0.116	0.087	kg
Soil	38.8	3.88	1.55	0.775	0.517	0.388	kg

The life cycle inventory data per use for secondary aluminum production are shown in Table 5.40.

Table 5.40: Life cycle inventory data per use for secondary aluminum production.

# of Uses:	1	10	25	50	75	100	
Energy	4570	457	183	91.4	60.9	45.7	MJ
Water	707	70.7	28.3	14.1	9.43	7.07	m^3
CO_2	167	16.7	6.70	3.35	2.23	1.67	kg
CH_4	1.89E-01	1.89E-02	7.55E-03	3.77E-03	2.52E-03	1.89E-03	kg
N_2O	2.04E+01	2.04E+00	8.17E-01	4.08E-01	2.72E-01	2.04E-01	kg
Emissions:							
Air	115	11.5	4.60	2.30	1.53	1.15	kg
Water	8.66	0.866	0.346	0.173	0.115	0.087	kg
Soil	2.36	0.236	0.094	0.047	0.031	0.024	kg

The production of the aluminum template requires a large amount of water- over $707m^3$. Much of this water is consumed during production of the chemicals used in electropolishing, anodizing and oxide removal, particularly the sodium chlorate used to produce perchloric acid.

5.7 Reduction of Inventory from Water Treatment and Chemical Recycling

In an industrial setting, the chemicals used for electropolishing, anodizing and oxide removal will not be completely replaced after one use (Munns 1993). These chemicals can be filtered or treated and reused multiple times. Doing so will diminish the amount of environmental impacts of chemical use in manufacturing a template that can be attributed to each template produced.

One method often used to filter chemical solutions used in anodizing processes is diffusion dialysis (US EPA 2000). In diffusion dialysis, a membrane is used to separate waste metals and contaminates from the acid solution (Munns 1993). Diffusion dialysis is typically used when the contaminants reach 1 gram per liter of solution. Energy consumption for solution pumping is small (Munns 1993), and will therefore be ignored. When employing diffusion dialysis to filter solutions, typically 80 to 95% of the solution is able to be reused, while 5 to 20% is waste and will need to be treated (US EPA 2000).

It is estimated that for every square meter of aluminum surface area anodized, 10 grams of aluminum are dissolved, and 2.1 kg of waste sludge are produced (Munns 1993). For 96.3974L of anodizing solution, this is a concentration of 22 grams of contamination per liter of anodizing solution. Therefore, the solution should be filtered after each part that is anodizing.

Approximately 5 to 20% of the total oxalic acid solution will need to be replaced after each anodized part. The life cycle inventory data of 5 to 20% of the total volume of oxalic acid solution are shown in Table 5.41.

Table 5.41: Inventory of 5 to 20% of oxalic acid replacement.

Waste of Filtration of Oxalic Acid			
	5%	**20%**	
Energy	11.1	44.3	MJ
Water	1.13	4.53	m^3
CO_2	0.284	1.14	kg
CH_4	0.000582	0.00233	kg
N_2O	1.35E-07	5.41E-07	kg
Air Emissions	0.960	3.84	kg
Water Emissions	0.0412	0.165	kg
Soil Emissions	0.00132	0.00528	kg

If a similar filtration and replacement scenario is also considered for electropolishing and oxide removal, then the total inventory of chemicals that can be attributed to each template produced will be 5 to 20% of the total of all chemicals used. The life cycle inventory of 5 to 20% of the total amount of chemicals is shown in Table 5.42.

Table 5.42: Inventory for 5 to 20% chemical replacement per template produced.

Waste of Filtration of Electropolishing Solution			
	5%	**20%**	
Energy	147.0997	588.3987	MJ
Water	33.45051	133.8021	m^3
CO_2	4.865088	19.46035	kg
CH_4	0.008419	0.033677	kg
NO_2	1.020719	4.082877	kg
Air Emissions	4.522094	18.08838	kg
Water Emissions	0.371027	1.484109	kg
Soil Emissions	0.005648	0.022591	kg

One must also consider the initial volume of oxalic acid used in anodizing. The life cycle inventory of the original volume of acid used to fill the tanks that can be attributed to each part is equal to that total volume divided by the number of times the acid is used. However, with enough uses of the oxalic acid, the inventory of the original acid that can be attributed to each part approaches zero; this would be the best scenario possible for the manufacture of the template.

The energy consumption of the production template for primary aluminum with 5% acid replacement per use of the chemicals, for ranges of times the template is used and times the anodizing chemicals are recycled, is shown in Figure 5.10.

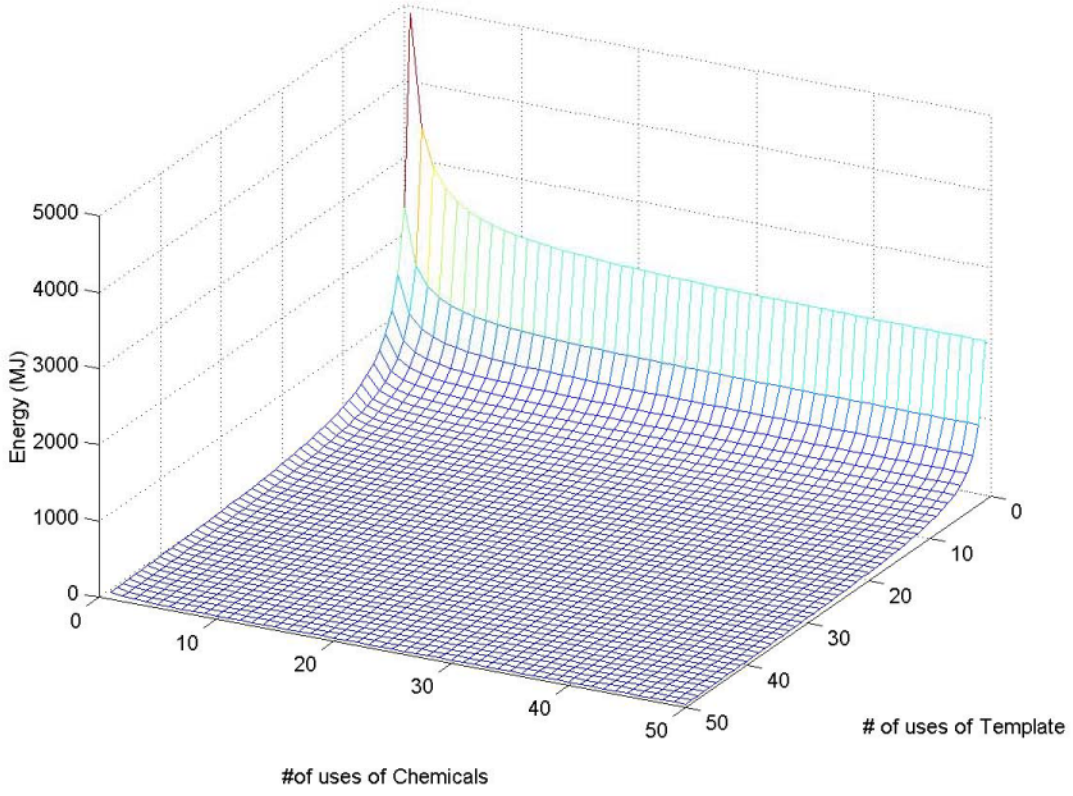

Figure 5.10: Energy consumption of production of aluminum template.

As shown above, the more times the chemicals can be recycled before replacement and the more times the template can be used, the less of the life cycle inventory that can be attributed to each m^2 of surface produced. Life cycle inventories for ranges of values of template uses, chemical uses and amount of chemical replaced per filtration have been calculated. Tables of these inventory values can be found in Appendix B.

However, each template may not be used the same number of times, and the anodizing chemicals may need to be replaced sooner than anticipated. Also, with a range

of possible values for the amount of chemicals lost after filtration (5 to 20%), it may not be possible to always replace the same amount. For these reasons, average or most likely values are need for the life cycle inventory of a self-cleaning surface produced with an anodized aluminum template. These values have been calculated with an uncertainty analysis; the method and results are described in Appendix D.

5.8 Parametric Analysis

The life cycle inventory of the production of the anodized aluminum template depends heavily on the size of the template. An increase in any dimension of the template increases the amount of aluminum, water and chemicals consumed. Because the thickness of the aluminum template was selected to be similar to the dimensions of the steel template and was not a value taken from experimental procedures, it may not represent a realistic value that a designer would choose. For these reasons, a parametric analysis was performed for the life cycle inventory of the production of this template.

A spreadsheet was developed in which a user can select the length, radius and thickness of the cylindrical templates. The amount of aluminum then is calculated, as well as the perchloric acid and ethanol needed for electropolishing, oxalic acid for anodizing and chromic and phosphoric acid for oxide removal. Updated values are obtained for the energy consumption and emissions of the applied voltages for electropolishing and anodizing. Approximate values of energy of heat transfer are calculated for the heating or cooling of the chemicals.

For example, with all other values kept the same, the thickness of the template was changed to 1 cm. The life cycle inventory values for this thickness are shown in Table 5.43.

Table 5.43: Inventory for the production of a template with thickness of 1cm.

Template Thickness 1cm			
	Primary	**Secondary**	
Energy	6020	4860	MJ
Water	670	670	m^3
CO_2	154	110	kg
CH_4	0.180	0.178	kg
N_2O	19.4	19.4	kg
Air Emissions	156	110	kg
Water Emissions	8.35	8.22	kg
Land Emissions	75.7	4.40	kg

5.9 Summary

The life cycle inventory for an anodized aluminum template used to produce a self-cleaning surface has been complied. This inventory includes: materials acquisition and production of aluminum; perchloric acid, ethanol, oxalic acid, chromic acid, and phosphoric acid production; energy consumption and emissions of applied voltages for electropolishing and anodizing; energy consumption and emissions for heating and cooling of chemicals; and energy consumption of heating the template to transfer the pattern to a polymeric surface.

Ranges of values for the inventory were calculated for varying total uses of the templates, total uses of the chemicals and amount of chemicals replaced per filtration and are given in Appendix B. A spreadsheet also was developed in which a user can change the dimensions of the template and received production life cycle inventory values. An uncertainty analysis was also performed; the procedure and results are described in Appendix D.

The total minimum energy consumed in the production of the particular template analyzed in this chapter is 4750MJ, for secondary sources of aluminum. This is more

than twice the total maximum energy used in the production of the laser ablated steel template. Although the inventory values for the production of the anodized aluminum template are higher than those of the steel template, the anodized aluminum template could have less environmental impacts, if efficient chemical recycling scenarios are employed.

CHAPTER 6

USE PHASE/CLEANING LIFE CYCLE INVENTORY

6.1 Self-Cleaning Surfaces

Self-cleaning surfaces are successfully cleaned with mist and fog (Fürstner and Barthlott 2005). Estimations of energy and water consumption and emissions for cleaning will be based on a mist cleaning process. The life cycle inventory data first will be determined for the ideal case, to determine a minimum, and then calculated for a more realistic scenario.

Self-cleaning surfaces require 1500 mL of water per square meter of surface for mist cleaning (Fürstner and Barthlott 2005):

$$V = 1500\frac{mL}{m^2}(A)$$

For the functional unit of $1m^2$, the total amount of water necessary for cleaning is 1.5 kg of water or 0.0015 m^2.

The minimum amount of energy used to clean the surface first is estimated using ideal thermodynamic principles. The water is assumed to be applied to the surface with a pump. The energy consumption of the pump is determined with the 1st law of thermodynamics:

$$\Delta E = Q_{12} - W_{12} + \Sigma m_{in}\left(h + \frac{s^2}{2} + gz\right)_{in} - \Sigma m_{out}\left(h + \frac{s^2}{2} + gz\right)_{out}$$

The equation is reduced for the case of steady-state, no heat transfer, no changes in potential or kinetic energy, and one inlet and one outlet. The pump is also assumed to be isentropic. The total work performed by such a pump is determined with:

$$W_{actual} = \frac{mv(P_2 - P_1)}{\eta_p}$$

The surface is cleaned with high pressure fog (Fürstner and Barthlott 2005). The high pressure of the fog is estimated to be 1000 psi, or 6895 kPa, from specifications of fog machines (Advanced Misting Systems). With a pump efficiency of 0.9, the total work performed by the pump is:

$$W_{actual} = \frac{1.5(6895 - 101)}{0.9} = 11.323kJ$$

This amount of work represents the minimum energy needed to power a pump to deliver the water to clean 1m^2 of self-cleaning surface. The emissions associated with powering this pump are determined assuming electricity is use. The emissions are $1.585 \times 10^{-6} tons\, CO_2$, $1.398 \times 10^{-8} kg\, CH_4$ and $3.18 \times 10^{-8} kg\, N_2O$. The energy consumption, water consumption, and emissions of cleaning 1 m^2 of self-cleaning surface are summarized in Table 6.1.

Table 6.1: Minimum energy, water consumption, and emissions of cleaning.

Cleaning of 1m^2 of surface with mist		
Energy	11.3	kJ
Water	0.0015	m^3
CO_2	0.00160	kg
CH_4	1.40E-8	kg
N_2O	3.18E-8	kg

More accurate life cycle inventory data are complied for the cleaning of a self-cleaning surface from the energy consumption specifics of the pump. For a pump that operates at 1000psi and can have a flow rate of either 0.5 or 1 gallons per minute, the

pump uses 110 V at 6 to 12 amps (Advanced Misting Systems). The minimum power consumption is:

$$110V \cdot 6A = 660W$$

and the maximum is

$$110V \cdot 12A = 1320W$$

For a flow rate of 1 gallon per minute, or 63.09mL/s, approximately 23.77 seconds are needed to deliver the 1500mL to clean $1m^2$. For a flow rate of 0.5gpm, or 31.545mL/s, the time increases to 47.55 seconds. The minimum total energy consumed by the pump is

$$660W \cdot 23.77s = 15.69kJ$$

while the maximum is

$$1320W \cdot 47.55s = 62.767kJ$$

The emissions of providing this power with only electricity are determined, and the life cycle data are shown in Table 6.2.

Table 6.2: Life cycle data for cleaning from pump specifications.

Cleaning of $1m^2$ of surface with mist			
	Minimum	**Maximum**	
Energy Consumed	15.7	62.8	kJ
Water Consumed	0.0015	0.0015	m^3
Carbon Dioxide	0.0022	0.0088	kg
Methane	1.94E-08	7.75E-08	kg
Nitrous oxide	4.41E-08	1.76E-07	kg

6.2 Industrial Cleaning

6.2.1 Functional Unit for Industrial Cleaning

Two commons ways to clean metal are ultrasonic cleaning and spray cleaning (Murphy 2000); these methods are described in more detail in Chapter 2. To summarize,

in ultrasonic cleaning, the part to be cleaned is submerged in a solution of water and solvent, and sound waves are used to produce bubbles through cavitation. The vibration of the bubbles removes contaminants from the part. In spray cleaning, a solution of water and solvent is sprayed from many angles onto a part. Spray cleaning machines often have additional rinse and drying stations.

These cleaning machines have a maximum volume capacity. An envelope volume for the part to be cleaned must be determined; this volume does not reflect the details of the part, simply the minimum prism volume in which the part can fit. A total of $1m^2$ of surface could occupy a large range of volumes; a very intricate part, such as a gear, will have a large surface area to volume ratio, while a simpler part could occupy a larger volume for the same surface area. Therefore, a range of part envelope volumes should be considered when estimating the necessary size and energy consumption of an industrial cleaning machine for the functional unit of $1m^2$.

In a recent life cycle assessment, the environmental impacts of remanufacturing parts was analyzed, including a cleaning step (Govetto 2008). One part analyzed in this assessment was a gear. The volume of enough such gears to provide $1m^2$ of surface area is calculated to be approximately 12L. This volume was selected as the lower bound for the new functional unit, as gears are more intricate parts and have a high surface area to volume ratio than other parts. An upper range of 150L for the part volume was selected, as this was the largest volume that a cleaning machine could hold analyzed in the remanufacturing LCA.

6.2.2 Spray Cleaning Energy

Energy consumption and other specifications were determined from spray cleaning machine industry websites (Uniwashers 2007). The spray cleaning machine requires that 2/3 of the tank capacity be reserved for solution. For 150 L volume part, with 300 L of solution, a total volume of 450 L is needed. The closest available spray cleaning machine has a capacity of 600 L; this machine consumes 25.4 kW (Uniwashers 2007). Cleaning times in cabinet spray cleaning machines range from 1-10 minutes (Murphy 2000). The range of energy consumptions to clean the 150L part is:

$$25.4\frac{kJ}{s}\cdot\frac{60s}{\min}\cdot t = 1.524(t)MJ$$

where t is the cleaning time, in minutes. The range of greenhouse gas emissions from cleaning this part, assuming electricity is used to power the spray machine, are $0.2133(t)kg\ CO_2$, $1.882\times10^{-6}(t)kg\,CH_4$, and $4.282\times10^{-6}(t)kg\,N_2O$. The energy consumption and associated emissions for the range of cleaning times is shown in Table 6.3.

Table 6.3: Energy consumption and emissions of spray cleaning a 150L part.

150L part Spray Cleaning Electricity			
	1 minute	10 minute	
Energy	1.52	15.2	MJ
CO_2	0.213	2.13	kg
CH_4	1.88E-06	1.88E-05	kg
N_2O	4.28E-06	4.28E-05	kg

When considering the energy consumption of cleaning the smaller 12 L volume part, a smaller machine is needed. However, the smallest capacity spray machine has a total tank volume of 200 L. The 200 L capacity machine uses 6.75 kW (Uniwashers 2007). The total energy consumption of this machine is:

$$6.75\frac{kJ}{s}\cdot\frac{60s}{\min}\cdot t = 405(t)kJ$$

where *t* is again the cleaning time in minutes. The green house gas emissions, assuming all electricity, are shown in Table 6.4 for a range of cleaning times.

Table 6.4: Energy consumption and emissions of spray cleaning a 12L part.

12L part Spray Cleaning Electricity			
	1 minute	10 minute	
Energy	0.405	4.05	MJ
CO_2	0.0567	0.567	kg
CH_4	5.00E-07	5.00E-06	kg
N_2O	1.14E-06	1.14E-05	kg

6.2.3 Ultrasonic Cleaning Energy

Energy consumption and specifications for ultrasonic cleaning machines were determined from a retailer's website (R.K. Transonic 2007). The manufacturers of the ultrasonic cleaning machine also recommend that 2/3 of the tank capacity volume be solution; there the total part envelope volumes can only be 1/3 of the machines capacity.

One available machine has a capacity of 450 L. This machine can clean a part or parts with a total volume of 150 L and requires 300 L of solution. The particular machine to clean a 150 L volume of parts uses 14.8 kW between heating and the ultrasonic power (R.K. Transonic 2007). The total cleaning time depends on the type and amount of contaminants. Ultrasonic cleaning machines are more efficient and therefore require shorter cleaning times than immersion cleaning (Murphy 2000). For this reason, a total cleaning time of 1-10 minutes will also be analyzed for ultrasonic cleaning scenarios. Therefore, the total energy consumption is

$$14.8\frac{kJ}{s}\cdot\frac{60s}{\min}\cdot t = 888(t)kJ$$

The energy consumptions and emissions from electricity are shown in Table 6.5, for the range of cleaning times.

Table 6.5: Energy and emissions from the ultrasonic cleaning of a 150L part.

150L part Ultrasonic Cleaning Electricity			
	1 minute	10 minute	
Energy	0.888	8.88	MJ
CO_2	0.12432	1.2432	kg
CH_4	1.10E-06	1.10E-05	kg
N_2O	2.50E-06	2.50E-05	kg

For the lower bound of a 12L part, 24 L of solution for cleaning is needed, for a total volume of 36 L. The smallest machine which could handle this volume has a tank capacity of 92 L and uses 4000 W for heating and cleaning (R.K. Transonic 2007). The range of energy consumed by this machine is:

$$4\frac{kJ}{s}\cdot\frac{60s}{\min}\cdot t = 240(t)kJ$$

The energy and emissions of electricity for a range of cleaning times is shown in Table 6.6.

Table 6.6: Energy and emissions of the ultrasonic cleaning of a 12L part.

12L part Ultrasonic Cleaning Electricity			
	1 minute	10 minute	
Energy	0.24	2.4	MJ
CO_2	0.0336	0.336	kg
CH_4	2.96E-07	2.96E-06	kg
N_2O	6.74E-07	6.74E-06	kg

6.2.4 Solvents

A commonly used solvent in the metal cleaning industry is trichloroethylene (US EPA 2004). The life cycle inventory data of trichloroethylene (TCE) was gathered from the EcoInvent database, and the fuel inputs are shown in Table 6.7 (Althaus et al. 2004).

Table 6.7: Energy inputs for the production of trichloroethylene.

Energy Inputs for Production of TCE		
Coal, Brown	0.006528	kg
Coal, Hard	0.40085	kg
Natural Gas	0.37535	m^3
Oil, Crude	0.4518	kg

The total energy consumed from combusting these fuels, using the energy content of each fuel, is $E = 40.24MJ$. The total CO_2, CH_4, and N_2O emissions from these fuels are $3.20kg\,CO_2$, $0.00212kg\,CH_4$, and $1.05\times10^{-5}\,kg\,N_2O$.

The life cycle inventory data for trichloroethylene (TCE) are shown in Table 6.8 (Althaus et al. 2004).

Table 6.8: Life cycle inventory data for the production of trichloroethylene.

Production of 1 kg of Trichloroethylene		
Energy	40.3	MJ
Water	0.0858	m^3
CO_2	3.22	kg
CH_4	0.00230	kg
N_2O	1.05E-5	kg
Air Emissions	0.0936	kg
Water Emissions	0.619	kg
Soil Emissions	6.56E-6	kg

Typical concentrations of solvent for spray cleaning range from 4 to 30 g/L (Murphy 2000). Both high and low concentrations are considered for each scenario of spray cleaning. For the case of a 150 L volume part and a solvent concentration of 4 g/L, the amounts of water and solvent necessary for 300 L of cleaning solution are determined from:

$$Water \cdot \frac{4g\,TCE}{L} \cdot \frac{1kg}{1000g} = Solvent$$

$$Water + Solvent\left(\frac{1L}{1.46kg}\right) = 300L$$

The solution to these two equations is 299.18L water and 1.1967 kg TCE. The inventory data of the production of 1.1967 kg of solvent and water consumption for 300L of solution are shown in Table 6.9.

Table 6.9: Life cycle inventory data for the production of 300L of cleaning solution, with 4g/L solvent, for spray cleaning.

Spray Cleaning - 4g/L – 300L Cleaning Solution		
Energy	48.17	MJ
Water	0.402	m^3
CO_2	3.85	kg
CH_4	0.003	kg
N_2O	1.26E-05	kg
Air Emissions	0.112	kg
Water Emissions	0.741	kg
Soil Emissions	7.85E-06	kg

This process is repeated for the range of solvent concentrations, part sizes, and for both spray and ultrasonic cleaning. The amount of water and tricholorethylene needed for each cleaning scenario is shown in Table 6.10.

Table 6.10: Water and TCE amounts for cleaning scenarios.

Cleaning Scenario	Water (L)	TCE (kg)
Spray 300L, 4g/L	299.18	1.1967
Spray 300L, 30g/L	293	8.82
Spray 24L, 4g/L	23.93	0.0957
Spray 24L, 30g/L	23.52	0.705
Ultrasonic 300L, 75g/L	285.34	21.4
Ultrasonic 24L, 75g/L	22.82	1.712

The equations used to determine the total amounts of water and tricholoethylene, and the resulting life cycle inventory of the total cleaning solution are shown in Appendix C.

6.2.5 Recycling of Aqueous Cleaning Solution

The cleaning solution used for both spray cleaning and ultrasonic cleaning can be filtered and reused, thereby lowering the environmental impact associated with each

cleaning cycle (US EPA 2000). Instead of attributing the production of 24 to 300L of cleaning solution to each part cleaned, only a fraction will be part of each cleaning cycle's inventory.

Aqueous cleaning solutions also can be filtered and reused with diffusion dialysis, as was investigated for the recycling of anodizing solutions (US EPA 2000). It is assumed that the cleaning solution will be filtered after each cleaning. Replacement rates of 5 and 20% of the solution per cleaning again will be analyzed, like for the recycling of the anodizing chemicals in Chapter 5. The life cycle inventory that can be attributed to each part cleaned is the total volume of cleaning solution needed to fill the machines divided by the number of times it will be recycled, in addition to the 5 to 20% of the solution that must be replaced after each filtering and the energy need to run the machines each time.

The life cycle inventory data including recycling are shown for multiple cleaning scenarios in Appendix C. Best and worst inventory values are selected for each part size and cleaning method, and are shown in the following four tables. The best scenario has the lowest cleaning time, lowest solvent concentration, 5% replacement per filtration and the initial volume of chemicals is used at least 100 times. In the worst scenario, the highest cleaning time and solvent concentration is used, and the chemicals are completely replaced after each cleaning cycle. The best and worst life cycle inventories are given for the range of parts sizes and for both spray and ultrasonic cleaning, in the following four tables.

Table 6.11: Best and worst scenarios for spray cleaning of 12L part.

12L Spray			
	Best	**Worst**	
Energy	0.636	32.4	MJ
Water	0.002	0.084	m^3
CO_2	0.075	2.838	kg
CH_4	1.37E-05	1.62E-03	kg
N_2O	1.20E-06	1.88E-05	kg
Air Emissions	0.001	0.0660	kg
Water Emissions	0.004	0.437	kg
Soil Emissions	3.76E-08	4.62E-06	kg

Table 6.12: Best and worst scenarios for spray cleaning of 150L part.

150L Spray			
	Best	**Worst**	
Energy	4.414	370	MJ
Water	0.024	1.05	m^3
CO_2	0.445	30.54	kg
CH_4	1.82E-04	0.020	kg
N_2O	5.04E-06	1.35E-04	kg
Air Emissions	0.007	0.825	kg
Water Emissions	0.044	5.46	kg
Soil Emissions	4.71E-07	5.78E-05	kg

Table 6.13: Best and worst scenarios for the ultrasonic cleaning of 12L part.

12L Ultrasonic			
	Best	**Worst**	
Energy	4.37	71.2	MJ
Water	0.01	0.170	m^3
CO_2	0.364	5.84	kg
CH_4	3.38E-02	3.92E-03	kg
N_2O	1.75E-06	2.47E-05	kg
Air Emissions	0.01	0.16	kg
Water Emissions	0.064	1.06	kg
Soil Emissions	6.72E-07	1.12E-05	kg

Table 6.14: best and worst scenarios for ultrasonic cleaning 150L part.

150L Ultrasonic			
	Best	**Worst**	
Energy	52.6	870	MJ
Water	0.127	2.12	m^3
CO_2	4.26	70.2	kg
CH_4	2.95E-03	4.91E-02	kg
N_2O	1.60E-05	2.50E-04	kg
Air Emissions	0.12	2.00	kg
Water Emissions	0.795	13.25	kg
Soil Emissions	8.40E-06	1.40E-04	kg

6.3 Summary

The life cycle inventory for the use phase, cleaning, has been complied. For the self-cleaning surfaces, cleaning is accomplished with high pressure mist. For the conventional cleaning, spray and ultrasonic cleaning methods are analyzed. A range of values for parts sizes, solvent concentration, solvent recycling and cleaning times is considered. Worst and best case scenarios are selected for each type of industrial cleaning, for the range of parts sizes.

The best industrial cleaning scenario is found to consume 10 times more energy than the maximum value of mist cleaning a self-cleaning surface. The mist cleaning uses less water than the industrial cleaning methods, and produces less greenhouse gasses. When considering just the use phase of the life cycle, self-cleaning surfaces are superior to industrial cleaning methods. The impacts of the entire life cycle of the self-cleaning surface, however, may be larger than the best industrial cleaning scenario. These impacts will be determined in Chapter 7.

CHAPTER 7

LIFE CYCLE IMPACT ASSESSMENT

7.1 Selection and Definition of Impact Categories

Impact Categories of interest in this study are:

- Energy Use
- Water Use
- Global Warming Potential
- Human Health

The first two impact categories have been selected because lowering resource consumption (energy and water) can be seen as more sustainable. The water use tallied in the life cycle inventory represents the throughput of water in each process; the water may be reused or recycled. Global warming potential is selected because climate change is currently an important issue amongst environmentalists, and lowering the greenhouse gas emissions of systems is a common goal of designers. Human health is selected as an impact category, as adverse effects to human health should be avoided when choosing the best design option.

7.2 Classification and Characterization

The following LCI data will be assigned the impact category of Global Warming:

- Carbon Dioxide (CO_2)
- Methane (CH_4)
- Nitrous Oxide (N_2O)

The water consumed in the life cycle will be classified to the categories of Water Use. The Human Health Impact Category is measured from the total air, water and soil release of the LCI data.

7.3 Global Warming Potential

To determine the total impact of the three gases which fall under the impact category of Global Warming Potential, the masses of each must be combined to form a mass of CO_2 equivalent, which gives their global warming potential (GWP) for 100 years. The international standards (IPCC 2001) for these equivalents are shown in Table 7.1.

Table 7.1: Greenhouse gasses CO_2 equivalencies.

Name	Formula	GWP
Carbon Dioxide	CO_2	1
Methane	CH_4	23
Nitrous oxide	N_2O	296

Global warming potential is calculated with:

$$GWP = \sum_i \left(m_i \times GWP_i \right)$$

7.4 Comparison of Three Methods of Producing a Self-Cleaning Surface

The life cycle inventory data for the three methods of producing a self-cleaning surface are shown in Table 7.2. The best scenarios have been selected for both templates methods. For the case of the laser ablated template, the best scenario is when the template can be used at least 100 times. For the anodized template, the best case occurs when the template is used at least 100 times, and the chemicals are recycled indefinitely, and when secondary aluminum sources are used.

Table 7.2: Average life cycle inventory values for all self-cleaning surface manufacture methods

	Chemical Coating	Laser Ablation - Best	Anodized - Best	
Energy	16.9	12.256	11.0025	MJ
Water	0.521	0.0090	0.33451	m^3
CO_2	0.764	1.6298	0.16835	kg
CH_4	3.42E-04	6.26E-06	8.54E-05	kg
N_2O	1.88E-01	1.92E-03	0.01021	kg
Waste:				
Air	0.0738	0.932	0.05197	kg
Water	0.121	0.003	0.00379	kg
Soil	5.46E-05	3.70E-01	0.02157	kg

7.4.1 Energy Consumption

The total energy consumption for the production of $1m^2$ of self-cleaning surface for each method of manufacture is shown in Figure 7.1.

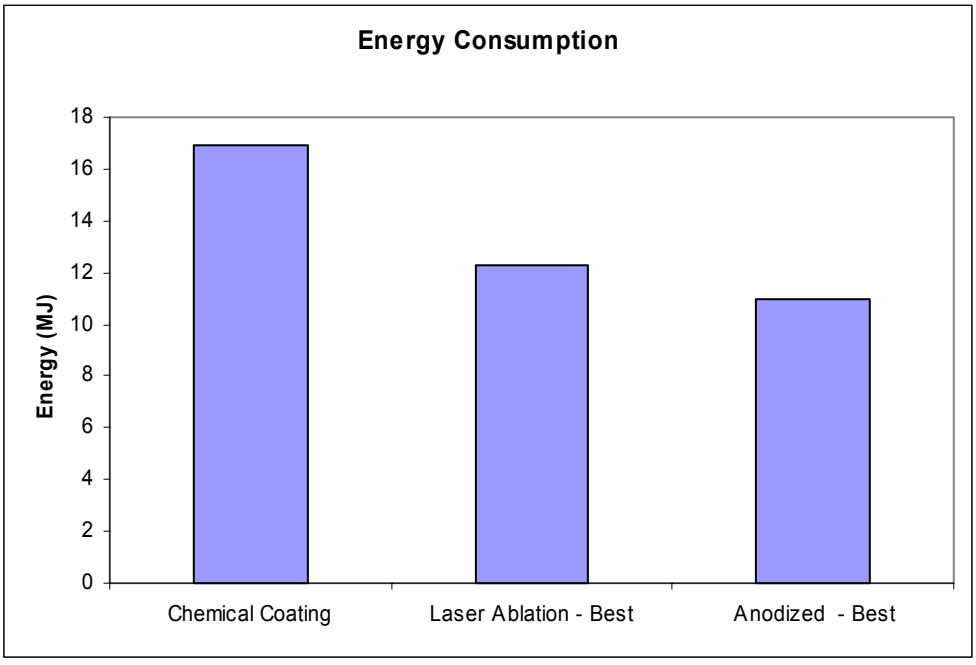

Figure 7.1: Energy consumption for manufacture of self-cleaning surface.

The energy consumption, as shown above, is the highest for chemical coating, at approximately 16.9MJ. The energy consumption of the two templates are similar, with 12.3 MJ used for the laser ablated template and 11.0MJ used by the anodized template. The energy values for the template methods represent scenarios in which the templates are used 100 times. However, and with a few less uses of the templates before replacement, both methods will consume more energy the chemical coating.

The energy consumption of producing $1m^2$ of self-cleaning surface is calculated for ranges of values of the efficiency of the heating device used to transfer the pattern from the template to the polymeric surface. This energy consumption is then compared to the energy consumption of producing $1m^2$ of self-cleaning surface with the chemical coating. The total number of times each template must be used to consume less energy than the chemical coating is calculated, for the range of heater efficiencies. These values are shown in Table 7.3.

Table 7.3: Uses of template to consume less energy than chemical coating.

heater efficiency	Min. uses of template to consume less energy than chemical coating			
	Min. scan speed	Max. scan speed	Secondary Al	Primary Al
1	65	152	64	100
0.9	67	156	65	100
0.8	70	162	65	101
0.75	71	165	65	101
0.66	75	174	65	101
0.5	87	202	66	102
0.4	104	242	66	103
0.33	132	307	67	104
0.25	259	600	68	106

7.4.2 Water Consumption

The water consumption for each manufacture method is shown in Figure 7.2.

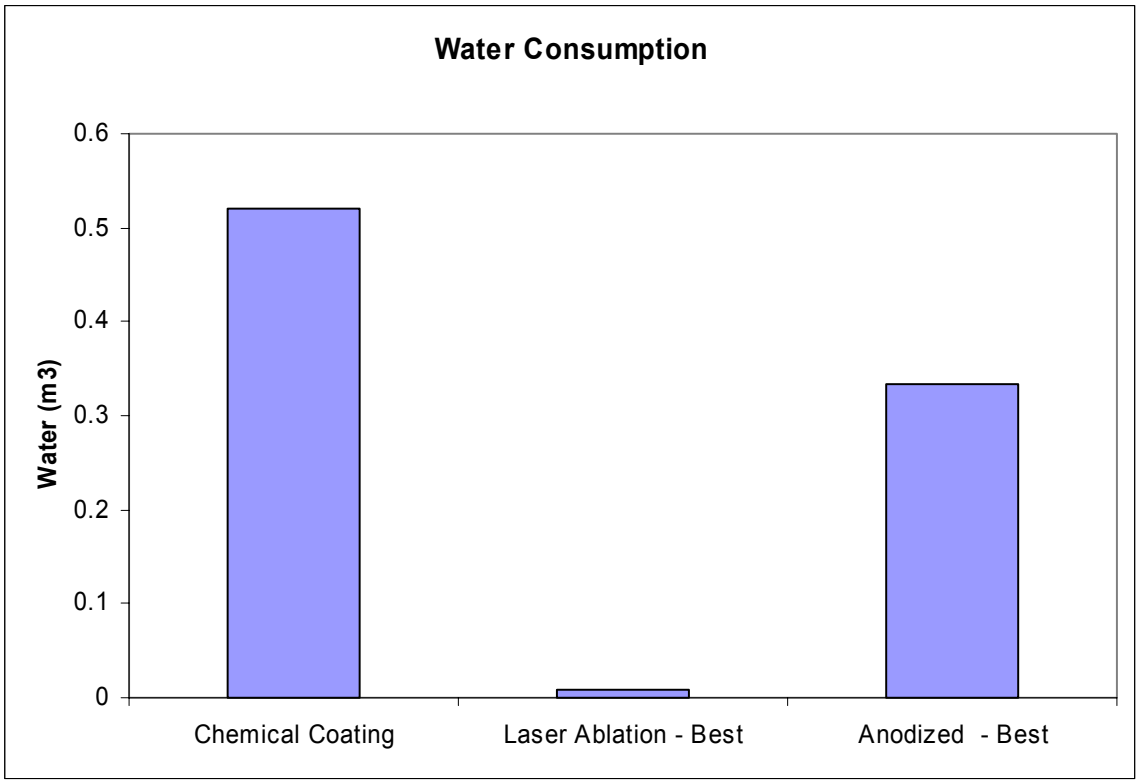

Figure 7.2: Water consumption for the production of a self-cleaning surface.

The water consumption of the production of chemical coating and the anodized template are similar, at 0.52 and 0.33 m^2, respectively. The laser ablated template uses much less water than the other two methods, at 0.009m^2. The chemical coating and anodized template method both use larger amounts of water because of the chemical production included in their life cycle inventories. The anodized template also consumes large amounts of water when diluting the chemicals to the proper concentration for anodizing and oxide removal.

The laser ablated steel template, produced with any scan speed, needs to be used only twice to consume less water per m^2 of self-cleaning surface than the chemical coating. The anodized aluminum template, when employing the best chemical recycling

scenario, will need to be used 65 times to consume less water than the chemical coating, for each m^2 of surface produced.

7.4.3 Global Warming Potential

The amount of CO_2 equivalent produced during the manufacture of the chemicals for the coating is

$$GWP = 0.764kg + 23(0.000342kg) + 296(0.188kg) = 56.4kg$$

The carbon dioxide equivalents total for chemical production, manufacture and cleaning of the coating is 56.5 kg. The process of calculating carbon dioxide equivalents was repeated for each method of producing a self cleaning surface, and the results are shown in Table 7.4.

Table 7.4: Global warming potentials for each method of producing a self-cleaning surface.

	Global Warming Potential (kg CO_2 equiv.)
Chemical Coating	56.5
Laser Ablation Best	2.19
Anodized Best	3.19

The global warming potential is highest for the self-cleaning chemical coating. In fact, it is 17 times more than the best scenario for the anodized aluminum template. A majority of this global warming potential can be attributed to the chemicals used in production, particularly the ethanol. The manufacture of ethanol from corn requires large amount of nitrogen containing fertilizer.

The number of times the template must be used to produce less CO_2 equivalents than the chemical coating is calculated, for each method and for a range of heater efficiency used in transferring the pattern to a polymeric surface. It is found that for a laser ablated template produced with the highest scan speed, the template must be used at

least 4 times, for the whole range of heater efficiencies analyzed. For the template produced with the lowest laser scan speed, then template must be used more than six times. When considering the template produced with anodizing, the template composed of primary aluminum will need to be used at least five times, while the secondary aluminum template must be used at least 6 times. It is found that with regards to global warming potential that the heater efficiency does not have much of an effect on how many times the template must be used, as only a small amount of greenhouse gasses are produced during the pattern transfer step.

7.4.4 Total Waste

The total waste produced by each method of production is shown in Figure 7.3.

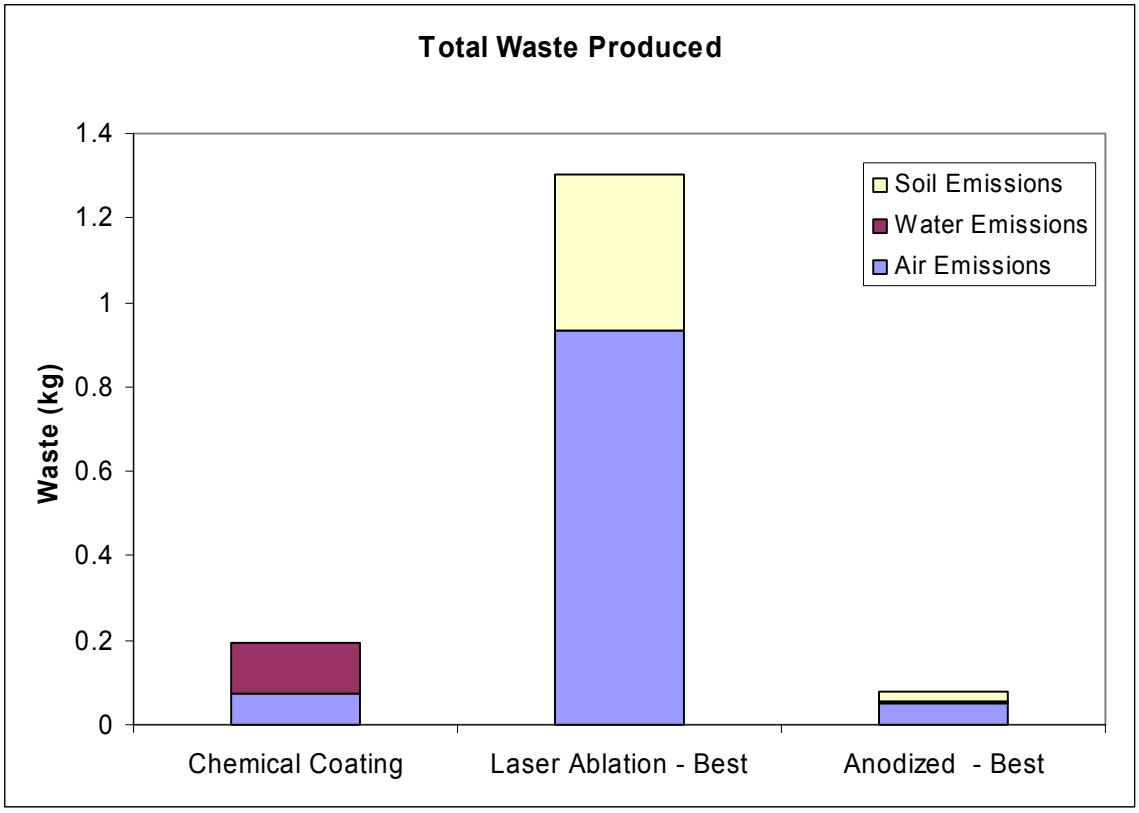

Figure 7.3: Total waste produced by manufacture of self-cleaning surfaces.

The manufacture of the laser ablated templates produced the most total waste (2.54 kg). This waste can all be attributed to the production of the steel, as electricity is the only input to every other stage of this template's production. The next highest amount of total waste is produced by the chemical coating, with 0.18kg of total emissions per m^2 of surface produced.

The anodized template made with recycled aluminum is the next best option in regards to waste produced, with 0.077kg of emissions per m^2 self-cleaning surface produced. The use of recycled aluminum prevents the production of additional waste associated with the aluminum mining and manufacturing process. Increasing uses of the aluminum template and the anodizing chemicals decrease the total waste attributed to each m^2 of surface produced. With less than ideal chemical recycling scenarios, the total waste produced by the anodized aluminum template becomes higher than that of the chemical coating.

For the laser ablated template produced with any laser scan speed, the template will need to be used at least 669 times to produce less waste than the chemical coating, per m^2 of self-cleaning surface produced. The anodized aluminum template produced with secondary aluminum will need to be used at least 40 times, and the primary aluminum template used at least 347 times, to produce less total waste per m^2 of self-cleaning surface produced, than the chemical coating.

7.4.5 Summary of Impacts of Each Production Method

The environmental impacts of each method of producing a self-cleaning surface have been determined for ranges of template uses and heating efficiencies in the case of the template methods. The template methods have been compared to the chemical

coating, and total uses of the template were calculated to determine how many uses are necessary for the template methods to be environmentally superior to the chemical coating, for each impact category. The necessary uses of the template for each method and each impact category are summarized in Table 7.5.

Table 7.5: Total uses of template to have smaller environmental impacts than chemical coating.

	Min. uses of template to produce less impacts than chemical coating			
Impact	Laser Ablated Min. scan speed	Laser Ablated Max. scan speed	Anodized Secondary Al	Anodized Primary Al
Energy	87	202	66	102
Water	2	2	65	65
GWP	4	6	5	6
Waste	669	669	40	357

The laser ablated templates will need to used at least 770 times each to have smaller overall environmental impacts than the chemical coating. The anodized templates produced with secondary aluminum will need to used at least 66 times and the primary aluminum template at least 357, to have lower environmental impacts than the chemical coating for each m^2 of self-cleaning surface produced.

7.5 Comparison of Self-Cleaning Surfaces to Industrial Cleaning

Having compared each of the three methods of producing a self-cleaning surface, the use phase is now considered. The life cycle inventory of each method of producing a self-cleaning surface is summed with the inventory of one mist cleaning cycle, determined in Chapter 6. These impacts are then compared to those of the industrial aqueous cleaning methods. The life cycle inventories of the best scenarios are chosen for the template methods of producing a self-cleaning surface and for the industrial cleaning methods.

The total life cycle inventory for each method is shown in Table 7.6.

Table 7.6: Best life cycle inventory for all scenarios.

	Chemical Coating	Laser Ablation - Best	Anodized - Best	12L Spray Best	150L Spray Best	12L Ultrasonic Best	150L Ultrasonic Best	
Energy	17.0	12.3	11.1	0.636	4.41	4.37	52.6	MJ
Water	0.523	0.011	0.336	0.002	0.024	0.01	0.127	m^3
CO_2	0.773	1.64	0.177	0.075	0.445	0.364	4.26	kg
CH_4	3.42E-4	6.34E-06	8.55E-5	1.37E-5	1.82E-4	3.38E-2	2.95E-3	kg
N_2O	1.88E-1	1.92E-03	1.02E-2	1.20E-6	5.04E-6	1.75E-6	1.60E-5	kg
Waste:								
Air	0.061	0.932	0.0520	0.001	0.007	0.01	0.12	kg
Water	0.119	0.003	0.00379	0.004	0.044	0.064	0.795	kg
Soil	4.88E-5	0.370	0.0216	3.76E-8	4.71E-7	6.72E-7	8.40E-6	kg

The data shown above are used to calculate the impacts in the following three sections.

7.5.1 Energy Consumption

The total energy consumption for all cleaning methods is shown in Figure 7.4.

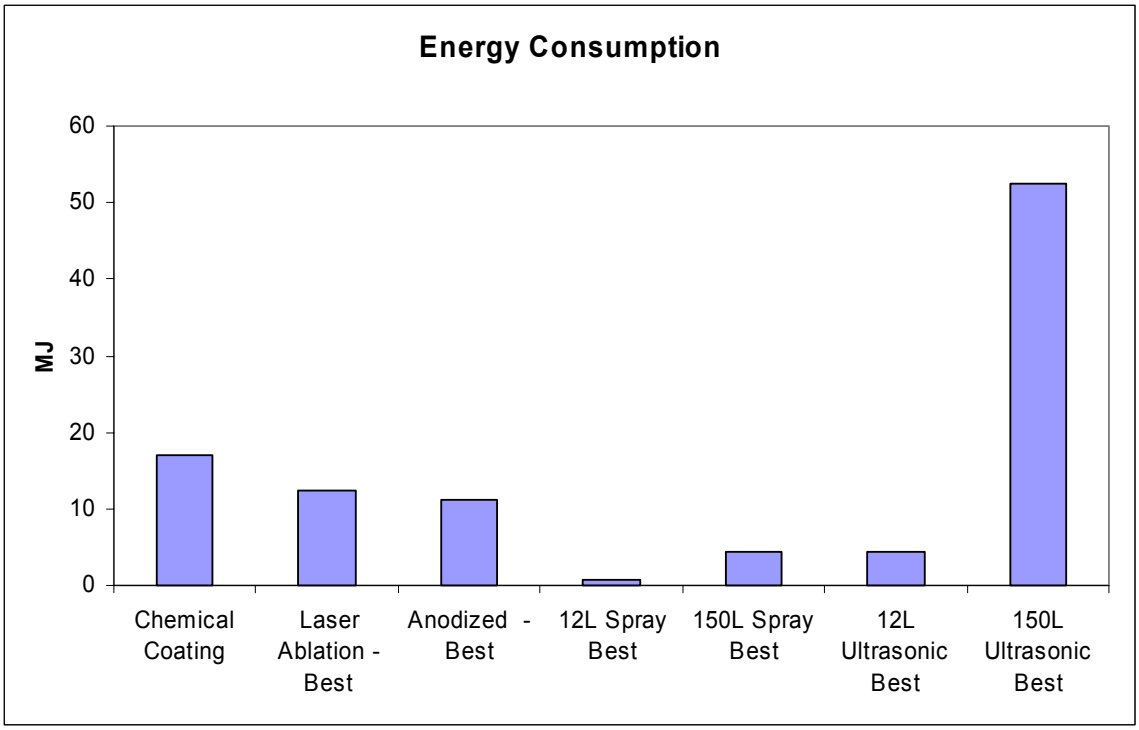

Figure 7.4: Total energy consumption for cleaning.

The minimum average energy used in the four aqueous cleaning scenarios is 0.636 MJ, for the case of the spray cleaning of a 12L part. This is less than the energy consumption of all methods of producing a self-cleaning surface with one mist cleaning.

The template process may not even be able to produce small intricate parts, so the comparison may not be applicable. If the anodizing process were used to create molds for smaller, more intricate parts, additional energy would be needed for aluminum machining, and the environmentally superior choice would be to use aqueous cleaning.

The chemical coating, primary anodized aluminum template and minimum laser ablated steel template methods of producing a self-cleaning surface all consume less energy than the best scenario for the ultrasonic cleaning of a large volume part. The energy consumption of each method of producing and cleaning a self-cleaning surface falls within the range of energy consumption of spray cleaning a large part; spray

cleaning could use more or less energy, depending on the cleaning time, solvent concentration and the cleaning solution recycling.

If the surface of a part will need to be cleaned multiple times in its lifetime, the self-cleaning surface option will eventually be environmentally superior to even the best of the aqueous cleaning methods. The energy consumption of the production and mist cleaning of the chemical coated surface and an average value (determined from the uncertainty analysis in Appendix D) of the spray cleaning of a small part are shown in Figure 7.5

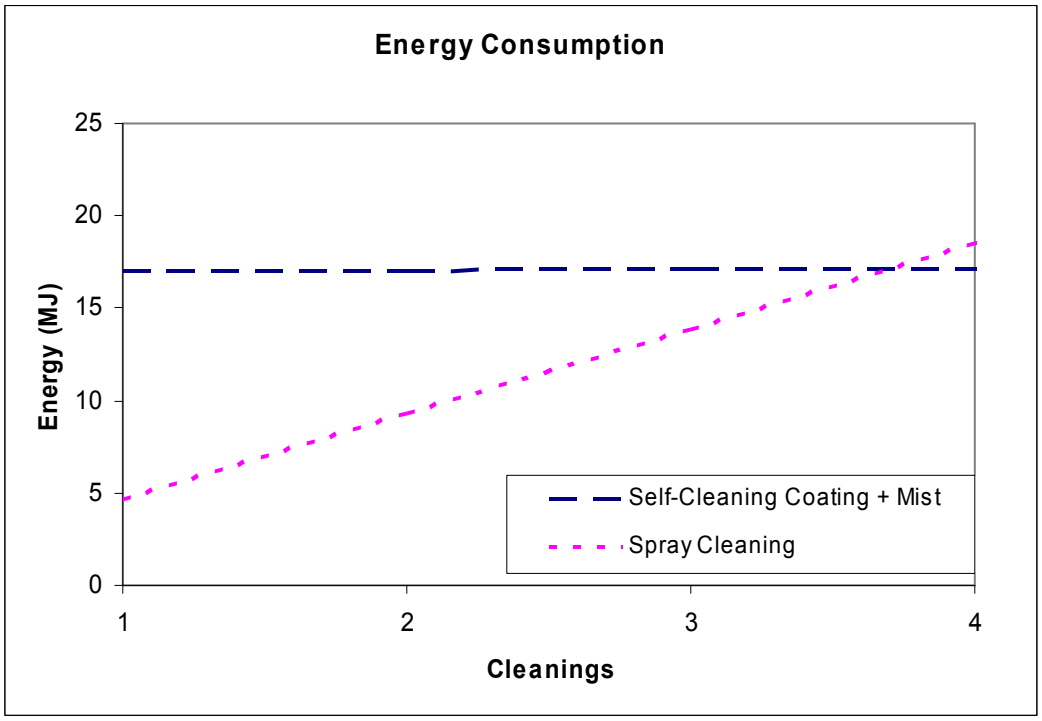

Figure 7.5: Two cleaning methods for increasing number of cleaning cycles.

As shown above, the total energy associated with the misting cleaning of the self-cleaning surface increases only slightly for each additional cleaning cycle. The spray cleaning, however, doubles for each cleaning cycle. For the case of the chemical coating, the self-cleaning surface will be environmentally superior in terms of energy

consumption, if the surface must be washed at least 4 times in its lifetime. For other methods of producing a self-cleaning surface, a similar number could be determined, but is dependent on how many times the template can be used, among other parameters.

Multiple cleanings are given further consideration. For each method of producing a self-cleaning surface, the number of times it must be cleaned to consume less energy than the best industrial cleaning scenario was calculated. For the template methods of producing a surface, the total number of cleaning cycles was calculated for both 100 and 1000 uses of the template, and for a heater efficiency of 50%. The total number of cleaning cycles for each method to consume less energy than the best industrial cleaning scenario is shown in Table 7.7.

Table 7.7: Total cleaning cycles to use less energy than best industrial cleaning method.

	# of cleaning cycles with 100 uses of templates	# of cleaning cycles with 1000 uses of templates
Laser min scan speed	28	14
Laser Max scan speed	48	16
Secondary anodized Al	20	3
Primary anodized Al	30	4
Chemical Coating	30	

7.5.2 Water Consumption

The total water consumed by production and one mist cleaning of the self-cleaning surfaces and of the industrial cleaning methods is shown in Figure 7.6.

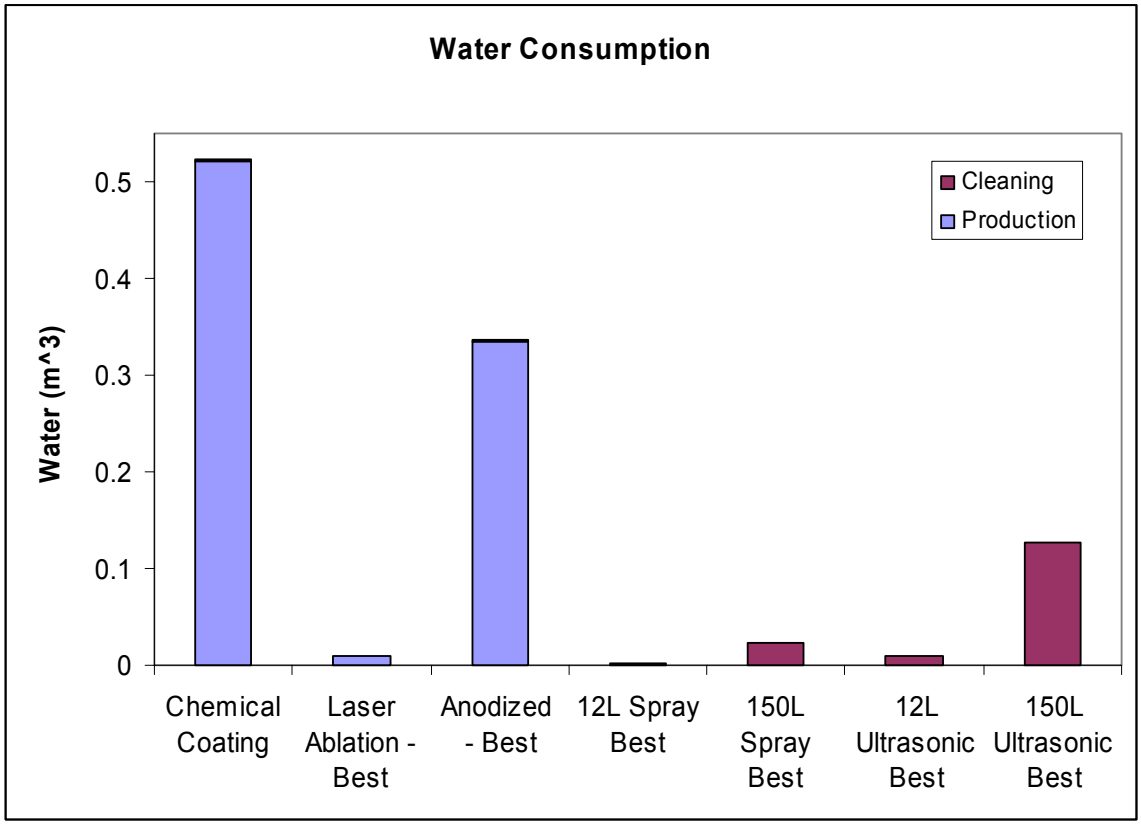

Figure 7.6: Water consumption for production and cleaning.

The water savings of the mist cleaning of the self-cleaning surface are overshadowed by water necessary for manufacture of the template. When comparing just the mist cleaning of the self-cleaning surface to the industrial cleaning methods, there are obvious water savings. The best minimum industrial cleaning method uses mores water than the mist cleaning ($0.0020m^3$ as compared to $0.0015m^3$). When considering the entire life cycle, the water savings of mist cleaning a self-cleaning surface disappear.

The chemical coating, when compared to the best scenarios of other methods of cleaning, consumes the most water between production and cleaning. The next highest water consumption is the best scenario for the production and cleaning of the anodized aluminum template; a slight change in parameters may cause this method to use the most

water. For example, when the chemical recycling scenario is kept the same, but the anodized template is only used 50 times (instead of 100), the template will use more water than the chemical coating per m^2 of surface created. A finite number of times that the chemicals can be recycled (instead of indefinitely) is also enough to cause the anodized template method to use more water than all other methods.

The ultrasonic cleaning of a large part is again the worst choice of the four industrial cleaning methods. The water use of both the spray cleaning and ultrasonic cleaning of a small part are low, lower than the laser ablated template created surface with mist cleaning. The water consumption of the worst spray and ultrasonic cleaning scenarios are 0.084 and 1.70 m^3, respectively. The water consumption of the laser ablated template method with mist cleaning falls in range of water consumption of spray and ultrasonic cleaning, and therefore has the potential to use less water than an industrial cleaning method.

Multiple cleaning cycles are again considered. The water consumption of each method of producing a self-cleaning surface and mist cleaning is compared to the best industrial cleaning scenario. The total number of times the self-cleaning surface must be cleaned to consume less total water than the best industrial cleaning method is calculated, for both 100 and 100 uses of the two different templates. The number of cleaning cycles for each method is shown in Table 7.8.

Table 7.8: Total cleaning cycles to use less water than best industrial cleaning method.

	# of cleaning cycles with 100 uses of templates	# of cleaning cycles with 1000 uses of templates
Laser Ablated	19	2
Anodized Aluminum	669	70
Chemical Coating	1042	

7.5.3 Global Warming Potential

The global warming potential of each method of producing a self-cleaning surface plus one mist cleaning and the aqueous cleaning methods is shown in Figure 7.7.

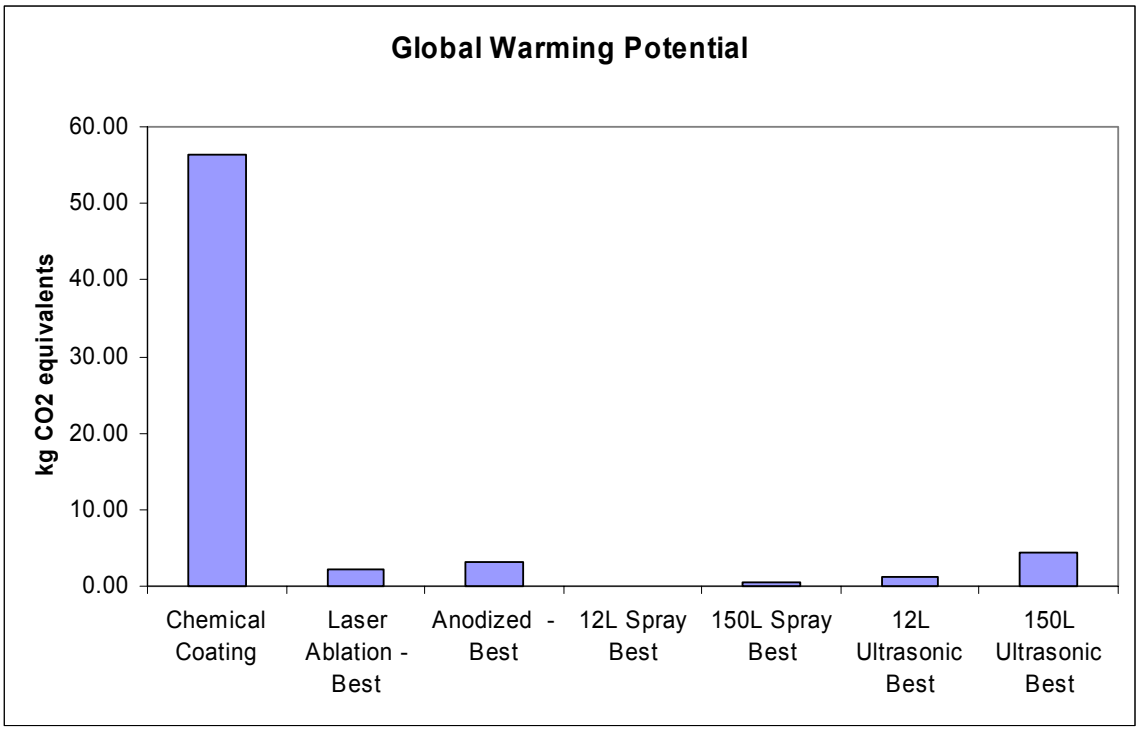

Figure 7.7: Global warming potential of each method of cleaning, for one cleaning.

The ultrasonic cleaning of a large part produced the most greenhouse gasses of the industrial cleaning methods, followed by the ultrasonic cleaning of a small part, and then spray cleaning. The lowest greenhouse gas emissions of the template methods are higher

than those of the best spray cleaning scenarios. However, if the cleaning solution used in the spray cleaning machines can only be recycled a finite amounts of times, the template methods have the potential to create less greenhouse gases and therefore cause less global warming.

The global warming potential of multiple cleanings of the same surface is considered. Again, each method of producing a self-cleaning surface and mist cleaning it is compared to the best industrial cleaning method. The total number of times the surface needs to be cleaned before it produces less total global warming potential than the industrial cleaning is calculated and is shown in Table 7.9.

Table 7.9: Total cleaning cycles to produce less global warming potential than the best industrial cleaning method.

	# of cleaning cycles with 100 uses of templates	# of cleaning cycles with 1000 uses of templates
Laser min scan speed	40	17
Laser Max scan speed	194	152
Secondary anodized Al	46	6
Primary anodized Al	49	6
Chemical Coating	793	

7.5.4 Total Waste

The total waste produced by each cleaning method is shown in Figure 7.8.

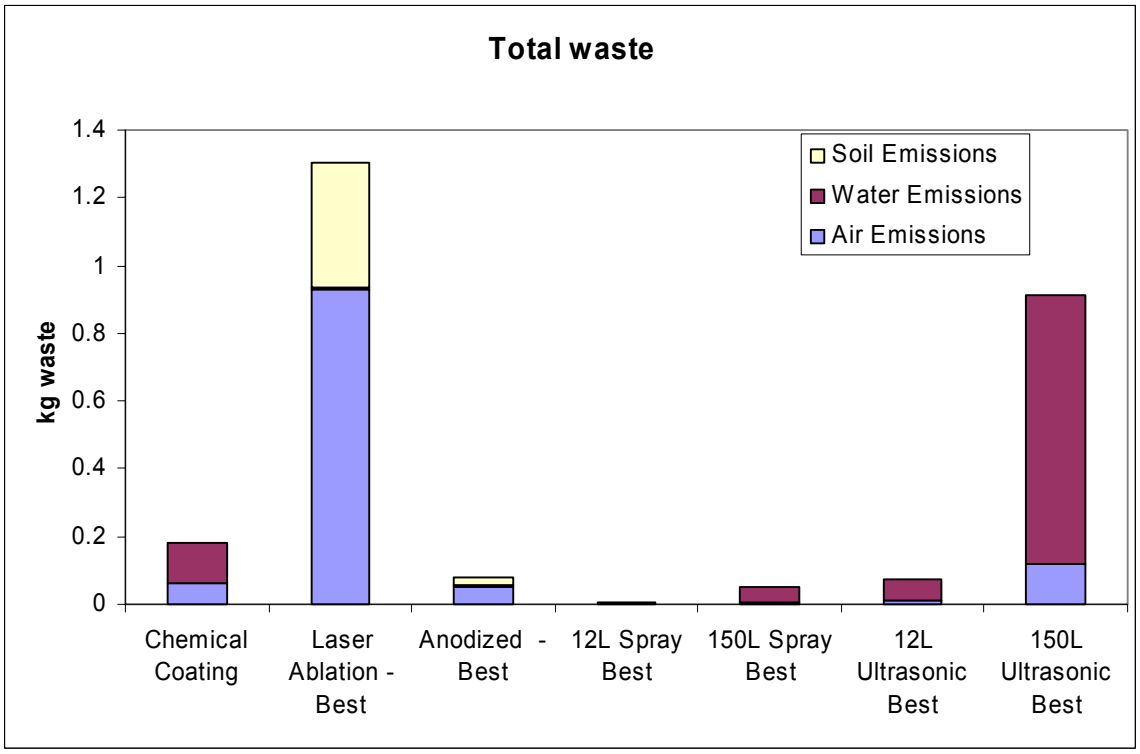

Figure 7.8: Total waste produced by each method of cleaning.

The laser ablation template with mist cleaning is the worst option, when considering the total waste produced. The large amounts of waste from the laser ablated template come from the production of the steel. The next worst is the ultrasonic cleaning a large part. The total waste shown above is for the best scenarios, so any change in parameters, such as the number of times the template can be used or the number of times the cleaning solution can be recycled, will only increase the amount of waste produced.

The best spray cleaning scenarios produce less waste than the chemical coating and best anodized template scenario. Again, a change in the cleaning solution recycling scenario or total cleaning time may cause the anodized template or chemical coating to be the best overall option in terms of waste produced.

The total waste of multiple cleaning cycles is calculated. The waste of each method of producing a self-cleaning surface and mist cleaning it was compared to the

waste of the best industrial cleaning scenario. The number of cleaning cycles necessary for each method to produce less total best than the best industrial cleaning method was calculated and is shown in Table 7.10.

Table 7.10: Total cleaning cycles to produce total waste than the best industrial cleaning method.

	# of cleaning cycles with 100 uses of templates	# of cleaning cycles with 1000 uses of templates
Laser ablated steel	261	27
Secondary anodized Al	16	2
Primary anodized Al	136	14
Chemical Coating	39	

7.5.5. Summary of Environmental Impacts of Cleaning Methods

The environmental impacts of each method of producing a self-cleaning surface and mist cleaning, as well as various ways to industrially clean a surface, have been determined for ranges cleaning solution recycling scenarios and total cleaning cycles. The impacts of producing a self-cleaning surface and mist cleaning it were compared to the impacts of industrial cleaning methods. Multiple cleanings of the same surface were considered, and a total number of cleaning cycles necessary for each self-cleaning surface production method to have smaller environmental impacts than industrial cleaning was calculated. The total cleaning cycles for each method and each impact category are summarized in Table 7.11.

Table 7.11: Total cleaning cycles of self-cleaning surface to have smaller environmental impacts than industrial cleaning.

	Min. cleaning cycles to produce less impacts than industrial cleaning				
Impact	Laser Ablated Min. scan speed	Laser Ablated Max. scan speed	Anodized Secondary Al	Anodized Primary Al	Chemical Coating
Energy	28	48	20	30	30
Water	19	19	669	669	1042
GWP	40	194	46	49	793
Waste	261	261	16	136	39

For the self-cleaning surface with mist cleaning to be environmentally superior to the industrial cleaning with respect to all impact categories, the laser ablated must be clean 261, the anodized template 669 times, and the chemical coating 1042 times, assuming the templates are used 100 times.

7.6 Life Cycle Interpretation

Life cycle interpretation is the final phase of the life cycle assessment (International Standards Organization 2006). In this phase, the results of the LCI and LCIA are evaluated and analyzed to draw conclusions, identify and explain limitations and provide recommendations for how designers should proceed with this information. This step also is used to neatly present the results of the life cycle assessment (SAIC 2006).

7.6.1 Significant Issues

In this step of the interpretation phase, the data are reviewed from LCIA to determine what most affects its results (SAIC 2006). This is done for each method of producing a self-cleaning surface and for the industrial cleaning methods.

One significant environmental issue is the greenhouse gas emissions of the chemical coating. At more than 56 kg of CO_2 equivalents for the production of the

coating, it is much higher than the other alternatives for producing a self-cleaning surface. This is mostly due to the high amount of nitrogen used as fertilizer to grow the corn for ethanol. Most of the coating is comprised of ethanol. Therefore, a better method of producing ethanol would reduce the global warming potential of the chemical coating. Production of ethanol from different plants besides corn can be considered for a reduction in the life cycle inventory.

Other significant environmental issues are present in the use of ultrasonic cleaning for large parts. The life cycle inventory indicates that this option uses much more energy than any other industrial cleaning option. This option has the highest greenhouse gas emissions of all alternatives. Also, the total emissions to water and soil are the highest for this alternative. These two high impacts are caused in part by the large amounts of trichloroethylene needed for cleaning. If a lower concentration could be used, or if a more environmentally friendly solvent were substituted, these two inventory categories could be reduced.

7.6.2 Completeness Check

The first part of this step of life cycle interpretation is the completeness check. In this part, the data used throughout the life cycle assessment is checked for availability and completeness (SAIC 2006). The data are checked for completeness against the system boundaries and the goals of the study.

The data of this study are fairly complete with regards to the goals of the study. As many inputs and processes were included as possible; this is in agreement with the scope of the study, which is to include all major environmental impacts. Some data are omitted, however, such as catalysts in the chemical reactions for some inputs to the self-

cleaning coating and tetrafluoroethylene, for which no life cycle data was available, in the water repellent solution. These chemicals comprise such a small percentage of the total mass of the coating (less than 2% of the total mass), that results should not be strongly affected by this omission. The end-of-life also is omitted, but the systems boundaries can be set to only include material acquisition, manufacture and use.

7.6.3 Sensitivity Check

The next part of this step is the sensitivity check. The significant issues raised in the previous step are analyzed to determine if any uncertainty surrounding them will affect the results and conclusions of the study (SAIC 2006). This step also is used to determine which data have the largest effect on the life cycle impacts. The sensitivity check can be performed by a contribution analysis (SAIC 2006). A contribution analysis was performed on all cleaning alternatives and is described in the following sections.

7.6.3.1 Anodized Aluminum Template

The effect of different parameters on the total life cycle data for the production of the anodized aluminum template was determined with an uncertainty analysis and is shown in Appendix D. A tornado graph is produced to show these effects. In a tornado graph, the increase or decrease of the output caused by an increase of one standard deviation of the input is shown. The effect of changes in parameters on the total energy consumption per m^2 of surface produced is shown in Figure 7.9.

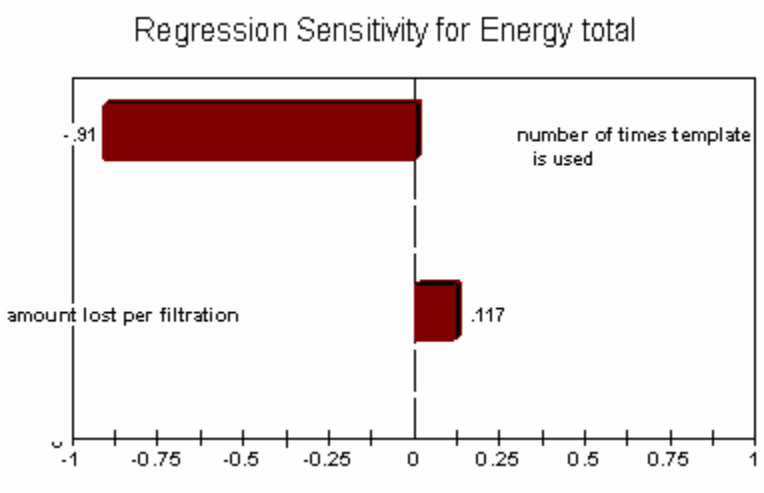

Figure 7.9: Effect of variables on energy consumption of anodized template.

For the case of the total energy consumed, this impact is most affected by how many times the template can be used. The amount of anodizing chemicals which need to be replaced after each filtration has a smaller effect on the total energy, while the amount of times the chemicals can be recycled has little to no effect.

The effect of the variables on the water consumption of the anodized aluminum template used to produce a self-cleaning surface is shown in Figure 7.10.

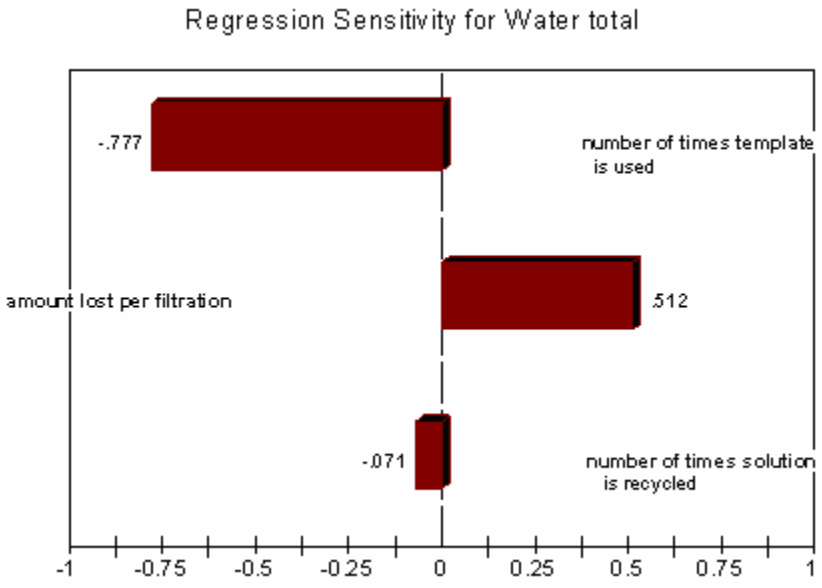

Figure 7.10: Effect of variables on total water consumption of anodized aluminum template.

Like for energy consumption, the number of times the template can be used has the largest effect on the total water consumption of the template. The inputs have a different affect on the global warming potential, as shown in Figure 7.11.

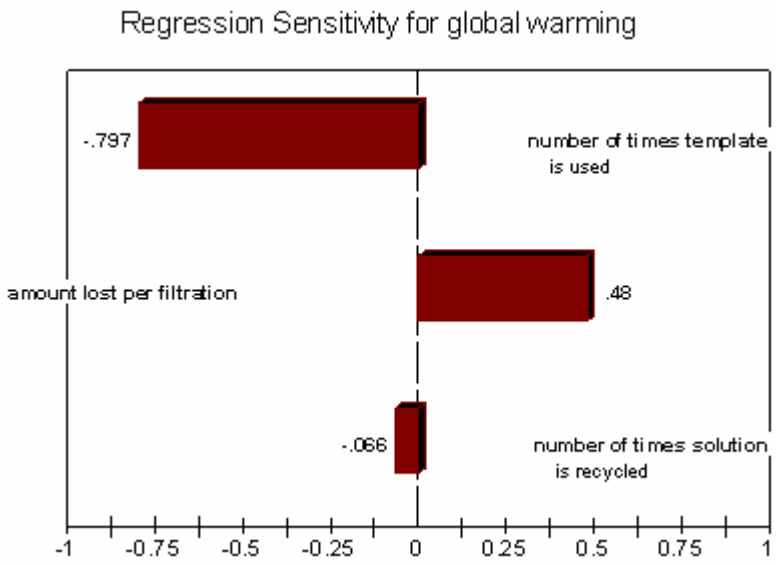

Figure 7.11: Effect of inputs on global warming potential of anodized template.

The global warming potential is most affected by the number of times the template can be used, followed by parameters associated with chemical recycling.

The results of this analysis show that the life cycle impacts are most affected by the number of times the template can be used. For this reason, any efforts to improve the environmental impact of this technology should be focused on making longer lasting, more durable templates.

7.6.3.2 Laser Ablated Template

The percentage of total energy consumption of each stage of production of the laser ablated template is shown in Figure 7.12.

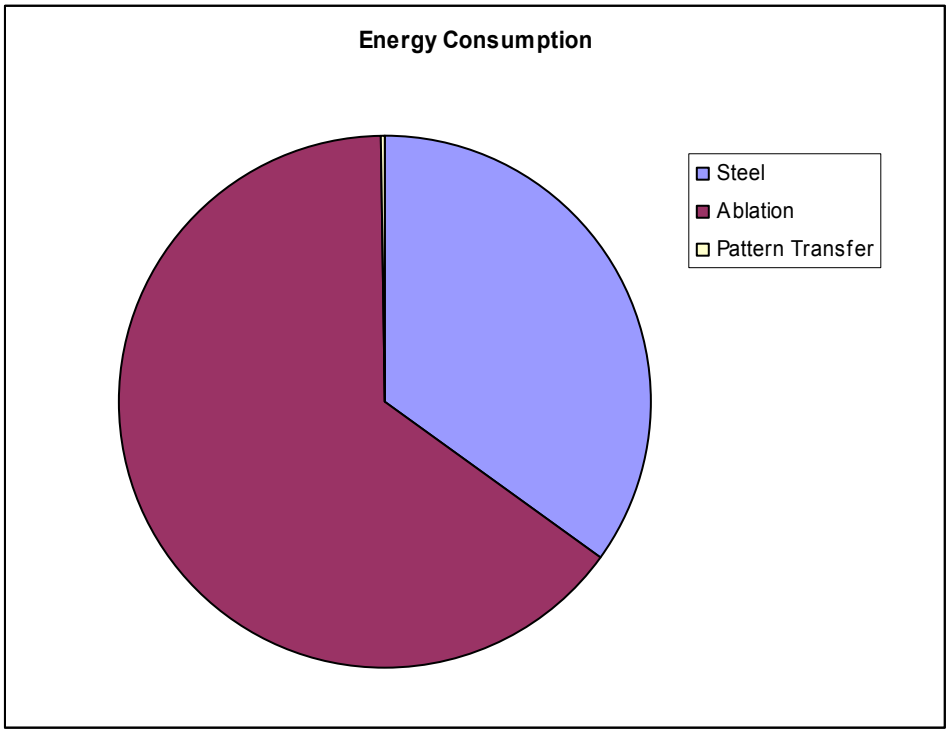

Figure 7.12: Total energy consumption of production of laser ablated template.

As shown above, the laser ablation process is responsible for most the energy used in producing the template. The materials acquisition and production of the steel for the template also contribute significantly. These two processes therefore have room for improvement.

7.6.3.3 Chemical Coating

The percentage of the total energy used to for chemical production per chemical is shown in Figure 7.13.

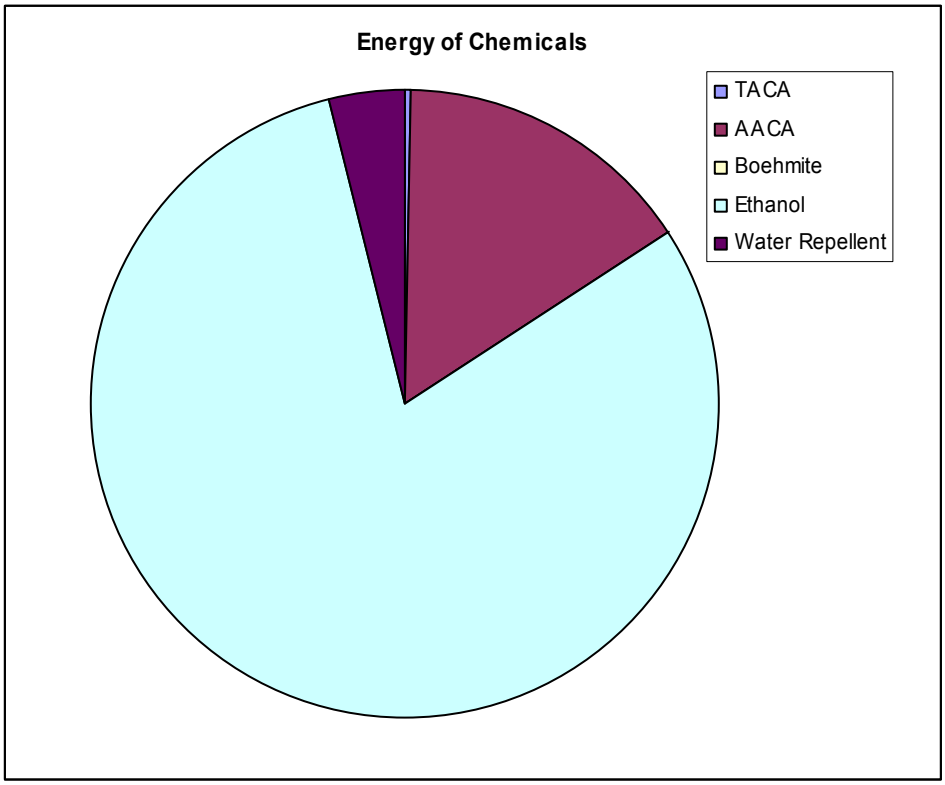

Figure 7.13: Energy consumption per chemical.

Ethanol, which composes most of the mass of the chemicals, uses the most energy in its production. Therefore, improvements in the production of ethanol have the greatest potential to improve the energy consumption associated with the life cycle of the chemical coating. The same can be said for the other environmental impacts, particularly global warming potential. In the production of ethanol, large amounts of nitrogen based fertilizers are used. A different method of producing the ethanol could drastically reduce the global warming potential caused by the chemical coating.

7.6.3.4 Industrial Cleaning

The effect of the input parameters on the energy use of the spray cleaning of a 150L part is shown in Figure 7.14.

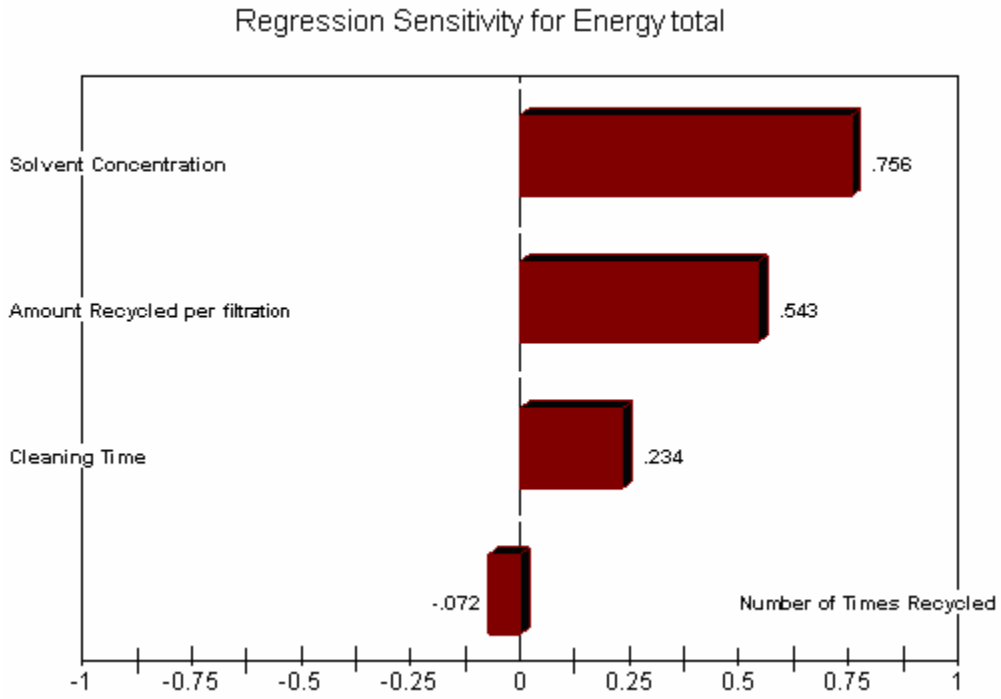

Figure 7.14: Effect of inputs on energy consumption of spray cleaning a 150L part.

The energy consumption of spray cleaning is most affected by the solvent concentration, then by the amount of cleaning solution which must be replaced after each filtration. This suggests that the majority of the energy consumption of the life cycle is from the production of trichloroethylene and not the electricity to run the cleaning machines.

The effect of the inputs on the water consumption is shown in Figure 7.15.

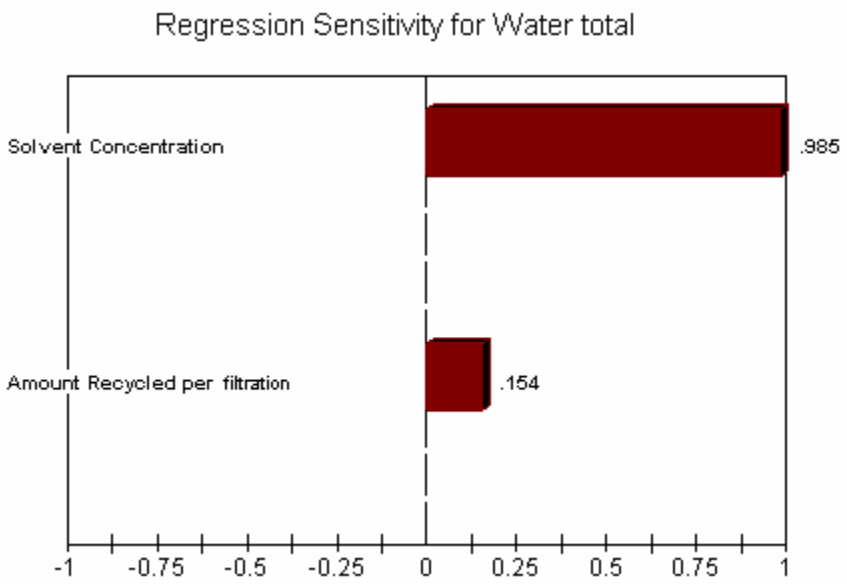

Figure 7.15: Effect of inputs on water consumption of industrial cleaning.

Solvent concentration has the largest effect on the water consumption of industrial cleaning methods; as the concentration increases, so does the water consumption.

The effect of the input parameters on the global warming potential is shown in Figure 7.16.

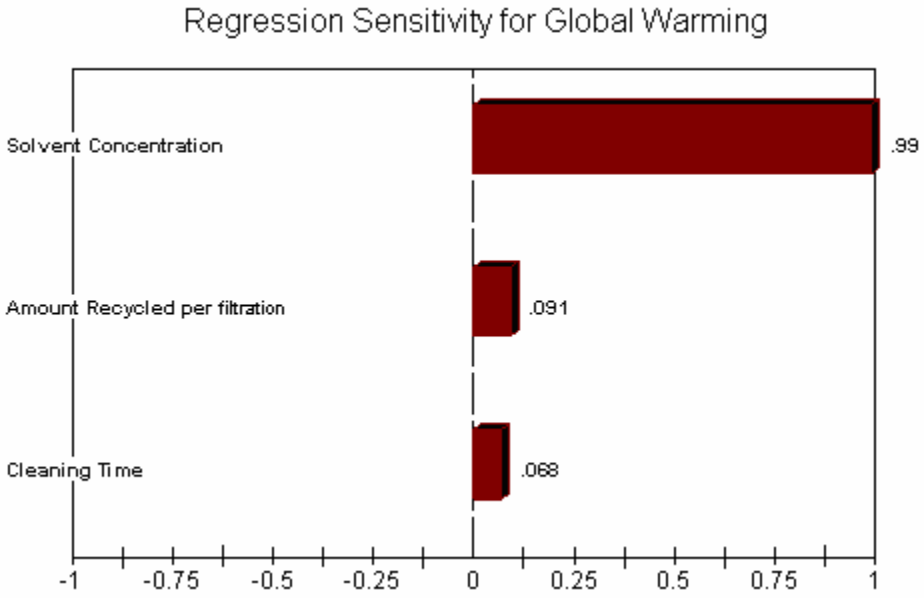

Figure 7.16: Effect of inputs on global warming potential of industrial cleaning.

Because solvent concentration has the largest effect on the life cycle inventory of industrial cleaning methods, the lowest solvent concentration as possible should be used. Also, if more environmentally friendly solvents can be used in place of trichloroethylene, the impact of industrial will be lowered more than with improvements in the recycling of the cleaning solution.

7.6.4 Consistency Check

Finally, a consistency check is performed. In this check, assumptions, methods and data used throughout the assessment are compared to determine any inconsistencies (SAIC 2006). The methods and assumptions are checked to see if they are consistent with the goals and scope of the study. Inconsistencies are allowed, if they do not affect the goal or scope of the study (SAIC 2006).

Inconsistencies exist in the data sources of various parts of the life cycle inventory. Some data are from established LCI databases, other data are from literature, and some data are based on theoretical models. Data accuracy is also not consistent throughout the study; some LCI data are taken from detailed accounts of actual chemical plants while other chemical data are based on assumptions of the balanaced chemical reaction.

Despite these data inconsistencies, the methods used are not inconsistent with the goals and scope of the study. The scope of this analysis was defined as capturing the main environmental impacts of the methods of producing a self-cleaning surface. As these methods are new technologies, it is simply not possible to have detailed, industrial scale life cycle inventory data of all processes included in production. Therefore it is

necessary to include models based on limited data and assumptions, in order to estimate the environmental impacts of all parts of the life cycle of these methods of production.

7.6.5 Conclusions and Recommendations

The results of the life cycle assessment indicate that the best method to produce a self-cleaning surface is dependent on the impact category of importance to the designer. The life cycle impacts for each method of producing and cleaning a surface once are summarized in Table 7.12.

Table 7.12: Summary of environmental impacts for production and cleaning of a surface.

	Chemical Coating	Laser Ablation - Best	Anodized - Best	12L Spray Best	150L Spray Best	12L Ultrasonic Best	150L Ultrasonic Best	
Energy	16.9	12.3	11.1	**0.636**	4.41	4.37	52.6	MJ
Water	0.523	0.0105	0.336	**0.002**	0.024	0.01	0.127	m3
GWP	56.43	2.21	3.20	**0.08**	0.45	1.14	4.33	kg
Waste	0.1800	1.31	0.0773	**0.0050**	0.0510	0.0740	0.915	kg

When selecting the best method of producing a self-cleaning surface, the best option depends on the impact category. If energy consumption is the most important impact category, the chemical coating should be selected, assuming templates can only be used a few times. However, for more ideal conditions, the anodized aluminum template will consume the least amount of energy. For water consumption, the laser ablated template method of producing a self-cleaning surface is the best. For the global warming potential impact, the laser ablated template method is against the best, with the anodized templates following closely behind. Finally, in terms of total waste produced, the anodized

aluminum template is the best option, for the best scenario for chemical recycling and high total uses of the template.

From the results of the life cycle assessment, the best option for cleaning is not clear cut. Many parameters affect the impacts of each option. Although the best scenario for spray cleaning has the lowest impact in most impact categories, uncertainty in the results could mean that another option is environmentally superior. With experimentation to determine how many uses are possible with the nanostructured templates, and better information about the recycling of cleaning solution, some uncertainty could be removed and a more definite choice could be made. Also, the spray cleaning will not be the best option, if multiple cleanings of the same surface are performed.

Significant differences between the impacts of a few alternatives are not present. Without a larger difference between the results it is hard to choose one option as overall environmentally superior. Though this analysis has uncertainty associated with a few aspects, it is clear that the biologically inspired alternative is not automatically the environmentally superior choice, despite the resource savings in the use phase.

Although no clear environmentally superior choice exists, one alternative can be ruled out. The ultrasonic cleaning of a larger part uses the most energy, even with the lowest possible cleaning time and best possible cleaning solution recycling. This alternative, as currently analyzed with 75g/L of trichloroethylene, should not be used to clean.

CHAPTER 8

DISCUSSION AND CLOSURE

In this chapter, the work completed in this thesis is summarized and discussed. The answers to the research questions posed in Chapter 1 are given. The limitations of this work are acknowledged, and areas of future work are outlined.

8.1 Summary of Results

The life cycle of three methods of producing a self-cleaning surface has been analyzed: a chemical coating, a laser ablated template and an anodized template. The two template methods were analyzed for varying times that they could be used before disposal and for the case of the anodized template, varying chemical recycling scenarios. The life cycle of industrial cleaning methods also has been considered, for a range of parts sizes, cleaning times, solvent concentration, wastewater recycling scenarios, and for both ultrasonic and spray cleaning.

When comparing the different ways of cleaning a surface, no clear environmentally superior choice exists. When considering just the use phase of the different systems, the self-cleaning surface has excellent water and energy savings, as compared to the industrial cleaning methods. However, when a life cycle perspective is taken, these benefits do not remain. The production of a self-cleaning surface uses large amounts of resources and produces enough waste to overshadow the comparatively small impacts of the use phase.

These results are contrary to what is expected of a biologically inspired design. Many researchers expect ideas taken from nature to automatically lead to environmentally superior products. The lotus leaf, as a symbol of purity, may falsely lead people to believe the engineering equivalent is also pure. The results of this life cycle assessment have shown that sustainability is not a convenient byproduct of using a biologically inspired idea. Designers must be concerned about the environment impact of their biomimetic design when sustainability is a design objective, and they should utilize already existing design methods to produce environmentally friendly products and systems.

8.2 Summary of Answers to Research Questions

In this section, the research questions posed in Chapter 1 are answered, using the results of the life cycle assessment. The first research question is:

- What overall environmental benefits are associated with using biologically inspired self-cleaning surfaces when cleaning, as compared to current cleaning methods?

This question was broken into two parts in Chapter 1:

- What environmental burdens are associated with producing hydrophobic surfaces?
- What environmental benefits are associated with self-cleaning hydrophobic surfaces?

The environmental burdens associated with the production of the three different self-cleaning surfaces have been summed in Chapters 3 to 5. The environmental burdens of using a self-cleaning were quantified in Chapter 6, as well as the burdens of conventional

cleaning methods. The environmental impacts of production and use were determined in Chapter 7.

It is found that obvious environmental savings are associated with the use of the self-cleaning surface when compared to aqueous cleaning methods requiring a solvent. The cleaning of a self-cleaning surface requires much less water and energy than the aqueous cleaning machines. When including the environmental impacts of producing the surface, however, there are no clear environmental advantages. In fact, for certain impact categories, such as greenhouse gas emissions, there are environmental disadvantages associated with the self-cleaning surface.

The overall environmental benefits or burdens of the self-cleaning surface depend heavily on how they are used. Because there are excellent water and energy savings in the cleaning of a self-cleaning surface as compared to the water and water use of industrial cleaning, self-cleaning surfaces are perhaps best used on products or systems which will be cleaned numerous times during its life cycle. The overall environmental impacts also depend on how soiled the surface may become, how often templates can be used in production before disposal, and how the chemicals used in production or the cleaning solutions are recycled.

The answer to the first research question is: **No clear environmental benefits exist for the use of a self-cleaning surface, when considering the entire life cycle.**

The second research question is:

- Do biologically inspired designs produce environmentally superior products or systems, as compared to conventionally designed products or systems?

As shown by the results of the life cycle assessment, using a biologically inspired design does not automatically or always lead to an environmentally superior design. The use of self-cleaning surfaces has benefits, but overall they do not. As illustrated by this example, a life cycle perspective is needed when using biologically inspired solutions for environmentally benign or sustainable products. Traditional guidelines and techniques for producing environmentally friendly products should still be used, in conjunction with the biologically inspired design.

The answer to the second research question is: **Biologically inspired designs are not necessarily environmentally superior designs.**

8.3 Research Contributions

The completion of this life cycle assessment has resulted in a few research contributions. A literature review of naturally occurring self-cleaning surfaces, methods of production, models and optimization and commercial products using these surfaces has been completed.

The environmental impacts of three different methods of producing a self-cleaning surface have been quantified; the three methods are a chemical coating, a laser ablated template and an anodized aluminum template. The analysis of the chemical coating includes the life cycle of chemicals for which no public life cycle inventory data exists. The results of this research are the first life cycle assessment of the manufacture and use of a self-cleaning surface.

A parametric model has been developed for the production of the anodized aluminum template. A spreadsheet was used to develop a tool in which a designer can

select the length, radius and thickness of a cylindrical aluminum template. The spreadsheet provides the life cycle inventory of each material input and stage of production.

In a more abstract sense, the environmental impacts of two manufacture methods have been quantified; no public life cycle data was available at the time of this research for anodizing, and laser ablation appears to be an emerging manufacturing technology, with little environmental data available. The life cycle data complied in this study may be used by other researchers when analyzing systems which include anodizing or laser machining.

The environmental impacts of industrial cleaning methods also have been quantified. Spray and ultrasonic aqueous cleaning methods have been analyzed, for various solvent concentrations, cleaning times, parts sizes and recycling scenarios. This life cycle data will be helpful for further comparisons or studies involving cleaning.

8.4 Limitations of this Research

The results and conclusions drawn from this research are limited in a few ways. The main limitation of this work is associated with the assumptions made about the life cycle inventory of certain chemicals. For chemicals that have no public LCI data, assumptions were made about their manufacture. The results therefore are not completely accurate, and the data quality of the inventory associated with the chemical coating and the anodized template is limited.

The life cycle inventory of the manufacture of the chemical coating and the anodized aluminum template were modeled after laboratory procedures. These procedures may not accurately represent how such surfaces would be produced on a

larger, industrial scale. Industrial scale production may be more efficient, requiring fewer resources and producing fewer emissions.

The environmental impacts of the template methods of producing a self-cleaning surfaces are only quantified for flat surfaces, as additional energy and resources would be needed to produce a self-cleaning surface with this methods on complex geometries. Limitations also are associated with the functional unit used for industrial cleaning. Because a surface area is used for the functional unit of the life cycle the self-cleaning surface, a surface area also should be used for industrial cleaning life cycle. Because the same surface area for the self-cleaning surface was represented as range of volumes for industrial cleaning, it is hard to determine an accurate comparison between the two. With a range of volumes investigated, multiple comparisons can be made, which may somewhat alleviate this particular limitation.

8.5 Future Work

The future work associated with this area of research will be the extending of the application of the life cycle study. Other uses of the self-cleaning surface, and therefore different cleaning scenarios should be analyzed. This current work only investigates the case of a self-cleaning surface used on parts and surfaces which will need to be industrially cleaned. Outside of industrial metal cleaning, there are many other possible applications of self-cleaning surfaces.

Life cycle inventories could be assembled for other traditional cleaning scenarios, such as the cleaning of the outside of buildings or cars, on textiles, or common household surfaces. The life cycle inventories then could be compared to the production and use of

a self-cleaning surface in the same situation. It then could be determined if self-cleaning surfaces are the environmentally superior choice for these scenarios.

A life cycle assessment could be performed on self-cleaning surfaces used on molds for injection molding. The same methods of production for the templates (laser ablation and anodizing) would be analyzed, with the additional impacts of producing the mold included. This life cycle assessment would be of interest, because it would quantify the environmental impacts of self-cleaning surfaces used on non-flat surfaces.

The life cycle inventories of the production of the chemical coating and the anodized template, as mentioned above, were modeled after small scale laboratory procedures. Future work of this life cycle assessment should include larger scale anodizing, such as in a factory. The same considerations should be given to the production of the chemical coating. Once modeled on a larger scale production basis, the life cycle inventory of both the anodized aluminum template and the chemical coating will more accurately represent real life manufacturing processes.

Another area of future work related to this particular life cycle assessment will include refinement of chemical life cycle inventories. Currently, many assumptions are made about the resource consumption and emissions of chemicals for which no public life cycle data are available. These inventories could be improved by gathering actual data from chemical plants about energy consumption and byproducts. Such data would serve to improve the data quality of this life cycle assessment.

The life cycle inventory of the mist cleaning of a self-cleaning surface should also be refined. Experimentation with self-cleaning surfaces will results in improved knowledge about the resource consumption and emissions associated with cleaning these

surfaces. Experiments should be performed, in which self-cleaning surfaces are soiled with common industrial contaminants. The surface then should be cleaned, measuring the amount of water necessary to removed all contaminants. The information gained from these experiments can then be used to validate and refine the calculated values for water and energy consumption of cleaning a self-cleaning surface.

A final area of future work relating to this research is in creating a "principle of life," as discussed in Chapter 1. Further study should be completed of how systems in nature clean themselves, or more generally how systems in nature use their surfaces. This information can be used to form a principle of life relating to the use of surfaces. If this principle can be successfully translated into an engineering guideline, it may lead to more novel or sustainable products.

APPENDIX A

CHEMICAL LCI DATA FOR SELF-CLEANING COATING AND ANODIZING

A.1 Aluminum Sulphate

The fuel inputs for producing one kilogram of aluminum sulphate are shown in Table A.1 (Althaus et al. 2004).

Table A.1: Fuel inputs for production of aluminum sulphate.

Fuel Inputs for 1kg of Aluminum Sulphate		
Coal, Brown	0.099881	kg
Coal, Hard	0.060067	kg
Natural Gas	0.028873	m^3
Oil, Crude	0.060186	kg
Uranium	0.000005187	kg

The total energy from these fuels is calculated using the energy contents listed above and is:

$$E = 8\frac{MJ}{kg}\cdot 0.099881kg + 18\frac{MJ}{kg}\cdot 0.060067kg + 36.6\frac{MJ}{m^3}\cdot 0.028873m^3$$
$$+42.6\frac{MJ}{kg}\cdot 0.060186kg + 451000\frac{MJ}{kg}\cdot 5.187\times 10^{-6}kg$$

$$E = 7.84MJ$$

The total CO_2, CH_4, and N_2O emissions from these fuels are

$$0.0999kg\cdot\frac{1.5kg}{kg} + 0.060kg\cdot\frac{2.84kg}{kg} + 0.029m^3\cdot\frac{1.92kg}{m^3} + 0.060kg\cdot\frac{2.95kg}{kg} = 2.45kg\,CO_2$$

$$0.0999kg\cdot\frac{0.0034kg}{kg} + 0.060kg\cdot\frac{0.0052kg}{kg} + 0.029m^3\cdot\frac{3.68\times 10^{-5}kg}{m^3} = 6.53\times 10^{-4}kg\,CH_4$$

$$0.0999kg\cdot\frac{1.16\times 10^{-5}kg}{kg} + 0.060kg\cdot\frac{2.60\times 10^{-5}kg}{kg} = 2.72\times 10^{-6}kg\,N_2O$$

The life cycle inventory data for the production of one kilogram of aluminum sulphate are shown in Table A.2 (Althaus et al. 2004).

Table A.2: Complied life cycle inventory data for the production of aluminum sulphate.

Production of 1 kg of Aluminum Sulphate		
Energy	8.01004	MJ
Water	3.014867	m^3
CO_2	0.456246	kg
CH_4	0.00061	kg
N_2O	0	kg
Air Emissions	0.4704	kg
Water Emissions	0.0429	kg
Soil Emissions	0.000312	kg

A.2 Acetone

The fuel inputs for the production of one kilogram of acetone are shown in Table A.3 (Althaus et al. 2004).

Table A.3: Fuel energy inputs for the production of acetone.

Energy Inputs for Production of 1kg of Acetone		
Coal, Brown	0.018329	kg
Coal, Hard	0.07767	kg
Natural Gas	1.06	m^3
Oil, Crude	0.52118	kg
Uranium	3.3937E-06	kg

The total energy from these fuels is $E = 64.07 MJ$. The total CO_2, CH_4, and N_2O emissions from these fuels are $3.82 kg\, CO_2$, $5.01 \times 10^{-4} kg\, CH_4$ and $2.21 \times 10^{-6} kg\, N_2O$. The life cycle inventory data for acetone is shown in Table A.4 (Althaus et al. 2004).

Table A.4: Complied life cycle inventory data for the production of acetone.

Production of 1 kg of Acetone		
Energy	64.083	MJ
Water	0.064451	m^3
CO_2	1.99471	kg
CH_4	0.003753	kg
N_2O	0	kg
Air Emissions	1.99458	kg
Water Emissions	0.022726	kg
Soil Emissions	5.18E-07	kg

A.3 Acetic Anhydride

The energy inputs for the production of acetic anhydride is shown in Table A.5 (Althaus et al. 2004).

Table A.5: Fuel inputs for the production of acetic anhydride.

Energy Inputs for Production of 1kg of Acetic Anhydride		
Coal, Brown	0.3358	kg
Coal, Hard	0.23709	kg
Natural Gas	0.89287	m^3
Oil, Crude	0.53856	kg
Uranium	1.77E-5	kg

The total energy from the fuel inputs is $E = 70.5587 MJ$. The total CO_2, CH_4, and N_2O emissions from these fuels are $4.48 kg\, CO_2$, $0.0024 kg\, CH_4$, and $1.01 \times 10^{-5} kg\, N_2O$.

The life cycle inventory data for acetic anhydride is shown in Table A.6 (Althaus et al. 2004).

Table A.6: Complied life cycle inventory data for the production of acetic anhydride.

Production of 1 kg of Acetic Anhydride		
Energy	71.3502	MJ
Water	10.6774	m^3
CO_2	2.319872	kg
CH_4	0.012267	kg
N_2O	0	kg
Air Emissions	2.368155	kg
Water Emissions	0.088435	kg
Soil Emissions	0.002975	kg

A.4 Aluminum Oxide

The energy inputs of the production of 1 kilogram of aluminum oxide are shown in Table A.7 (PRé Consultants 1996).

Table A.7: Energy inputs for the production of aluminum oxide.

Energy Inputs for Production of 1kg of Aluminum Oxide		
Coal, Brown	0.0425	kg
Coal, Hard	0.0456	kg
Natural Gas	0.0607	m^3
Oil, Crude	0.324	kg
Uranium	3.92E-6	kg

The total energy from these fuels is $E = 18.95MJ$. The total CO_2, CH_4, and N_2O emissions from these fuels are $0.405kg\,CO_2$, $3.84\times10^{-4}\,kg\,CH_4$, and $1.68\times10^{-6}\,kg\,N_2O$. The life cycle inventory data for aluminum oxide are shown in Table A.8 (PRé Consultants 1996).

Table A.8: Complied life cycle inventory data for the production of aluminum oxide.

Production of 1 kg of Aluminum Oxide		
Energy	18.85192	MJ
Water	0.00384	m3
CO_2	1.3	kg
CH_4	0.00164	kg
N_2O	0	kg
Air Emissions	1.398287	kg
Water Emissions	0.019976	kg
Soil Emissions	0	kg

A.5 Sodium Carbonate

The energy input for the production of sodium carbonate are shown in Table A.9 (Althaus et al. 2004).

Table A.9: Energy inputs for the production of sodium carbonate.

Energy Inputs for Production of 1kg of Sodium Carbonate		
Coal, Brown	0.027101	kg
Coal, Hard	0.16086	kg
Natural Gas	0.009386	m^3
Oil, Crude	0.015743	kg
Uranium	1.49E-6	kg

The total energy from these input fuels is $E = 4.80 MJ$. The total CO_2, CH_4, and N_2O emissions from these fuels are $0.562 kg\, CO_2$, $9.30 \times 10^{-4} kg\, CH_4$, and $4.50 \times 10^{-6} kg\, N_2O$. The life cycle inventory data for sodium carbonate are shown in Table A.10 (Althaus et al. 2004).

Table A.10: Complied life cycle inventory data for the production of sodium carbonate.

Production of 1 kg of Sodium Carbonate		
Energy	5.04779	MJ
Water	1.385525	m^3
CO_2	0.425975	kg
CH_4	0.000991	kg
N_2O	0	kg
Air Emissions	0.432359	kg
Water Emissions	0.155653	kg
Soil Emissions	0.000152	kg

A.6 Titanium Dioxide

The energy inputs for the production of titanium dioxide are shown in Table A.11 (Althaus et al. 2004).

Table A.11: Energy inputs for the production of titanium dioxide.

Energy Inputs for Production of 1kg of Titanium Dioxide		
Coal, Brown	0.61589	kg
Coal, Hard	0.3604	kg
Natural Gas	0.78979	m^3
Oil, Crude	0.64302	kg
Uranium	3.21E-5	kg

These inputs represent a total energy input of $E = 82.19 MJ$. The total CO_2, CH_4, and N_2O emissions from these fuels are $5.36 kg\, CO_2$, $0.0040 kg\, CH_4$, and $1.65 \times 10^{-5} kg\, N_2O$.

The life cycle inventory data for titanium dioxide are shown in Table A.12 (Althaus et al. 2004).

Table A.12: Complied life cycle inventory data for the production of titanium dioxide.

Production of 1 kg of Titanium Dioxide		
Energy	83.2477	MJ
Water	18.92572	m^3
CO_2	3.825051	kg
CH_4	0.007041	kg
N_2O	0	kg
Air Emissions	3.865409	kg
Water Emissions	0.472564	kg
Soil Emissions	0.003676	kg

A.7 Carbon

The energy inputs for the production of carbon, in the form of graphite, are shown in Table A.13 (Althaus et al. 2004).

Table A.13: Energy inputs for the production of carbon.

Energy Inputs for Production of 1kg of Carbon		
Coal, Brown	0.005555	kg
Coal, Hard	0.003211	kg
Natural Gas	0.001464	m^3
Oil, Crude	0.003707	kg
Uranium	2.866E-7	kg

These energy inputs represent a total energy of $E = 0.44285MJ$. The total CO_2, CH_4, and N_2O emissions from these fuels are $0.0312kg\,CO_2$, $3.57\times10^{-4}\,kg\,CH_4$, and $1.48\times10^{-7}\,kg\,N_2O$. The life cycle inventory data for the production of 1kg of carbon are shown in Table A.14 (Althaus et al. 2004).

Table A.14: Compiled life cycle inventory data for the production of carbon.

Production of 1 kg of Carbon		
Energy	0.450159	MJ
Water	0.165645	m^3
CO_2	0.027504	kg
CH_4	3.01E-05	kg
N_2O	0	kg
Air Emissions	0.041946	kg
Water Emissions	0.000911	kg
Soil Emissions	1.94E-05	kg

A.8 Chlorine

The energy inputs for the production of chlorine are shown in Table A.15 (Althaus et al. 2004).

Table A.15: Energy inputs for the production of chlorine.

Energy Inputs for Production of 1kg of Chlorine		
Coal, Brown	0.30121	kg
Coal, Hard	0.17812	kg
Natural Gas	0.073294	m^3
Oil, Crude	0.051699	kg
Uranium	1.56E-5	kg

These fuel inputs represent a total energy of $E = 17.54MJ$. The total CO_2, CH_4, and N_2O emissions from these fuels are $1.25kg\,CO_2$, $0.00195kg\,CH_4$, and $8.22\times10^{-6}\,kg\,N_2O$. The life cycle inventory data for the production of chlorine are shown in Table A.16 (Althaus et al. 2004).

Table A.16: Compiled life cycle inventory data for the production of chlorine.

Production of 1 kg of Chlorine		
Energy	18.0877	MJ
Water	9.025745	m^3
CO_2	2.200463	kg
CH_4	0.00338	kg
N_2O	8.22E-6	kg
Air Emissions	0.959829	kg
Water Emissions	0.048306	kg
Soil Emissions	4.03E-04	kg

A.9 Silicon

The energy inputs for the production of silicon are shown in Table A.17.

Table A.17: Energy inputs for production of silicon.

Energy Inputs for Production of 1kg of Silicon		
Coal, Brown	0.064716	kg
Coal, Hard	1.7674	kg
Natural Gas	0.05242	m^3
Oil, Crude	0.69822	kg
Uranium	3.9E-6	kg

A total of 65.474 MJ of energy is extracted from these fuels. Using these fuels emits 8.8653 kg CO_2, 0.0094 kg CH_4 and 4.67E-5 kg N_2O. The total life cycle inventory data for 1 kg of silicon is shown in Table A.18.

Table A.18: Life cycle inventory for silicon.

Production of 1 kg of Silicon		
Energy	88.23439	MJ
Water	13.15227	m3
CO_2	15.35	kg
CH_4	0.02736	kg
N_2O	4.67E-05	kg
Air Emissions	6.597363	kg
Water Emissions	0.099741	kg
Soil Emissions	3.72E-03	kg

A.10 Hydrochloric Acid

The energy inputs for the production of hydrochloric acid are shown in Table A.19.

Table A.19: Energy inputs for production of hydrochloric acid.

Energy Inputs for Production of 1kg of Hydrochloric Acid		
Coal, Brown	0.051134	kg
Coal, Hard	0.035826	kg
Natural Gas	0.043532	m^3
Oil, Crude	0.047888	kg
Uranium	2.7E-6	kg

A total of 5.906519 MJ are extracted from these fuels. A total of 0.40330 kg CO_2, 3.617E-4 kg CH_4, and 1.5246E-6 kg N_2O are emitted when using these fuels. The total life cycle inventory is shown in Table A.20.

Table A.20: Life cycle inventory of hydrochloric acid.

Production of 1 kg of Hydrochloric Acid		
Energy	6.162194	MJ
Water	1.830249	m^3
CO_2	0.783717	kg
CH_4	0.000867	kg
N_2O	1.52E-06	kg
Air Emissions	0.385303	kg
Water Emissions	0.054015	kg
Soil Emissions	4.15E-04	kg

A.11 Nitric Acid

The energy inputs for the production of nitric acid are shown in Table A.21.

Table A.21: Energy inputs for the production of nitric acid.

Energy Inputs for Production of 1kg of Nitric Acid		
Coal, Brown	0.02654	kg
Coal, Hard	0.020977	kg
Natural Gas	0.2512	m^3
Oil, Crude	0.13837	kg
Uranium	1.417E-6	kg

The total energy content of these fuels is 16.287 MJ. The total emissions of these fuels are 0.9904 kg CO_2, 2.044E-4 kg CH_4, and 8.53E-7 kg N_2O. The total life cycle inventory for the production of 1 kg of nitric acid is shown in Table A.22.

Table A.22: Life cycle inventory of nitric acid.

Production of 1 kg of Nitric Acid		
Energy	16.56267	MJ
Water	1.106286	m3
CO_2	1.84808	kg
CH_4	0.001808	kg
N_2O	8.53E-07	kg
Air Emissions	0.876926	kg
Water Emissions	0.021572	kg
Soil Emissions	0.000768	kg

A.12 Methanol

The energy inputs to the production of methanol are shown in Table A.23.

Table A.23: Energy inputs for methanol.

Energy Inputs for Production of 1kg of Methanol		
Coal, Brown	0.02041	kg
Coal, Hard	0.012896	kg
Natural Gas	0.94034	m^3
Oil, Crude	0.005712	kg
Uranium	1.06E-6	kg

These fuels contain 35.529 MJ of energy, and their emissions are 1.8895 kg CO_2, 1.71E-4 kg CH_4, and 5.72E-7 kg N_2O. The total life cycle inventory of methanol is shown in Table A.24.

Table A.24: Life cycle inventory data of methanol.

Production of 1 kg of Methanol		
Energy	35.55848	MJ
Water	0.646951	m3
CO_2	1.9893	kg
CH_4	0.004367	kg
N_2O	5.72E-07	kg
Air Emissions	0.640534	kg
Water Emissions	0.006445	kg
Soil Emissions	1.31E-04	kg

A.13 Fluorine

The energy inputs to the production of fluorine are shown in Table A.25.

Table A.25: Energy inputs for fluorine.

Energy Inputs for Production of 1kg of Fluorine		
Coal, Brown	2.644	kg
Coal, Hard	1.507	kg
Natural Gas	0.63254	m^3
Oil, Crude	0.46843	kg
Uranium	0.000137	kg

These fuels contain 152.8065 MJ of energy, and their emissions are 10.8428 kg CO_2, 0.01685 kg CH_4, and 9.6857E-5 kg N_2O. The total life cycle inventory of methanol is shown in Table A.26.

Table A.26: Life cycle inventory data for fluorine.

Production of 1 kg of Fluorine		
Energy	156.9287	MJ
Water	77.3895	m^3
CO_2	18.9318	kg
CH_4	2.90E-02	kg
N_2O	6.90E-05	kg
Air Emissions	8.213197	kg
Water Emissions	0.243668	kg
Soil Emissions	2.94E-03	kg

A.14 Ethylene

The energy inputs to the production of ethylene are shown in Table A.27.

Table A.27: Energy inputs for ethylene.

Energy Inputs for Production of 1kg of Ethylene		
Coal, Brown	0.000715	kg
Coal, Hard	0.017953	kg
Natural Gas	0.79801	m^3
Oil, Crude	0.75004	kg
Uranium	8.43E-7	kg

These fuels contain 61.56792 MJ of energy, and their emissions are 3.7968 kg CO_2, 0.000125 kg CH_4, and 4.75E-7 kg N_2O. The total life cycle inventory of ethylene is shown in Table A.28.

Table A.28: Life cycle inventory data for ethylene.

Production of 1 kg of Ethylene		
Energy	61.57616	MJ
Water	0.064524	m^3
CO_2	4.95868	kg
CH_4	4.20E-03	kg
N_2O	4.75E-07	kg
Air Emissions	1.0827	kg
Water Emissions	0.002133	kg
Soil Emissions	1.36E-07	kg

A.15 Sodium Chlorate

The energy inputs to the production of sodium chlorate are shown in Table A.29.

Table A.29: Energy inputs for sodium chlorate.

Energy Inputs for Production of 1kg of Sodium Chlorate		
Coal, Brown	0.000715	kg
Coal, Hard	0.017953	kg
Natural Gas	0.79801	m^3
Oil, Crude	0.75004	kg
Uranium	8.43E-7	kg

These fuels contain 53.4483 MJ of energy, and their emissions are 3.792389 kg CO_2, 0.006085 kg CH_4, and 2.522E-5 kg N_2O. The total life cycle inventory of sodium chlorate is shown in Table A.30.

Table A.30: Life cycle inventory data for sodium chlorate.

Production of 1 kg of Sodium Chlorate		
Energy	54.87043	MJ
Water	27.97997	m^3
CO_2	6.603721	kg
CH_4	0.012682	kg
N_2O	2.52E-05	kg
Air Emissions	2.89488	kg
Water Emissions	0.13991	kg
Soil Emissions	8.40E-04	kg

A.16 Sulfuric Acid

The energy inputs to the production of sulfuric acid are shown in Table A.31.

Table A.31: Energy inputs for sulfuric acid.

Energy Inputs for Production of 1kg of Sulfuric Acid		
Coal, Brown	0.011379	kg
Coal, Hard	0.008604	kg
Natural Gas	0.005269	m^3
Oil, Crude	0.026086	kg
Uranium	6.09E-7	kg

These fuels contain 1.82483 MJ of energy, and their emissions are 0.128575 kg CO_2, 8.36E-5 kg CH_4, and 3.557E-7 kg N_2O. The total life cycle inventory of sulfuric acid is shown in Table A.32.

Table A.32: Life cycle inventory data for sulfuric acid.

Production of 1 kg of Sulfuric Acid		
Energy	1.919393	MJ
Water	0.49585	m^3
CO_2	0.251525	kg
CH_4	0.000223	kg
N_2O	3.56E-07	kg
Air Emissions	0.141382	kg
Water Emissions	0.007691	kg
Soil Emissions	1.59E-04	kg

A.17 Ethylene Glycol

The energy inputs to the production of ethylene glycol are shown in Table A.33.

Table A.33: Energy inputs for ethylene glycol.

Energy Inputs for Production of 1kg of Ethylene Glycol		
Coal, Brown	0.16362	kg
Coal, Hard	0.10797	kg
Natural Gas	0.51875	m^3
Oil, Crude	0.47807	kg
Uranium	8.97E-6	kg

These fuels contain 46.64803 MJ of energy, and their emissions are 2.958371 kg CO_2, 0.001137 kg CH_4, and 4.7052 E-6 kg N_2O. The total life cycle inventory of ethylene glycol is shown in Table A.34.

Table A.34: Life cycle inventory data for ethylene glycol.

Production of 1 kg of Ethylene Glycol		
Energy	47.07653	MJ
Water	5.041298	m^3
CO_2	4.338158	kg
CH_4	0.004416	kg
N_2O	4.71E-06	kg
Air Emissions	7.054236	kg
Water Emissions	0.316873	kg
Soil Emissions	2.10E-04	kg

A.18 Chromium Ore

The energy inputs to the production of chromium ore (chromite) are shown in Table A.35.

Table A.35: Energy inputs for chromite.

Energy Inputs for Production of 1kg of Chromite		
Coal, Brown	0.003344	kg
Coal, Hard	0.002828	kg
Natural Gas	0.001841	m^3
Oil, Crude	0.003334	kg
Uranium	1.78E-7	kg

These fuels contain 0.3672 MJ of energy, and their emissions are 0.0264 kg CO_2, 2.614E-5 kg CH_4, and 1.123 E-7 kg N_2O. The total life cycle inventory of chromite is shown in Table A.36.

Table A.36: Life cycle inventory data for chromite.

Production of 1 kg of Chromite		
Energy	0.413195	MJ
Water	1.173303	m^3
CO_2	0.0527	kg
CH_4	5.68E-05	kg
N_2O	1.12E-07	kg
Air Emissions	0.028087	kg
Water Emissions	0.001301	kg
Soil Emissions	1.80E-05	kg

A.19 Platinum

The life cycle inventory data for platinum was obtained on per 1000 kg basis (Overcash 2008), and is shown in Table A.37.

Table A.37: Life cycle inventory data for platinum.

Production of 1000 kg of Platinum		
Energy	125000	MJ
Water	0	m^3
CO_2	428	kg
CH_4	0	kg
N_2O	0	kg
Air Emissions	30.4	kg
Water Emissions	0	kg
Soil Emissions	3820	kg

A.20 Sodium Chloride

The energy inputs for the production of sodium chloride are shown in Table A.38 (PRé Consultants 1996).

Table A.38: Energy inputs for the production of sodium chloride.

Energy Inputs for Production of 1000kg of Sodium Chloride		
Coal, Brown	7.3	kg
Coal, Hard	16	kg
Natural Gas	43	m^3
Oil, Crude	15	kg
Uranium	4.7E-4	kg

These fuels contain 2771 MJ of energy, and their emissions are 388 kg CO_2, 0.00342 kg CH_4, and 0.00779 kg N_2O. The total life cycle inventory of sodium chloride per kg is complied and is shown in Table A.39.

Table A.39: Life cycle inventory data for the production of sodium chloride.

Production of 1 kg of Sodium Chloride		
Energy	2.82	MJ
Water	0.0046	m^3
CO_2	0.563	kg
CH_4	3.73E-4	kg
N_2O	7.79E-6	kg
Air Emissions	0.182	kg
Water Emissions	0.0425	kg
Soil Emissions	0.035	kg

A.21 Total Life Cycle Inventory of Chemical Coating

A.21.1 TACA, AACA, Boehmite and Ethanol Mixture

The total life cycle inventory for this mixture per chemical is shown in Table A.40.

Table A.40: Total life cycle inventory of chemical mixture.

Chemical Name	ENERGY	WATER	CO2	CH4	N2O	AIR RELEASES	WATER RELEASES	SOIL RELEASES
Titanium Acetylacetonate	0.00326	0.0007	0.0005	4E-09	9.2E-09	4.1254E-07	1.0293E-05	0
Oxychloride	0.00176	0.00038	0.0002	2.2E-09	5E-09	1.438E-07	5.1022E-06	0
Titanium Chloride	0.00168	0.00056	0.0002	2.1E-09	4.7E-09	2.5454E-07	0.11449197	0
Rutile	0.00285	0.00078	0.0004	4.6E-07	6.8E-10	0.00015993	1.9552E-05	1.5209E-07
Chlorine	0.00081	0.00066	0.0002	2.5E-07	6E-10	7.0505E-05	3.5483E-06	2.9603E-08
Carbon	4E-06	2.1E-06	7E-07	4.8E-09	1.8E-12	5.2172E-07	1.1331E-08	2.4129E-10
Water	0	0.00887	0	0	0	0	0	0
Acetylacetone	0.00262	0.00056	0.0004	3.2E-09	7.4E-09	3.1546E-07	7.8704E-06	0
Acetone	0.00358	3.7E-06	0.0003	2.4E-07	1.3E-10	0.00011409	1.3E-06	2.963E-11
Acetic Anhydride	0.00637	0.00107	0.0007	1.5E-06	1E-09	0.00023806	8.89E-06	2.9907E-07
Sodium Carbonate	0.00022	6.9E-05	5E-05	9.5E-08	2.2E-10	2.1431E-05	7.7153E-06	7.5342E-08
Aluminum acetylacetonate	0.39278	0.08417	0.055	4.9E-07	1.1E-06	5.6901E-05	0.00141963	0
Aluminum Sulphate	0.08374	0.04453	0.0429	1.9E-05	4E-08	0.0069474	0.0006336	4.608E-06
Acetylacetone	0.38307	0.08209	0.0536	4.7E-07	1.1E-06	4.6075E-05	0.00114954	0
Acetone	0.55603	0.00054	0.0486	3.6E-05	1.8E-08	0.0166643	0.00018987	4.3278E-09
Acetic Anhydride	0.93041	0.15677	0.0998	0.00022	1.5E-07	0.03477111	0.00129847	4.3681E-05
Boehmite	0.02411	5.4E-06	0.0024	2.8E-06	2.4E-09	0.00196152	2.8022E-05	0
Ethanol	12.076	0.02454	0.1449	0	0.18823	0	0	0
TOTALS	14.4693	0.4063	0.4502	0.00028	0.18823	0.06105297	0.11927539	4.885E-05
	MJ	m^3	kg	kg	kg	kg	kg	kg

A.21.2 Total Water Repellent Solution Inventory

The life cycle inventory per chemical for the water repellent solution is shown in Table A.41.

Table A.41: Total life cycle inventory of water repellent solution.

	Energy	Water	CO2	CH4	N2O	Air	Water	Soil
Total mass of water	0	0.0002	0	0	0	0	0	0
Total mass of FAS	0.083	0.0166	0.0116	1E-07	2.33E-07	1.41E-05		0
Sodium Methoxide	0.0194	3E-06	0.0027	2.4E-08	5.45E-08	0	0	0
Methanol	0.0367	0.0007	0.0021	4.5E-06	5.9E-10	0.000661	6.65E-06	1.35E-07
Sodium Chloride	0.0051	8E-06	0.001	6.8E-07	1.42E-08	0.000331	7.73E-05	6.37E-05
Methanol	0.2486	0.0045	0.0139	3.1E-05	4E-09	0.004479	4.51E-05	9.16E-07
Trichlorosilane	0.0025	0	0.0003	3.1E-09	6.96E-09	8.82E-06	0.00022	0
Silicon	0.0725	0.0108	0.0126	2.2E-05	3.84E-08	0.005422	8.2E-05	3.06E-06
Hydrochloric acid	0.0221	0.0066	0.0028	3.1E-06	5.46E-09	0.001383	0.000194	1.49E-06
Chloroplatinic acid	0.0002	4E-05	3E-05	2.2E-10	5.03E-10	1.8E-08	4.5E-07	0
Platinum	0.2232	0	0.0252	2.2E-07	5.06E-07	0	0	0
Nitric acid	6E-05	4E-06	7E-06	7E-09	3.29E-12	5.11E-06	1.26E-07	4.48E-09
Hydrochloric acid	1E-05	4E-06	2E-06	1.9E-09	3.3E-12	8.36E-07	1.17E-07	9E-10
Methanol	0.0003	6E-06	2E-05	4E-08	5.2E-12	5.83E-06	5.86E-08	1.19E-09
1H,1H,2H,2H-heptad	0.1161	0.0232	0.0163	1.4E-07	3.26E-07	1.05E-05	0.000262	0
Ethylene	0.0158	2E-05	0.0013	1.1E-06	1.22E-10	0.000277	5.46E-07	3.48E-11
Iodoperfluorooctane	0.1496	0.0299	0.0209	1.8E-07	4.2E-07	1.05E-05	0.000262	0
Tetrafluoroethylene								
Pentafluoroethyl Iodi	0.0708	0.0142	0.0099	2.9E-09	1.99E-07	4.97E-06	0.000124	0
Tetrafluoroethylene								
Iodine	0.0185	0.0037	0.0021	1.7E-06	0.000315	0.000602	5.4E-05	2.35E-05
Iodine Pentafluoride	0.0134	0.0027	0.0019	1.7E-08	3.77E-08	9.42E-07	2.35E-05	0
Iodine	0.0074	0.0015	0.0008	6.6E-07	0.000137	0.00024	2.16E-05	9.37E-06
Fluorine	0.0096	0.0047	0.0012	1.8E-06	4.22E-09	0.000503	1.49E-05	1.8E-07
TOTAL	1.115	0.1194	0.1267	6.7E-05	0.000454	0.013958	0.001388	0.000102
	MJ	m^3	kg	kg	kg	kg	kg	kg

APPENDIX B

LIFE CYCLE INVENTORIES OF ANODIZED ALUMINUM TEMPLATE

The life cycle inventories for the anodized aluminum template for various total template uses, total chemical uses and various chemical replacement per filtration are given in this appendix.

B.1 Best Case Scenario – Indefinite Chemical Use

In this scenario, secondary aluminum is used. The chemicals are assumed to filtrated definitely; therefore, no amount of the initial volume of chemicals is attributed to the template. The replacement rate is 5% of the total volume of chemicals per filtration, and it is assumed that both anodizing and oxide removal cycles are performed before filtering. This inventory is shown in Table B.1, for increasing values of the total use of the template.

Table B.1: Best case scenario for inventory of anodized aluminum template.

Best Case Scenario - chemicals used indefinitely, secondary aluminum, 5% replacement							
Uses of Template:	**1**	**10**	**25**	**50**	**75**	**100**	
Energy	1068.9	106.891	42.756	21.3782	14.2521	10.6891	**MJ**
Water	33.451	3.34505	1.338	0.66901	0.44601	0.33451	**m^3**
CO_2	12.447	1.24466	0.4979	0.24893	0.16595	0.12447	**kg**
CH_4	0.0085	0.00085	0.0003	0.00017	0.00011	8.5E-05	**kg**
N_2O	1.0209	0.10209	0.0408	0.02042	0.01361	0.01021	**kg**
Air Emissions	5.1968	0.51968	0.2079	0.10394	0.06929	0.05197	**kg**
Water Emissions	0.379	0.0379	0.0152	0.00758	0.00505	0.00379	**kg**
Soil Emissions	2.1571	0.21571	0.0863	0.04314	0.02876	0.02157	**kg**

The inventory for secondary aluminum with a 20% chemical replacement rate after filtration is shown in Table B.2.

Table B.2: Inventory for secondary aluminum, with 20% chemical replacement rate per filtration.

Best Case Scenario - chemicals used indefinitely, secondary aluminum, 20% replacement							
Uses of Template:	**1**	**10**	**25**	**50**	**75**	**100**	
Energy	1510.21	151.021	60.408	30.204	20.1361	15.102	**MJ**
Water	133.802	13.3802	5.3521	2.676	1.78403	1.338	**m^3**
CO_2	27.0418	2.70418	1.0817	0.5408	0.36056	0.2704	**kg**
CH_4	0.03374	0.00337	0.0013	0.0007	0.00045	0.0003	**kg**
N_2O	4.08302	0.4083	0.1633	0.0817	0.05444	0.0408	**kg**
Air Emissions	18.7631	1.87631	0.7505	0.3753	0.25017	0.1876	**kg**
Water Emissions	1.49203	0.1492	0.0597	0.0298	0.01989	0.0149	**kg**
Soil Emissions	2.17402	0.2174	0.087	0.0435	0.02899	0.0217	**kg**

The inventory for the best case scenario with primary aluminum is shown in Table B.3, for increasing uses of the template.

Table B.3: Inventory for best case scenario of primary anodized aluminum template.

Best Case Scenario - chemicals used indefinitely, primary aluminum, 5% replacement							
Uses of Template:	**1**	**10**	**25**	**50**	**75**	**100**	
Energy	1661.8	166.176	66.47	33.2351	22.1567	16.6176	**MJ**
Water	33.451	3.34505	1.338	0.66901	0.44601	0.33451	**m^3**
CO_2	34.759	3.47586	1.3903	0.69517	0.46345	0.34759	**kg**
CH_4	0.0093	0.00093	0.0004	0.00019	0.00012	9.3E-05	**kg**
N_2O	1.0209	0.10209	0.0408	0.02042	0.01361	0.01021	**kg**
Air Emissions	28.643	2.86429	1.1457	0.57286	0.38191	0.28643	**kg**
Water Emissions	0.4435	0.04435	0.0177	0.00887	0.00591	0.00443	**kg**
Soil Emissions	38.558	3.85576	1.5423	0.77115	0.5141	0.38558	**kg**

The inventory for indefinite chemical use, primary aluminum and 20% replacement rate per filtration is shown in Table B.4.

Table B.4: Inventory for primary aluminum template, with 20% replacement rate per filtration.

Best Case Scenario - chemicals used indefinitely, primary aluminum, 20% replacement							
Uses of Template:	**1**	**10**	**25**	**50**	**75**	**100**	
Energy	2103.05	210.305	84.122	42.061	28.0407	21.031	**MJ**
Water	133.802	13.3802	5.3521	2.676	1.78403	1.338	**m^3**
CO_2	49.3538	4.93538	1.9742	0.9871	0.65805	0.4935	**kg**
CH_4	0.03457	0.00346	0.0014	0.0007	0.00046	0.0003	**kg**
N_2O	4.08305	0.4083	0.1633	0.0817	0.05444	0.0408	**kg**
Air Emissions	42.2092	4.22092	1.6884	0.8442	0.56279	0.4221	**kg**
Water Emissions	1.55658	0.15566	0.0623	0.0311	0.02075	0.0156	**kg**
Soil Emissions	38.5745	3.85745	1.543	0.7715	0.51433	0.3857	**kg**

B.2 Chemicals Recycled Finite Times

In the best case scenario, the chemicals are used indefinitely. In a more realistic scenario, the chemicals will be filtrated a finite number of times before being completely replaced. In the following sections, the inventory is calculated for various total times that the chemicals are recycled.

B.2.1 Chemicals Recycled One Hundred Times

The inventory for the production of the template with secondary aluminum, 5% replacement, and one hundred uses of the initial volume of chemicals is shown in Table B.5, for increasing uses of the template.

Table B.5: Inventory for 100 uses of chemicals, secondary aluminum and 5% chemical replacement rate.

Chemicals recycled 100 times before replacement, 5% replacement, secondary

Uses of Template:	1	10	25	50	75	100	
Energy	1098.3	109.833	43.933	21.9666	14.6444	10.9833	**MJ**
Water	40.141	4.01406	1.6056	0.80281	0.53521	0.40141	**m^3**
CO_2	13.42	1.34196	0.5368	0.26839	0.17893	0.1342	**kg**
CH_4	0.0102	0.00102	0.0004	0.0002	0.00014	0.0001	**kg**
N_2O	1.225	0.1225	0.049	0.0245	0.01633	0.01225	**kg**
Air Emissions	6.1012	0.61012	0.244	0.12202	0.08135	0.06101	**kg**
Water Emissions	0.4532	0.04532	0.0181	0.00906	0.00604	0.00453	**kg**
Soil Emissions	2.1582	0.21582	0.0863	0.04316	0.02878	0.02158	**kg**

The same scenario for the use of primary aluminum is shown in Table B.6.

Table B.6: Inventory for 100 uses of chemicals, primary aluminum and 5% chemical replacement rate.

Chemicals recycled 100 times before replacement, 5% replacement, primary

Uses of Template:	1	10	25	50	75	100	
Energy	1691.2	169.118	67.647	33.8235	22.549	16.9118	**MJ**
Water	40.141	4.01406	1.6056	0.80281	0.53521	0.40141	**m^3**
CO_2	35.732	3.57316	1.4293	0.71463	0.47642	0.35732	**kg**
CH_4	0.011	0.0011	0.0004	0.00022	0.00015	0.00011	**kg**
N_2O	1.225	0.1225	0.049	0.0245	0.01633	0.01225	**kg**
Air Emissions	29.547	2.95473	1.1819	0.59095	0.39396	0.29547	**kg**
Water Emissions	0.5177	0.05177	0.0207	0.01035	0.0069	0.00518	**kg**
Soil Emissions	38.559	3.85587	1.5423	0.77117	0.51412	0.38559	**kg**

B.2.2 Chemicals Recycled 50 Times

The inventory for a secondary aluminum template, with chemicals replaced after 50 uses and 5% replacement per filtration is shown in Table B.7.

Table B.7: Inventory for 50 uses of chemicals, secondary aluminum and 5% replacement per filtration.

Chemicals recycled 50 times before replacement, 5% replacement, secondary							
Uses of Template:	**1**	**10**	**25**	**50**	**75**	**100**	
Energy	1127.8	112.775	45.11	22.555	15.0367	11.2775	**MJ**
Water	46.831	4.68307	1.8732	0.93661	0.62441	0.46831	**m^3**
CO_2	14.393	1.43926	0.5757	0.28785	0.1919	0.14393	**kg**
CH_4	0.0119	0.00119	0.0005	0.00024	0.00016	0.00012	**kg**
N_2O	1.4292	0.14292	0.0572	0.02858	0.01906	0.01429	**kg**
Air Emissions	7.0057	0.70057	0.2802	0.14011	0.09341	0.07006	**kg**
Water Emissions	0.5274	0.05274	0.0211	0.01055	0.00703	0.00527	**kg**
Soil Emissions	2.1593	0.21593	0.0864	0.04319	0.02879	0.02159	**kg**

The inventory for 50 uses of the initial volume of chemicals and 5% replacement per filtration, for a primary aluminum template, is shown in Table B.8.

Table B.8: Inventory for 50 uses of chemicals, primary aluminum and 5% replacement rate.

Chemicals recycled 50 times before replacement, 5% replacement, primary							
Uses of Template:	**1**	**10**	**25**	**50**	**75**	**100**	
Energy	1720.6	172.06	68.824	34.4119	22.9413	17.206	**MJ**
Water	46.831	4.68307	1.8732	0.93661	0.62441	0.46831	**m^3**
CO_2	36.705	3.67046	1.4682	0.73409	0.48939	0.36705	**kg**
CH_4	0.0127	0.00127	0.0005	0.00025	0.00017	0.00013	**kg**
N_2O	1.4292	0.14292	0.0572	0.02858	0.01906	0.01429	**kg**
Air Emissions	30.452	3.04518	1.2181	0.60904	0.40602	0.30452	**kg**
Water Emissions	0.5919	0.05919	0.0237	0.01184	0.00789	0.00592	**kg**
Soil Emissions	38.56	3.85598	1.5424	0.7712	0.51413	0.3856	**kg**

B.2.3 Chemicals Recycled 25 Times

The inventory for a secondary aluminum template, with chemicals replaced after 25 uses and 5% replacement per filtration is shown in Table B.9.

Table B.9: Inventory for secondary aluminum and 5% replacement per filtration.
Chemicals recycled 25 times before replacement, 5% replacement, secondary

Uses of Template:	1	10	25	50	75	100	
Energy	1186.6	118.659	47.464	23.7318	15.8212	11.8659	**MJ**
Water	60.211	6.02109	2.4084	1.20422	0.80281	0.60211	**m^3**
CO_2	16.339	1.63386	0.6535	0.32677	0.21785	0.16339	**kg**
CH_4	0.0152	0.00152	0.0006	0.0003	0.0002	0.00015	**kg**
N_2O	1.8374	0.18374	0.0735	0.03675	0.0245	0.01837	**kg**
Air Emissions	8.8145	0.88145	0.3526	0.17629	0.11753	0.08815	**kg**
Water Emissions	0.6758	0.06758	0.027	0.01352	0.00901	0.00676	**kg**
Soil Emissions	2.1616	0.21616	0.0865	0.04323	0.02882	0.02162	**kg**

The inventory for the primary aluminum template, with chemicals replaced after 25 uses and 5% replacement is shown in Table B.10.

Table B.10: Inventory for primary aluminum and 10% replacement per filtration.
Chemicals recycled 25 times before replacement, 5% replacement, primary

Uses of Template:	1	10	25	50	75	100	
Energy	1779.4	177.944	71.177	35.5887	23.7258	17.7944	**MJ**
Water	60.211	6.02109	2.4084	1.20422	0.80281	0.60211	**m^3**
CO_2	38.651	3.86506	1.546	0.77301	0.51534	0.38651	**kg**
CH_4	0.016	0.0016	0.0006	0.00032	0.00021	0.00016	**kg**
N_2O	1.8375	0.18375	0.0735	0.03675	0.0245	0.01837	**kg**
Air Emissions	32.261	3.22606	1.2904	0.64521	0.43014	0.32261	**kg**
Water Emissions	0.7403	0.07403	0.0296	0.01481	0.00987	0.0074	**kg**
Soil Emissions	38.562	3.85621	1.5425	0.77124	0.51416	0.38562	**kg**

APPENDIX C

LIFE CYCLE INVENTORY OF INDUSTRIAL CLEANING WITH RECYCLING

C.1 Cleaning Solution LCI

For the case of 150 L part volume and a solvent concentration of 30 g/L, the amounts of water and solvent necessary for 300L of cleaning solution are:

$$Water \cdot \frac{30g\,TCE}{L} \cdot \frac{1kg}{1000g} = Solvent$$

$$Water + Solvent\left(\frac{1L}{1.46kg}\right) = 300L$$

Solving these two equations yields a total water of 293 L and 8.82 kg of solvent. The inventory data of the production of 8.82 kg of solvent and water for 300L of cleaning solution are shown in Table C.1.

Table C.1: Life cycle inventory data for production of 300L cleaning solution, at 30g/L solvent, for spray cleaning.

Spray Cleaning - 30g/L – 300L Cleaning Solution		
Energy	355.045	MJ
Water	1.05	m^3
CO_2	28.406	kg
CH_4	0.020	kg
N_2O	9.26E-05	kg
Air Emissions	0.826	kg
Water Emissions	5.462	kg
Soil Emissions	5.79E-05	kg

For the 12 L part which requires 24 L of cleaning and a solvent concentration of 4 g/L, the amounts of water and solvent are determined from:

$$Water \cdot \frac{4g\,TCE}{L} \cdot \frac{1kg}{1000g} = Solvent$$

$$Water + Solvent\left(\frac{1L}{1.46kg}\right) = 24L$$

The total water needed is 23.93L and the total required solvent is 95.7g. The inventory data for the production of 95.7 g of solvent and the water to form the cleaning solution are shown in Table C.2.

Table C.2: Life cycle inventory data for 24L of cleaning solution, at 4g/L solvent, for spray cleaning.

Spray Cleaning - 4g/L – 24L Cleaning Solution		
Energy	3.852	MJ
Water	0.032	m^3
CO_2	0.308	kg
CH_4	2.20E-04	kg
N_2O	1.00E-06	kg
Air Emissions	0.009	kg
Water Emissions	0.059	kg
Soil Emissions	6.28E-07	kg

For the 200 L capacity machine and a solvent concentration of 30 g/L, the necessary amounts of water and solvent are determined from:

$$Water \cdot \frac{30g\,TCE}{L} \cdot \frac{1kg}{1000g} = Solvent$$

$$Water + Solvent\left(\frac{1L}{1.46kg}\right) = 24L$$

Solving these equations yields 23.52L water and 0.705 kg solvent. The inventory data for the production of 705 g of solvent and 23.52L of cleaning water are shown in Table C.3.

Table C.3: Life cycle inventory data for the production of 24L of cleaning solution, at 30g/L solvent, for spray cleaning.

Spray Cleaning - 30g/L – 24L Cleaning Solution		
Energy	28.379	MJ
Water	0.084	m^3
CO_2	2.271	kg
CH_4	1.62E-03	kg
N_2O	7.40E-06	kg
Air Emissions	0.066	kg
Water Emissions	0.437	kg
Soil Emissions	4.62E-06	kg

The typical concentration of solvent for ultrasonic cleaning is 75 g/L (Murphy 2000). For the part which is 150L in volume, a total of 300L of solution is needed. The total water and solvent which comprise the cleaning solution, using the fact that the density of TCE is $\frac{1.46kg}{1L}$, can be solved from:

$$Water \cdot \frac{75g\,TCE}{L} \cdot \frac{1kg}{1000g} = Solvent$$

$$Water + Solvent\left(\frac{1L}{1.46kg}\right) = 300L$$

The solution to these equations is 285.34 L of water and 21.4 kg of TCE. The inventory data of producing 21.4 kg of solvent and the water used in the cleaning solution are shown in Table C.4.

Table C.4: Life cycle inventory data for the production of 300L of cleaning solution for ultrasonic cleaning.

Ultrasonic Cleaning -300L Cleaning Solution		
Energy	861.446	MJ
Water	2.121	m^3
CO_2	68.922	kg
CH_4	4.91E-02	kg
N_2O	2.25E-04	kg
Air Emissions	2.003	kg
Water Emissions	13.254	kg
Soil Emissions	1.40E-04	kg

The second ultrasonic cleaning scenario (12 L part volume) has a total cleaning solution volume of 24L. The total amounts of water and solvent which comprise this volume are determined from:

$$Water \cdot \frac{75g\,TCE}{L} \cdot \frac{1kg}{1000g} = Solvent$$

$$Water + Solvent\left(\frac{1L}{1.46kg}\right) = 24L$$

Solving these equations yields a water volume of 22.83 L and 1.71 kg of solution. The life cycle inventory data for 1.71 kg of TCE are shown in Table C.5.

Table C.5: Life cycle inventory data for the production of 24L of cleaning solution for ultrasonic cleaning.

Ultrasonic Cleaning – 24L Cleaning Solution		
Energy	68.835	MJ
Water	0.170	m^3
CO_2	5.507	kg
CH_4	3.92E-03	kg
N_2O	1.80E-05	kg
Air Emissions	0.160	kg
Water Emissions	1.059	kg
Soil Emissions	1.12E-05	kg

C.2 Recycling of Cleaning Solution Scenarios

The life cycle inventory of aqueous cleaning are calculated for the minimum and maximum value of each variable. These variables are: solvent concentration (4g/L to 30 g/L for spray cleaning), cleaning time (1 to 10 minutes), and amount of chemicals replaced per filtration (5% to 20%). Each life cycle inventory is shown for increasing uses of the initial volume of cleaning solution used in the cleaning machines.

C.2.1 Spray Cleaning

The life cycle inventory data of various cleaning scenarios for spray cleaning are shown in Table C.6 through Table C.13.

Table C.6: Inventory of spray cleaning of 150L part, with low concentration and cleaning time and 5% replacement per filtration.

Spray Cleaning - 150L 4g/L 1 minute - 5% replacement							
# of Uses:	**1**	**10**	**25**	**50**	**75**	**100**	
Energy	52.105	8.750	5.860	4.896	4.575	4.414	MJ
Water	0.422	0.060	0.036	0.028	0.025	0.024	m^3
CO_2	4.260	0.791	0.560	0.483	0.457	0.445	kg
CH_4	3.15E-03	4.52E-04	2.72E-04	2.12E-04	1.92E-04	1.82E-04	kg
N_2O	1.75E-05	6.17E-06	5.42E-06	5.16E-06	5.08E-06	5.04E-06	kg
Waste:							
Air	0.118	0.017	0.010	0.008	0.007	0.007	kg
Water	0.778	0.111	0.067	0.052	0.047	0.044	kg
Soil	8.24E-06	1.18E-06	7.07E-07	5.50E-07	4.97E-07	4.71E-07	kg

Table C.7: Inventory of spray cleaning of 150L part, with low concentration and cleaning time and 20% replacement per filtration.

Spray Cleaning - 150L 4g/L 1 minute - 20% replacement							
# of Uses:	**1**	**10**	**25**	**50**	**75**	**100**	
Energy	59.331	15.976	13.085	12.122	11.801	11.640	MJ
Water	0.482	0.121	0.096	0.088	0.086	0.084	m^3
CO_2	4.838	1.370	1.138	1.061	1.036	1.023	kg
CH_4	3.60E-03	9.02E-04	7.22E-04	6.62E-04	6.42E-04	6.32E-04	kg
N_2O	1.94E-05	8.06E-06	7.31E-06	7.05E-06	6.97E-06	6.93E-06	kg
Waste:							
Air	0.134	0.034	0.027	0.025	0.024	0.024	kg
Water	0.889	0.222	0.178	0.163	0.158	0.156	kg
Soil	9.42E-06	2.36E-06	1.88E-06	1.73E-06	1.67E-06	1.65E-06	kg

Table C.8: Inventory of spray cleaning of 150L part, with high concentration and cleaning time and 5% replacement per filtration.

Spray Cleaning - 150L 30g/L 10 minute - 5% replacement							
# of Uses:	**1**	**10**	**25**	**50**	**75**	**100**	
Energy	388.039	68.499	47.196	40.096	37.729	36.545	MJ
Water	1.102	0.157	0.094	0.073	0.066	0.063	m^3
CO_2	31.960	6.395	4.690	4.122	3.933	3.838	kg
CH_4	2.10E-02	3.02E-03	1.82E-03	1.42E-03	1.29E-03	1.22E-03	kg
N_2O	1.40E-04	5.67E-05	5.12E-05	4.93E-05	4.87E-05	4.84E-05	kg
Waste:							
Air	0.867	0.124	0.074	0.058	0.052	0.050	kg
Water	5.736	0.819	0.492	0.382	0.346	0.328	kg
Soil	6.07E-05	8.67E-06	5.20E-06	4.05E-06	3.66E-06	3.47E-06	kg

Table C.9: Inventory of spray cleaning of 150L part, with high concentration and cleaning time and 20% replacement per filtration.

Spray Cleaning - 150L 30g/L 10 minute - 20% replacement							
# of Uses:	**1**	**10**	**25**	**50**	**75**	**100**	
Energy	441.296	121.756	100.453	93.352	90.985	89.802	MJ
Water	1.260	0.315	0.252	0.231	0.224	0.220	m^3
CO_2	36.221	10.656	8.951	8.383	8.194	8.099	kg
CH_4	2.40E-02	6.02E-03	4.82E-03	4.42E-03	4.29E-03	4.22E-03	kg
N_2O	1.54E-04	7.06E-05	6.51E-05	6.32E-05	6.26E-05	6.23E-05	kg
Waste:							
Air	0.991	0.248	0.198	0.182	0.176	0.173	kg
Water	6.555	1.639	1.311	1.202	1.165	1.147	kg
Soil	6.94E-05	1.73E-05	1.39E-05	1.27E-05	1.23E-05	1.21E-05	kg

Table C.10: Inventory of spray cleaning a 12L part, with low concentration and cleaning time, and 5% replacement per filtration.

Spray Cleaning - 12L 4g/L 1 minute - 5% replacement							
# of Uses:	**1**	**10**	**25**	**50**	**75**	**100**	
Energy	4.450	0.983	0.752	0.675	0.649	0.636	MJ
Water	0.034	0.005	0.003	0.002	0.002	0.002	m^3
CO_2	0.380	0.103	0.084	0.078	0.076	0.075	kg
CH_4	2.32E-04	3.35E-05	2.03E-05	1.59E-05	1.44E-05	1.37E-05	kg
N_2O	2.19E-06	1.29E-06	1.23E-06	1.21E-06	1.20E-06	1.20E-06	kg
Waste:							
Air	0.009	0.001	0.001	0.001	0.001	0.001	kg
Water	0.062	0.009	0.005	0.004	0.004	0.004	kg
Soil	6.58E-07	9.41E-08	5.64E-08	4.39E-08	3.97E-08	3.76E-08	kg

Table C.11: Inventory of spray cleaning a 12L part, with low concentration and cleaning time, and 20% replacement per filtration.

Spray Cleaning - 12L 4g/L 1 minute - 20% replacement							
# of Uses:	**1**	**10**	**25**	**50**	**75**	**100**	
Energy	5.028	1.561	1.330	1.253	1.227	1.214	MJ
Water	0.039	0.010	0.008	0.007	0.007	0.007	m^3
CO_2	0.426	0.149	0.131	0.124	0.122	0.121	kg
CH_4	2.65E-04	6.65E-05	5.33E-05	4.89E-05	4.74E-05	4.67E-05	kg
N_2O	2.34E-06	1.44E-06	1.38E-06	1.36E-06	1.35E-06	1.35E-06	kg
Waste:							
Air	0.011	0.003	0.002	0.002	0.002	0.002	kg
Water	0.071	0.018	0.014	0.013	0.013	0.012	kg
Soil	7.52E-07	1.88E-07	1.50E-07	1.38E-07	1.34E-07	1.32E-07	kg

Table C.12: Inventory of spray cleaning a 12L part, with high concentration and cleaning time, and 5% replacement per filtration.

Spray Cleaning - 12L 30g/L 10 minute - 5% replacement							
# of Uses:	**1**	**10**	**25**	**50**	**75**	**100**	
Energy	33.848	8.307	6.604	6.037	5.847	5.753	MJ
Water	0.088	0.013	0.008	0.006	0.005	0.005	m^3
CO_2	2.952	0.908	0.771	0.726	0.711	0.703	kg
CH_4	1.71E-03	2.48E-04	1.51E-04	1.18E-04	1.08E-04	1.02E-04	kg
N_2O	1.92E-05	1.25E-05	1.20E-05	1.19E-05	1.18E-05	1.18E-05	kg
Waste:							
Air	0.069	0.010	0.006	0.005	0.004	0.004	kg
Water	0.458	0.065	0.039	0.031	0.028	0.026	kg
Soil	4.85E-06	6.93E-07	4.16E-07	3.23E-07	2.93E-07	2.77E-07	kg

Table C.13: Inventory of spray cleaning a 12L part, with high concentration and cleaning time, and 20% replacement per filtration.

Spray Cleaning - 12L 30g/L 10 minute - 20% replacement							
# of Uses:	**1**	**10**	**25**	**50**	**75**	**100**	
Energy	38.105	12.564	10.861	10.293	10.104	10.010	MJ
Water	0.101	0.025	0.020	0.018	0.018	0.018	m^3
CO_2	3.292	1.248	1.112	1.067	1.051	1.044	kg
CH_4	1.95E-03	4.91E-04	3.94E-04	3.61E-04	3.51E-04	3.45E-04	kg
N_2O	2.03E-05	1.36E-05	1.32E-05	1.30E-05	1.30E-05	1.29E-05	kg
Waste:							
Air	0.079	0.020	0.016	0.015	0.014	0.014	kg
Water	0.524	0.131	0.105	0.096	0.093	0.092	kg
Soil	5.54E-06	1.39E-06	1.11E-06	1.02E-06	9.86E-07	9.70E-07	kg

C.2.2 Ultrasonic Cleaning

The life cycle inventory of ultrasonic cleaning are shown in the following tables, for varying part size, cleaning time, and amount of cleaning solution lost per filtration. These data are all give for increasing uses of the initial cleaning solution, before it is entirely replaced.

Table C.14: Inventory of ultrasonic cleaning a 150L part, with 1 minute cleaning time, and 5% replacement per filtration.

Ultrasonic cleaning - 150L - 1 minute - 5% replacement							
# of Uses:	**1**	**10**	**25**	**50**	**75**	**100**	
Energy	905.407	130.105	78.418	61.189	55.446	52.575	MJ
Water	2.227	0.318	0.191	0.148	0.134	0.127	m^3
CO_2	72.492	10.463	6.327	4.949	4.489	4.260	kg
CH_4	5.16E-02	7.37E-03	4.42E-03	3.44E-03	3.11E-03	2.95E-03	kg
N_2O	2.39E-04	3.62E-05	2.27E-05	1.82E-05	1.67E-05	1.60E-05	kg
Waste:							
Air	2.103	0.300	0.180	0.140	0.127	0.120	kg
Water	13.916	1.988	1.193	0.928	0.839	0.795	kg
Soil	1.47E-04	2.10E-05	1.26E-05	9.80E-06	8.87E-06	8.40E-06	kg

Table C.15: Inventory of ultrasonic cleaning a 150L part, with 1 minute cleaning time, and 20% replacement per filtration.

Ultrasonic cleaning - 150L- 1 minute - 20% replacement							
# of Uses:	**1**	**10**	**25**	**50**	**75**	**100**	
Energy	1034.624	259.322	207.635	190.406	184.663	181.792	MJ
Water	2.545	0.636	0.509	0.467	0.453	0.445	m^3
CO_2	82.831	20.801	16.666	15.287	14.828	14.598	kg
CH_4	5.89E-02	1.47E-02	1.18E-02	1.08E-02	1.05E-02	1.03E-02	kg
N_2O	2.72E-04	7.00E-05	5.65E-05	5.20E-05	5.05E-05	4.97E-05	kg
Waste:							
Air	2.404	0.601	0.481	0.441	0.427	0.421	kg
Water	15.904	3.976	3.181	2.916	2.827	2.783	kg
Soil	1.68E-04	4.20E-05	3.36E-05	3.08E-05	2.99E-05	2.94E-05	kg

Table C.16: Inventory of ultrasonic cleaning a 150L part, with 10 minute cleaning time, and 5% replacement per filtration.

Ultrasonic cleaning - 150L - 10 minute - 5% replacement							
# of Uses:	**1**	**10**	**25**	**50**	**75**	**100**	
Energy	913.399	138.097	86.410	69.181	63.438	60.567	MJ
Water	2.227	0.318	0.191	0.148	0.134	0.127	m^3
CO_2	73.611	11.582	7.446	6.068	5.608	5.379	kg
CH_4	5.16E-02	7.38E-03	4.43E-03	3.45E-03	3.12E-03	2.96E-03	kg
N_2O	2.61E-04	5.87E-05	4.52E-05	4.07E-05	3.92E-05	3.85E-05	kg
Waste:							
Air	2.103	0.300	0.180	0.140	0.127	0.120	kg
Water	13.916	1.988	1.193	0.928	0.839	0.795	kg
Soil	1.47E-04	2.10E-05	1.26E-05	9.80E-06	8.87E-06	8.40E-06	kg

Table C.17: Inventory of ultrasonic cleaning a 150L part, with 10 minute cleaning time, and 20% replacement per filtration.

Ultrasonic cleaning - 150L - 10 minute - 20% replacement							
# of Uses:	**1**	**10**	**25**	**50**	**75**	**100**	
Energy	1042.616	267.314	215.627	198.398	192.655	189.784	MJ
Water	2.545	0.636	0.509	0.467	0.453	0.445	m^3
CO_2	83.950	21.920	17.784	16.406	15.947	15.717	kg
CH_4	5.89E-02	1.47E-02	1.18E-02	1.08E-02	1.05E-02	1.03E-02	kg
N_2O	2.95E-04	9.25E-05	7.90E-05	7.45E-05	7.30E-05	7.22E-05	kg
Waste:							
Air	2.404	0.601	0.481	0.441	0.427	0.421	kg
Water	15.904	3.976	3.181	2.916	2.827	2.783	kg
Soil	1.68E-04	4.20E-05	3.36E-05	3.08E-05	2.99E-05	2.94E-05	kg

Table C.18: Inventory of ultrasonic cleaning a 12L part, with 1 minute cleaning time, and 5% replacement per filtration.

Ultrasonic cleaning - 12L - 1 minute - 5% replacement							
# of Uses:	**1**	**10**	**25**	**50**	**75**	**100**	
Energy	72.517	10.565	6.435	5.058	4.600	4.370	MJ
Water	0.178	0.025	0.015	0.012	0.011	0.010	m^3
CO_2	5.816	0.860	0.529	0.419	0.382	0.364	kg
CH_4	3.77E-02	3.42E-02	3.40E-02	3.39E-02	3.38E-02	3.38E-02	kg
N_2O	1.96E-05	3.37E-06	2.29E-06	1.93E-06	1.81E-06	1.75E-06	kg
Waste:							
Air	0.168	0.024	0.014	0.011	0.010	0.010	kg
Water	1.112	0.159	0.095	0.074	0.067	0.064	kg
Soil	1.18E-05	1.68E-06	1.01E-06	7.84E-07	7.09E-07	6.72E-07	kg

Table C.19: Inventory of ultrasonic cleaning a 12L part, with 1 minute cleaning time, and 20% replacement per filtration.

Ultrasonic cleaning - 12L- 1 minute - 20% replacement							
# of Uses:	**1**	**10**	**25**	**50**	**75**	**100**	
Energy	82.842	20.891	16.760	15.384	14.925	14.695	MJ
Water	0.203	0.051	0.041	0.037	0.036	0.036	m^3
CO_2	6.642	1.686	1.355	1.245	1.208	1.190	kg
CH_4	3.83E-02	3.48E-02	3.45E-02	3.45E-02	3.44E-02	3.44E-02	kg
N_2O	2.23E-05	6.07E-06	4.99E-06	4.63E-06	4.51E-06	4.45E-06	kg
Waste:							
Air	0.192	0.048	0.038	0.035	0.034	0.034	kg
Water	1.271	0.318	0.254	0.233	0.226	0.222	kg
Soil	1.34E-05	3.36E-06	2.69E-06	2.46E-06	2.39E-06	2.35E-06	kg

Table C.20: Inventory of ultrasonic cleaning a 12L part, with 10 minute cleaning time, and 5% replacement per filtration.

Ultrasonic cleaning - 12L - 10 minute - 5% replacement							
# of Uses:	**1**	**10**	**25**	**50**	**75**	**100**	
Energy	74.677	12.725	8.595	7.218	6.760	6.530	MJ
Water	0.178	0.025	0.015	0.012	0.011	0.010	m^3
CO_2	6.118	1.162	0.832	0.721	0.685	0.666	kg
CH_4	3.40E-01	3.37E-01	3.36E-01	3.36E-01	3.36E-01	3.36E-01	kg
N_2O	2.56E-05	9.44E-06	8.36E-06	8.00E-06	7.88E-06	7.82E-06	kg
Waste:							
Air	0.168	0.024	0.014	0.011	0.010	0.010	kg
Water	1.112	0.159	0.095	0.074	0.067	0.064	kg
Soil	1.18E-05	1.68E-06	1.01E-06	7.84E-07	7.09E-07	6.72E-07	kg

Table C.21: Inventory of ultrasonic cleaning a 12L part, with 10 minute cleaning time, and 20% replacement per filtration.

Ultrasonic cleaning - 12L - 10 minute - 20% replacement							
# of Uses:	**1**	**10**	**25**	**50**	**75**	**100**	
Energy	85.002	23.051	18.920	17.544	17.085	16.855	MJ
Water	0.203	0.051	0.041	0.037	0.036	0.036	m^3
CO_2	6.944	1.988	1.658	1.548	1.511	1.492	kg
CH_4	3.41E-01	3.37E-01	3.37E-01	3.37E-01	3.37E-01	3.37E-01	kg
N_2O	2.83E-05	1.21E-05	1.11E-05	1.07E-05	1.06E-05	1.05E-05	kg
Waste:							
Air	0.192	0.048	0.038	0.035	0.034	0.034	kg
Water	1.271	0.318	0.254	0.233	0.226	0.222	kg
Soil	1.34E-05	3.36E-06	2.69E-06	2.46E-06	2.39E-06	2.35E-06	kg

APPENDIX D

UNCERTAINTY ANALYSIS

D.1 Laser Ablated Template

The more times the template can be used, the less of an environmental impact that can be attributed to each m^2 of self-cleaning surface produced. With no experimental data available about the lifetime of a laser ablated template, it cannot be determined how many times the template will be used before needing to be replaced. Also, each template may not have the same lifetime.

For these reasons, an uncertainty analysis is performed. Using the @Risk software, a distribution of Triangular(20,50,100) is inputted for the number of times the template is used. The analysis uses 1000 iterations and Monte Carlo sampling. This analysis is performed to determine an average or most likely value for the life cycle inventory of the template per use. The average per use values are found for the template produced with a 2000mm/s scan speed and are shown in Table D.1.

Table D.1: Average inventory values for the production of a laser ablated template with a high scan speed.

Steel Template – 2000mm/s- Production		
Energy	17.27	MJ
Water	1.80E-2	m^3
CO_2	2.25	kg
CH_4	4.02E-6	kg
N_2O	3.85E-3	kg
Air Emissions	1.82	kg
Water Emissions	4.95E-3	kg
Soil Emissions	0.720	kg

The process is repeated for a laser scan speed of 250mm/s, and the inventory data are shown in Table D.2

Table D.2: Average inventory values for the production of a laser ablated template with a low scan speed.

Steel Template – 250mm/s- Production		
Energy	40.03	MJ
Water	1.80E-2	m^3
CO_2	5.436	kg
CH_4	3.21E-5	kg
N_2O	3.91E-3	kg
Air Emissions	1.82	kg
Water Emissions	4.95E-3	kg
Soil Emissions	0.720	kg

D.2 Anodized Aluminum Template

The average, or most likely, values of the life cycle inventory are determined with an uncertainty analysis. Distributions are selected for each of the input variables. The variables and their distributions are shown in Table D.3.

Table D.3: Variable distributions for the production of an anodized aluminum template.

Variable	Distribution
Number of times template is used	Uniform (20,100)
Amount Recycled per filtration	Uniform(0.05, 0.2)
Number of Times Recycled	Triangular(20,50,100)

First, the production of the anodized template from primary aluminum is considered. The risk analysis software @RISK is used with Excel to run a Monte Carlo selection from these distributions. The simulation is run for 1000 iterations, and average values for each life cycle inventory category are determined. The averages for a 150L part spray cleaned are shown in Table D.4.

Table D.4: Average life cycle inventory values for the production of an anodized aluminum template.

Aluminum Template - Averages		
Energy Consumed	34.25	MJ
Water Consumed	1.735	m^3
Carbon Dioxide emitted	1.47	kg
Methane emitted	4.46E-4	kg
Nitrous oxide	0.0529	kg
Total Air Releases	0.248	kg
Total Water Releases	0.02087	kg
Total Soil Releases	0.0447	kg

This process is repeated for the use of secondary aluminum. The same distributions are used for this analysis. The results of this analysis are shown in Table D.5.

Table D.5: Average life cycle inventory values for the production of an anodized aluminum template from secondary aluminum.

Aluminum Template - Averages		
Energy Consumed	47.39	MJ
Water Consumed	1.74	m^3
Carbon Dioxide emitted	1.97	kg
Methane emitted	4.66E-4	kg
Nitrous oxide	0.0532	kg
Total Air Releases	0.744	kg
Total Water Releases	0.0208	kg
Total Soil Releases	0.813	kg

D.3 Industrial Cleaning

Obviously, the lowest life cycle inventory occurs when cleaning the smallest part, with the lowest solvent concentration, for the shortest cleaning time, replacing only 5% of the solution each time and reusing the solution as many times as possibly. However, these ideal conditions will not occur for each part cleaned. The chemical solution, although filtered after cleaning, may be periodically disposed of and completely replaced. To account for variations in these parameters, a uncertainty analysis is performed on the cleaning scenarios.

Distributions are selected for each of the input variables. The variables and their distributions are shown in Table D.6.

Table D.6: Variable distributions for industrial cleaning of 150L part.

Variable	Distribution
Cleaning Time	Uniform(1,10)
Solvent Concentration	Uniform(4,30)
Amount Recycled per filtration	Uniform(0.05,20)
Number of Times Recycled	Triang(20,50,100)

First, the spray cleaning of a 150L part is considered. The size of the part is not used as an input variable, as different sized parts require different sized machines to be cleaned. Therefore, separate analyses will be performed for 12L and 150L parts. The risk analysis software @RISK is used with Excel to run a Monte Carlo selection from these distributions. The simulation is run for 1000 iterations, and average values for each life cycle inventory category are determined. The averages for a 150L part spray cleaned are shown in Table D.7.

Table D.7: Average life cycle inventory values for spray cleaning a 150L part.

Spray Cleaning – 150L Part - Averages		
Energy	37.01	MJ
Water	0.812	m^3
CO_2	19.138	kg
CH_4	1.28E-2	kg
N_2O	8.21E-5	kg
Air Emissions	0.522	kg
Water Emissions	3.454	kg
Soil Emissions	3.66E-5	kg

The probabilistic analysis is repeated for the 12L part. The results of this analysis are shown in Table D.8.

Table D.8: Average life cycle inventory values for spray cleaning a 12L part.

Spray Cleaning – 12L Part - Averages		
Energy	4.63	MJ
Water	0.0653	m^3
CO_2	4.63	kg
CH_4	0.0654	kg
N_2O	1.12E-7	kg
Air Emissions	0.0422	kg
Water Emissions	0.279	kg
Soil Emissions	2.96E-6	kg

The probabilistic analysis is performed for the ultrasonic cleaning scenarios. The same distributions are used, with the exception of the solvent concentration which is held constant at 75g/L. The results for the ultrasonic cleaning of a 150L part are shown in Table D.9.

Table D.9: Average values for the ultrasonic cleaning of a 150L part.

Ultrasonic Cleaning – 150L Part - Averages		
Energy	130.67	MJ
Water	2.39	m^3
CO_2	78.33	kg
CH_4	0.0553	kg
N_2O	2.67E-4	kg
Air Emissions	2.256	kg
Water Emissions	14.93131	kg
Soil Emissions	1.577E-4	kg

The results of the uncertainty analysis for the ultrasonic cleaning of 12L part are shown in Table D.10.

Table D.10: Average values for ultrasonic cleaning of a 12L part.

Ultrasonic Cleaning – 12L Part - Averages		
Energy	11.34	MJ
Water	0.191	m^3
CO_2	6.38	kg
CH_4	4.42E-3	kg
N_2O	2.39E-5	kg
Air Emissions	0.180	kg
Water Emissions	1.19	kg
Soil Emissions	1.26E-5	kg

REFERENCES

Abbott, S. J. and P. H. Gaskell (2007). "Mass production of bio-inspired structured surfaces." Proceedings of the Institution of Mechanical Engineers, Part C: Journal of Mechanical Engineering Science **221**(10): 1181-1191.

Advanced Misting Systems. "High Pressure Modules Mist Pumps." 2008, Available online at http://www.advancedmistingsystems.com/mist_pumps.html.

Allen, D. T., D. J. Bauer, B. Bras, T. G. Gutowski, C. F. Murphy, T. S. Piwonka, P. S. Sheng, J. W. Sutherland, D. L. Thurston and E. E. Wolff (2002). "Environmentally Benign Manufacturing: Trends in Europe, Japan and the USA." ASME Journal of Manufacturing Science **124**(4): 908-920.

Althaus, H.-J., M. Chudacoff, R. Hischier, N. Jungbluth, M. Osses and A. Primas (2004). "Life Cycle Inventories of Chemicals. Final Report ecoinvent." Swiss Centre for Life Cycle Inventories **8**.

Arkles, B. (2000). Silicon Compounds, Silanes. Kirk-Othmer Encyclopedia of Chemical Technology, John Wiley & Sons.

ASM International (1996). Choosing a Cleaning Process. Materials Park, OH, ASM International.

Bado, P., W. Clark and A. Said. (2007). "Introduction to Micromachining." 2008, Available online at http://cmxr.com/Industrial/Handbook/Introduction.htm.

Bailey, W. I. and A. J. Woytek (2004). Halogen Fluoride. Kirk-Othmer Encyclopedia of Chemical Technology, John Wiley & Sons.

Barthlott, W. and C. Neinhuis (1997). "Purity of the sacred lotus, or escape from contamination in biological surfaces." Planta **202**: 1-8.

Baum, C., W. Meyer, R. Stelzer, L. G. Fleischer and D. Siebers (2002). "Average nanorough skin surface of the pilot whale (Globicephala melas, Delphinidae): considerations on the self-cleaning abilities based on nanoroughness." Marine Biology **140**: 653-657.

Beattie, A. and P. R. Erhlich (2001). Wild Solutions: How Biodeversity is Money in the Bank. New Haven, Yale University Press.

Benyus, J. M. (1997). Biomimicry: Innovation Inspired by Nature. New York, NY, Harper Perennial.

Bhushan, B. and Y. C. Jung (2006). "Micro- and nanoscale characterization of hydrophilic and hydrophilic leaf surfaces." Nanotechnology **17**: 2758-2772.

Bico, J., C. Marzolin and D. Quere (1999). "Pearl drops." Europhysics Letters **47**(2): 220-226.

Bico, J., U. Thiele and D. Quere (2002). "Wetting of textured surfaces." Colloids and Surfaces A: Physiochemical and Engineering Aspects **206**: 41-46.

Biomimicry Guild. (2007). "Life's Principles." Retrieved 2007, Available online at http://www.biomimicryinstitute.org/about-us/biomimicry-a-tool-for-innovation.html.

BIOPRO. (2006). "Botany meets textile technology." 2007, Available online at http://www.bio-pro.de/en/region/stern/magazin/02141/index.html.

Brezet, H. and C. V. Hemel (1997). Ecodesign: A Promising Approach to Sustainable Production and Consumption. Paris, France, UNEP/IE (United Nations ENvironment Programme/Industry and Environment).

Brombach Gess. (2007). "Nano E2C 121 - Easy-to-clean Coating for Marine Glass." 2007, Available online at http://www.brombach-gess.de/pdf_download/beschichtungen_da_E.pdf.

Cassie, A. B. D. and S. Baxter (1944). "Wettability of Porous Surfaces." Transactions of the Faraday Society **40**: 546-551.

Cheng, Y. T., D. E. Rodak, C. A. Wong and C. A. Hayden (2006). "Effects of micro- and nao-structures on the self-cleaning behaviour of lotus leaves." Nanotechnology **17**: 1359-1362.

Churchill, S. W. and H. H. S. Chu (1975). "Correlating Equations for Laminar and Turbulent Free Convection from a Horizontal Cylinder." International Journal of Heat and Mass Transfer **18**: 1049.

Churchill, S. W. and H. H. S. Chu (1975). "Correlating Equations for Laminar and Turbulent Free Convection from a Vertical Plate." International Journal of Heat and Mass Transfer **18**: 1323.

Coherent Inc. (2000). "RegA 9000/9050 - High Repetition Rate Ti:Sapphire Amplifier." 2008, Available online at http://www.coherentinc.com/downloads/RegA_9000_9500_DS.pdf.

Couden, M. (2008). "Aluminum Anodizing." 2008, Available online at http://www.pfonline.com/articles/pfdcouden01.html.

Delstar Metal Finishing Inc. (2003). "Electropolishing: A User's Guide to Applications, Quality Standards and Specifications." 2008, Available online at http://www.delstar.com/manual.htm.

Durkee, J. B. I. (2002). "Aqueous Cleaning Machines - Part I." Cleaning Times **100**(3): 51-54.

Durkee, J. B. I. (2002). "Aqueous Cleaning Machines - Part II." Cleaning Times **100**(5): 54-59.

Durkee, J. B. I. (2002). "Aqueous Cleaning Machines - Part III." Cleaning Times **100**(7): 27-31.

Ecological Coatings. (2008). "Advanced Environmental Coatings from Eccotech. Product Line." 2007, Available online at http://www.capital.net/com/eccotech/eproducts.htm.

EIA. "Voluntary Reporting of Greenhouse Gases Program: Fuel and Energy Source Codes and Emission Coefficients." 2008, Available online at http://www.eia.doe.gov/oiaf/1605/coefficients.html.

Eisch Glaskultur. "The No Drop Effect Cleaning Information." 2007, Available online at http://www.eisch.de/downloads/Information_NoDrop.pdf.

EKSPLA. "Pico Master Series Picosecond Laser Micromachining Workstation." 2008, Available online at http://www.ekspla.com/en/p/pico-master-series-picosecond-laser-micromachining-21152.

Electro Polish Systems Inc. (2006). "Electropolishing Solutions: Characteristics and Operating Parameters." 2008, Available online at http://www.ep-systems.com/favorite.htm.

Erlus. "Erlus Lotus: The first self-cleaning clay roof." 2007, Available online at http://www.erlus.com/uploads/pdf/dach/en_Lotus.pdf.

Extrand, C. W. (2002). "Model for Contact Angles and Hysteresis on Rough and Ultraphobic Surfaces." Langmuir **18**: 7991-7999.

Fisher, J. and T. A. Egerton (2001). Titanium Compounds, Inorganic. Kirk-Othmer Encyclopedia of Chemical Technology, John Wiley & Sons.

Fiskel, J. (1996). Design for Environment- Creating Eco-Efficient Products and Processes. New York, McGraw-Hill.

Fujii, H., T. Nagaiwa and H. Kusuno (2005). How to quantify the environmental profile of stainless steel. SETAC North American 26th Annual Meeting, Baltimore, Maryland.

Fürstner, R. and W. Barthlott (2005). "Wetting and Self-Cleaning Properties of Artificial Superhydrophobic Surfaces." Langmuir **21**: 956-961.

Govetto, S. (2008). Determining the Environmental Impact of Disposal, Recycling and Remanufacturing Strategies. G.W. Woodruff School of Mechanical Engineering. Atlanta, Georgia Institute of Technology. **Master of Science in Mechanical Engineering:** 299.

Groenendijk, M. and J. Meijer (2006). "Microstructuring using femtosecond pulsed laser ablation." Journal of Laser Applications **18**(3): 227-235.

Guo, C., L. Feng, J. Zhai, G. Wang, Y. Song, L. Jiang and D. Zhu (2004). "Large-Area Fabrication of a Nanostructure-Induced Hydrophobic Surface from a Hydrophilic Polymer." ChemPhysChem **5**: 750-753.

Hansen, W. R. and K. Autumn (2005). "Evidence for self-cleaning in gecko setae." Proceedings of the National Academy of Sciences **102**: 385-389.

Hischier, R., S. Hellweg, C. Capello and A. Primas (2005). "Establishing Life Cycle Inventories of Chemicals Based on Differing Data Availability." International Journal of Life Cycle Assessment **10**(1): 59-67.

Horn, M. and U. Horns (2000). Alkoxides, Metal. Kirk-Othmer Encyclopedia of Chemical Technology, John Wiley & Sons.

Incropera, F. P. and D. P. DeWitt (2002). Introduction to Heat Transfer, John Wiley & Sons.

International Standards Organization (2006). Environmental Management - Life Cycle Assessment - Principles and Framework ISO 14040.

IPCC. (2001). "Climate Change 2001: The Scientific Basis." 2007, Available online at http://www.grida.no/climate/ipcc_tar/wg1/index.htm.

Joanny, J. F. and P. G. d. Gennes (1984). "A model for contact angle hysteresis." Journal of Chemical Physics **81**(1): 552-562.

Katakura, R. and Y. Koide (2005). "One-step Synthesis of Aluminum Acetylaceontate from [AlO(OH)]n (Boehmite) in Water." Chemistry Letters **34**(10): 1448-1449.

Kern, W. (1993). "Handbook of Semiconductor Wafer Cleaning Technology - Science, Technology, and Applications." Retrieved 1/7, 2008, Available online at http://www.knovel.com/knovel2/Toc.jsp?BookID=132&VerticalID=0.

Kim, S. and B. E. Dale (2005). "Environmental aspects of ethanol derived from no-tilled corn grain: nonrenewable energy consumption and greenhouse gas emissions." Biomass and Bioenergy **28**: 475-489.

Kyle, B. G. (1984). Chemical and Process Thermodynamics. Englewood Cliffs, NJ, Prentice Hall.

Lafuma, A. and D. Quere (2003). "Superhydrophobic States." Natural Materials **2**: 457-460.

Lau, K. K. S., J. Bico, K. B. K. Teo, M. Chhowalla, G. A. J. Amaratunga, W. I. Milne, G. H. McKinley and K. K. Gleason (2003). "Superhydrophobic Carbon Nanotube Forests." Nano Letters **3**(12): 1701-1705.

Lee, W., M.-K. Jin, W.-C. Yoo and J.-K. Lee (2004). "Nanostructuring of a Polymeric Substrate with Well-Defined Nanometer-Scale Topography and Tailored Surface Wettability." Langmuir **20**(18): 7665-7669.

Lewis, R. J., Sr. (2002). Hawley's Condensed Chemical Dictionary, John Wiley & Sons.

Li, H., X. Wang, Y. Song, Y. Liu, Q. Li, L. Jiang and D. Zhu (2001). "Super-'Amphiphobic' Aligned Carbon Nanotube Films." Angewandte Chemie (International Edition) **40**(9): 1743-1746.

Madou, M. J. (2002). Fundamentals of Microfabrication: The Science of Miniaturization. Boca Raton, FL, CRC Press LLC.

Marmur, A. (2004). "The Lotus Effect: Superhydrophobicity and Metastability." Langmuir **20**: 3517-3519.

Mendiratta, S. K., R. L. Dotson and R. T. Brooker (2005). Perchloric Acid and Perchlorates. Kirk Othmer Encyclopedia of Chemical Technology, John Wiley & Sons.

Mendiratta, S. K. and B. L. Duncan (2003). Chloric Acid and Chlorates. Kirk Othmer Encyclopedia of Chemical Technology, John Wiley & Sons. **6**.

Munns, K. (1993). "Recycling and the Anodizer: Anodizing the recyclable metal with recyclable processes." 2008, Available online at http://www.p2pays.org/ref%5C02/01443.pdf.

Murphy, D. P. (2000). Metal Surface Treatments, Cleaning. Kirk-Othmer Encyclopedia of Chemical Technology, John Wiley & Sons.

Murphy, D. P. (2000). Metal Surface Treatments, Cleaning. Kirk-Othmer Encyclopedia of Chemical Technology, John Wiley & Sons.

Nakajima, A., A. Fujishima, K. Hashimoto and T. Watanabe (1999). "Preparation of Transparent Superhydrophobic Boehmite and Silica Films by Sublimation of Aluminum Acetyleacetonate." Advanced Materials **2**(16): 1365-1368.

Nakajima, A., K. Hashimoto and T. Watanabe (2001). "Recent Studies on Super-Hydrophobic Films." Monatshefte für Chemie **132**: 31-41.

Nakajima, A., K. Hasimoto and T. Watanabe (2000). "Transparent Superhydrophobic Thin Films with Self-Cleaning Properties." Langmuir **16**: 7044-7047.

Nano-X. "NANO-X Information." 2007, Available online at http://www.nano-x.de/pdf/Handout_Textil_englisch.pdf.

Neinhuis, C. and W. Barthlott (1997). "Characterization and Distribution of Water-repellent, Self-cleaning Plant Surfaces." Annals of Botany **79**: 667-677.

Nosonovsky, M. and B. Bhushan (2005). "Roughness optimization for biomimetic superhydrophobic surfaces." Microsystem Technology **11**: 535-549.

NREL. (2007). "Primary Aluminum Production." 2008, Available online at http://www.nrel.gov/lci.

Oberdörster, G., E. Oberdörster, and J. Oberdörster (2005). "Nanotoxicology: An Emerging Discipline Evolving from the Studies of Ultrafine Particles." Environmental Health Perspectives **113**(7): 823-839.

Overcash, M. (2008). Chemical life cycle inventory database. Raleigh, NC 27607.

Pacific Northwest Pollution Prevention Resource Center. (1996). "Aqueous Cleaning Technology Review." Available online at http://www.pprc.org/pubs/techreviews/aqueous/aqintro.html.

Patankar, N. A. (2003). "On the Modeling of Hydrophobic Contact Angles on Rough Surfaces." Langmuir **19**: 1249-1253.

Patzek, T. W. (2004). "Thermodynamics of the Corn-Ethanol Biofuel Cycle." Critical Reviews in Plant Sciences **23**(6): 519-567.

Petschel, M. and R. Hart (2000). Metal Surface Conversion Treatments. Kirk Othmer Encyclopedia of Chemical Technology, John Wiley & Sons.

Plating Sales Inc. (2005). "Anodizing Studio Kits and Anodizing Accessories ", 2008, Available online at http://www.platingsales.com/anodizingkits.html.

PRé Consultants (1996). Database Manual BUWAL 250 Library.

Procachem. "AD-500 Anti-Graffiti Coating Additive." 2008, Available online at http://www.procachem.com/Products/Composites-Elastomer-Coatings/Anti-Graffiti%20Coating%20Additive.htm.

Quitmeyer, J. A. (1995). "The Evolution of Aqueous Cleaner Technology." Metal Finishing **93**(9): 34-39.

R.K. Transonic. (2007). "Aqueous Ultrasonic Cleaners." Available online at http://www.ultrasonicindia.com/single-tank-ultrasonic-cleaners.html.

Richard, D. and D. Quéré (1999). ""Viscous drops rolling on a tilted non-wettable solid." Europhysics Letters **48**(3): 286-291.

Rickerby, D. G. and M. Morrison (2007). "Nanotechnology and the environment: A European perspective." Science and Technology of Advanced Materials **8**: 19-24.

Romenesko, D. J., I. Chorvath, C. W. Olsen and L. M. Tonge (2005). Poly(Fluorosilicones). Kirk-Othmer Encyclopedia of Chemical Technology, John Wiley & Sons.

SAIC. (2006). "Life Cycle Assessment: Principles and Practice." 2008, Available online at http://www.epa.gov/NRMRL/lcaccess/pdfs/600r06060.pdf.

Sandtex. (2006). "Sandtex - Microseal." 2007, Available online at http://www.sandtex.co.uk/microseal/index.html.

Sawada, H. and T. Murakami (2000). Oxalic Acid. Kirk Othmer Encyclopedia of Chemical Technology, John Wiley & Sons.

Schoelle Textiles. "3XDRY: The Feelgood Technology." 2007, Available online at http://www.schoeller-textiles.com/default.asp?cat1ID=128&cat2ID=134&pageID=83&emotionstate=0&emotionID=8&langID=2.

Schoelle Textiles. "Schoelle Textiles - Nanospheres." 2007, Available online at http://www.schoeller-textiles.com/nanosphere/main.asp?site=nanosphere&language=english&webpageID=255.

Smart, B. E. and R. E. Fernandez (2000). Fluorinated Aliphatic Compounds. Kirk-Othmer Encyclopedia of Chemical Technology, John Wiley & Sons.

Stainmaster Carpet. (2003). "Carpet design, Carpet construction, Carpet manufacturer - Stainmaster." 2007, Available online at http://www.stainmaster.com.au/construction.aspx.

Sto Corp. (2007). "Sto Lotusan - The Exterior Coating with Lotus-Effect." 2007, Available online at http://www.stocorp.com/allweb.nsf/lotusanpage.

Terörde, F. (2006). "Stainless Steel Recycling: Data and Scenarios Availability of Scrap." Available online at http://www.worldstainless.org/NR/rdonlyres/8FD08987-E98F-4BB8-9B33-99EEF0E8F938/2425/StainlessSteelRecyclingAvailabilityofscrap.pdf.

Thieme, M., R. Frenzel, S. Schmidt, F. Simon, A. Hennig, H. Worch, K. Lunkwitz and D. Scharnweber (2001). "Generation of Ultrahydrophobic Properties of Aluminum - A first Step to Self-cleaning Transparently Coated Metal Surfaces." Advanced Engineering Materials **3**(9): 691-695.

Thomas, C., T. Tennant, and J. Rolls (2000). "The GHG Indicator: UNEP Guidelines for Calculating Greenhouse Gas Emissions for Businesses and Non-Commercial Organisations." United Nations Environment Programme.

UN 'Brundtland' Commission (1987). Our Common Future, Report of the World Commission on Environment and Development. Oxford, Oxford University Press.

Uniwashers. (2007). "Industrial and automotive parts washers and spray wash cabinets." Available online at http://www.uniwashers.com/.

US EPA (1993). Life-Cycle Design Guidance Manual. Washington, D.C., US Environmental Protection Agency, Office of Research and Development.

US EPA. (1995). "Compilation of Air Pollutant Emission Factors, Volume 1: Stationary Point and Area Sources." 5th. 2008, Available online at http://www.epa.gov/ttn/chief/ap42/index.html.

US EPA. (2000). "Approaching Zero Discharge in Surface Finishing." 2008, Available online at http://www.epa.gov/nrmrl/pubs/625r99008/625r99008.pdf.

US EPA. (2004). "Inventory of U.S. Greenhouse Gas Emissions and Sinks: 1990-2004." Available online at http://yosemite.epa.gov/OAR/globalwarming.nsf/content/ResourceCenterPublicationsGHGEmissionsUSEmissionsInventory2006.html.

US EPA (2004). "The U.S. Solvent Cleaning Industry and the Transition to Non Ozone Depleting Substances."

Wagner, F. S. (2002). Acetic Anhydride. Kirk-Othmer Encyclopedia of Chemical Technology, John Wiley & Sons.

Wagner, T., C. Neinhuis and W. Barthlott (1996). "Wettability and Contaminability of Insect Wings as a Function of Their Surface Sculptures." Acta Zoologica **77**(3): 213-225.

Wenzel, R. (1936). "Resistance of Solid Surfaces to Wetting by Water." Industrial and Engineering Chemistry **28**(8): 988-994.

Yoshimitsu, Z., A. Nakajima, T. Watanabe, and K. Hashimoto (2002). "Effects of Surface Structure on the Hydrophobicity and Sliding Behavior of Water Droplets." Langmuir **18**: 5818-5822.

Yoshino, N., Y. Yamamoto, K. Hmano and T. Kawase (1993). "Syntheses and Reactions of Metal Organics. XVII. Syntheses of (1H,1H,2H,2H-Polyfluoroalkyl)trimethoxysilanes and Surface Modification of Glass Plate." Bulletins of the Chemical Society of Japan **66**(6): 1754-1758.

Zheng, Q. S., Y. Yu, and Z.H. Zhao (2005). "Effects of Hydraulic Pressure on the Stability and Transition of Wetting Modes of Superhydrophobic Surfaces." Langmuir **21**: 12207-12212.

Zorba, V., L. Persano, D. Pisignano, A. Athanassiou, E. Stratakis, R. Cingolani, P. Tzanetakis and C. Fotakis (2006). "Making silicon hydrophobic: wettability control by two-lengthscale simultaneous patterning with femtosecond laser irradiation." Nanotechnology **17**: 3234-3238.